UNIVERSIDADE D
COIMBRA

Daniela Pereira Santana Alho

Preparation and Biological Evaluation of New Triterpenoid Derivatives of Glycyrrhetinic Acid

Doctoral Thesis in Pharmaceutical Sciences in the Speciality of Pharmaceutical Chemistry, supervised by Professor Doctor Jorge António Ribeiro Salvador and presented to the Faculty of Pharmacy of the University of Coimbra

November 2022

Preparation and Biological Evaluation of New Triterpenoid Derivatives of Glycyrrhetinic Acid

Dissertation presented to the Faculty of Pharmacy of the University of Coimbra, to obtain the degree of Doctor of Philosophy in Pharmaceutical Sciences, in the specialty of Pharmaceutical Chemistry.

Daniela Pereira Santana Alho

2022

1 2 9 0

UNIVERSIDADE D
COIMBRA

Preparation and Biological Evaluation of New Triterpenoid Derivatives of Glycyrrhetinic Acid

Work developed under the scientific supervision of:

Professor Jorge António Ribeiro Salvador, PhD

Laboratory of Pharmaceutical Chemistry, Faculty of Pharmacy of the University of Coimbra

and

Center for Neuroscience and Cell Biology of the University of Coimbra.

With the collaboration of:

Professor Marta Cascante Serratosa, PhD

Department of Biochemistry and Molecular Biomedicine, Faculty of Biology, University of Barcelona.

This work was supported by **Fundação para a Ciência e para a Tecnologia (FCT)** under the Programa Operacional Potencial Humano (POPH) of Quadro de Referência Estratégico Nacional (QREN) Portugal 2007-2013.

SFRH / BD / 66020 / 2009

Agradecimentos / Acknowledgments

Ao Professor Doutor Jorge António Ribeiro Salvador expresso o meu agradecimento pela oportunidade e pela confiança que depositou em mim, pela sua competência científica, pelo entusiasmo e espírito otimista, pelo apoio e pela orientação no decorrer de todo o trabalho desenvolvido.

To Professor Marta Cascante Serratosa, PhD, I am grateful for the opportunity to work in your laboratory, for providing me all the conditions that I needed to perform the biological assays presented in this dissertation, and for the revision of my papers. I am also thankful for your kindness and your concern about my work and my well-being.

To Silvia Marin, PhD for welcoming me into the lab and for the teachings and support in the biological experiments. I am also grateful for your trust, for our work reflections and for your corrections of, and suggestions for my papers.

À Dra. Fátima Nunes e ao Dr. Pedro Cruz, pelo auxílio prestado na discussão de alguns aspetos relacionados com a elucidação estrutural dos compostos.

A todos os docentes do Laboratório de Química Farmacêutica da Faculdade de Farmácia da Universidade de Coimbra, gostaria de agradecer a simpatia, o apoio, a convivência e os ensinamentos que me foram gentilmente oferecidos.

À Dra. Vânia Moreira, agradeço por todos os ensinamentos e apoio na execução dos procedimentos experimentais químicos.

À Fundação para a Ciência e a Tecnologia, agradeço o apoio financeiro sob a forma de uma bolsa de doutoramento (SFRH / BD / 66020 / 2009).

À Graça Santiago, funcionária do Laboratório de Química Farmacêutica da Faculdade de Farmácia da Universidade de Coimbra, pela amizade, simpatia e cuidado com que sempre me tratou e por todo o apoio laboratorial prestado.

A todos os colegas do Laboratório de Química Farmacêutica com quem trabalhei agradeço por todo o companheirismo, partilha e apoio.

To all the colleagues at Marta Cascante's lab for the friendship, joy, support and for the assistance in the experiments.

Aos meus familiares e amigos que me apoiaram nesta jornada.

Ao Joaquim por todo o apoio e pelas palavras de incentivo que me fortaleceram.

A todos os que, de alguma forma, contribuíram para a realização deste trabalho, expresso a mais profunda gratidão.

Contents

Resumo

O cancro é uma das principais causas de morte em todo o mundo e prevê-se que a sua incidência aumente significativamente nas próximas décadas. Apesar dos avanços científicos alcançados na sua investigação, os fármacos anticancerígenos disponíveis na prática clínica corrente apresentam várias limitações de eficácia e segurança. Estes dados refletem a urgência no desenvolvimento de novos fármacos em quimioterapia.

Os produtos naturais têm sido a fonte principal de novos protótipos para o desenvolvimento de fármacos antitumorais. De facto, alguns medicamentos antineoplásicos derivados de compostos naturais constituem ainda a base da quimioterapia. Os triterpenóides pentacíclicos são um grupo de compostos naturais, amplamente distribuídos nas plantas, que apresentam uma grande variedade de atividades biológicas, incluindo antitumoral. Estes compostos têm demonstrado modular várias vias de sinalização e alvos moleculares do cancro, o que aumentou o seu interesse como protótipos para o desenvolvimento de novos fármacos.

O ácido glicirretínico é um triterpenóide pentacíclico que atua em vários alvos moleculares no cancro e que pode ser extraído em grande quantidade da sua fonte natural, o que o torna num protótipo comercialmente disponível e acessível.

O principal objetivo desta tese de doutoramento foi a síntese e a avaliação biológica de novos derivados do ácido glicirretínico, com o objetivo de melhorar a sua atividade antitumoral.

Este trabalho seguiu duas estratégias principais de semissíntese para modificar a estrutura do ácido glicirretínico: a introdução de diferentes anéis heterocíclicos conjugados com uma cetona α,β-insaturada no seu anel A, e a abertura do anel A juntamente com o acoplamento de um aminoácido. As estruturas dos novos derivados foram elucidadas com recurso a diferentes técnicas, incluindo espectroscopia de infravermelho, espectrometria de massa e ressonância magnética nuclear.

A atividade antiproliferativa dos derivados do ácido glicirretínico foi testada em várias linhas celulares humanas, de diferentes tipos de cancro. O derivado mais potente de cada série foi também testado na linha de células BJ não tumorais, para avaliar a sua seletividade. A linha celular Jurkat, na qual se obtiveram os melhores resultados de

inibição de proliferação para ambas as séries, foi selecionada para a realização de ensaios biológicos adicionais.

O derivado mais potente da primeira série foi o composto **2.9**, que possui um anel imidazol conjugado a uma cetona α, β-insaturada no anel A, tem um anel C reduzido e um éster metílico na posição C-30. Este composto apresentou um valor de IC_{50} de 1.1 μM nas células Jurkat, sendo assim 96 vezes mais potente do que o ácido glicirretínico e também demonstrou ser 4 vezes mais seletivo para essas células. Estudos biológicos adicionais mostraram que o composto **2.9** é um potente indutor de apoptose que ativa ambas as vias intrínseca e extrínseca, tendo este efeito sido detetado logo ao final de 6 horas de tratamento.

No segundo grupo de derivados, o composto **3.16**, com o anel A clivado, o anel C reduzido e uma cadeia de éster metílico de alanina na posição C-30, demonstrou ser o composto mais ativo. O seu valor de IC_{50} foi de 6.1 μM nas células Jurkat, sendo por isso 17 vezes mais potente do que o ácido glicirretínico e também demonstrou ser pelo menos 10 vezes mais seletivo para estas células. A investigação preliminar do seu mecanismo de ação indicou que a atividade antiproliferativa do composto **3.16** foi devida à paragem do ciclo celular na fase S e à indução de apoptose.

Em suma, este trabalho contribuiu com dois novos painéis de derivados do ácido glicirretínico com potência e seletividade melhoradas e que merecem um estudo mais aprofundado.

Palavras-chave: cancro, triterpenóides pentacíclicos, ácido glicirretínico, derivados semissintéticos, atividade antiproliferativa, apoptose, paragem do ciclo celular.

Abstract

Cancer is a leading cause of death worldwide and its incidence is expected to increase significantly over the next decades. Despite the scientific progress in cancer research, the anticancer drugs currently in clinical use have several limitations in efficacy and safety. These data demonstrate the urgency to develop new chemotherapeutic drugs.

Natural products have been the main source of new leads for anticancer drug development. In fact, some drugs derived from natural compounds are still the mainstay of cancer therapy. Pentacyclic triterpenoids are a group of natural compounds, widely distributed in plants, which display a broad range of biological activities, including antitumor activity. These compounds have been shown to modulate multiple signaling pathways and molecular targets of cancer, which increased their interest as leads for the development of new drugs.

Glycyrrhetinic acid is a pentacyclic triterpenoid with a promising multi-target profile that can be extracted from its natural source in high quantities, which make it a commercially available and affordable hit.

The main goal of this PhD thesis was the synthesis and the biological evaluation of new glycyrrhetinic acid derivatives, with the aim to improve its antitumor activity.

The work followed two main semisynthetic strategies to modify the glycyrrhetinic acid scaffold: the introduction of different heterocyclic rings conjugated with an α,β-unsaturated ketone in its ring A, and the opening of the ring A along with the coupling of an amino acid moiety. The structures of the new derivatives were elucidated using different techniques, including infrared spectroscopy, mass spectrometry and nuclear magnetic resonance.

The glycyrrhetinic acid derivatives were tested for their antiproliferative activity against several cancer lines. The most potent derivative of each series was also tested in the nontumoral BJ cell line, to evaluate their selectivity. The leukemia Jurkat cell line, in which the antiproliferative assays had the best results for both series, was selected to the execution of further biological assays.

The most potent derivative of the first series was compound **2.9**, which bears an imidazole ring conjugated to an α,β-unsaturated ketone in the ring A, has a reduced ring C

and a methyl ester at C-30 position. This compound had an IC_{50} value of 1.1 μM on Jurkat cells, which was 96-fold more potent than glycyrrhetinic acid and was also 4-fold more selective toward that cells. Further biological studies showed that compound **2.9** is a potent inducer of apoptosis that activates both the intrinsic and extrinsic pathways, as early as at 6 hours of treatment.

In the second group of derivatives, compound **3.16**, with a cleaved ring A, a reduced ring C and an alanine methyl ester chain at C-30 position, was the more active compound. It had an IC_{50} value of 6.1 μM on Jurkat cells, which was 17-fold more potent than that of glycyrrhetinic acid, and was up to 10 times more selective toward that cells. Preliminary mechanism investigation indicated that the antiproliferative activity of compound **3.16** was due to cell cycle arrest at the S phase and induction of apoptosis.

Overall, this work contributed with two new panels of novel glycyrrhetinic acid derivatives with enhanced potency and selectivity that warrant to be further studied.

Keywords: cancer, pentacyclic triterpenoids, glycyrrhetinic acid, semisynthetic derivatives, antiproliferative activity, apoptosis, cell cycle arrest.

Abbreviations

Apaf-1	Apoptotic protease activating factor-1
ATF-3	Activating transcription factor-3
Bcl-2	B-cell lymphoma 2
br	Broad
CA	Cinnamic acid
CBMI	1,1'-Carbonylbis(2'-methylimidazole)
CDI	1,1'-Carbonyldiimidazole
CDK	Cyclin-dependent kinase
CDT	1,1'-Carbonyl-di(1,2,4-triazole)
c-FLIP	Fas-associated death domain-like interleukin-1β converting enzyme inhibitory protein
CKI	Cyclin-dependent kinase inhibitor
CuAAc	Cu (I)-catalysed azide-alkyne cycloaddition
d	Doublet
DAPI	4',6-Diamidino-2'-phenylindole dihydrochloride
Deoxo-Fluor®	Bis(2-methoxyethyl)aminosulfur trifluoride
DISC	Death-inducing signaling complex
DMAPP	Dimethylallyl diphosphate
DMBA	7,12-Dimethylbenz(a)anthracene
DMEM	Dulbecco's Modified Eagle's Medium
DMSO	Dimethyl sulfoxide
DNA	Deoxyribonucleic acid
Egr-1	Early growth response-1
EMT	Epithelial-mesenchymal transition
ER	Endoplasmic reticulum
FACS	Fluorescence-activated cell sorter
ESI-MS	Electroscopy Ionization Mass Spectrometry
FADD	Fas-associated death domain
Fas-L	Fas ligand
FBS	Fetal Bovine Serum
FCC	Flash column chromatography
FLICE	Fas-associated death domain-like interleukin-1β converting enzyme
FPP	Farnesyl diphosphate
FPS	Farnesyl diphosphate synthase

GA	Glycyrrhetinic acid
GSH	Glutathione
HCC	Hepatocellular carcinoma
HDAC	Histone deacetylase
HTS	High throughput screening
HUVECs	Human umbilical vein endothelial cells
IAP	Inhibitors of apoptosis protein
IPP	Isopentenyl diphosphate
IC_{50}	Concentration that inhibits 50% of cellular growth
IR	Infrared
IUPAC	International Union for Pure and Applied Chemistry
J	Coupling constant
JNK	c-Jun NH2-terminal kinase
m	Multiplet
MAPK	Mitogen-activated protein kinase
***m*-CPBA**	*m*-Chloroperbenzoic acid
MEM	Minimum Essential Medium
MMP	Matrix metalloproteinase
MOMP	Mitochondrial outer membrane permeabilization
MS	Mass spectrometry
MTT	3-(4,5-Dimethylthiazol-2-yl)-3,5-diphenyltetrazolium bromide
MVA	Mevalonic acid
MVE	Methylerythritol phosphate
m/z	Mass-to-charge ratio
M^+	Molecular ion
m.p.	Melting point
NAG-1	Nonsteroidal anti-inflammatory drug-activated gene-1
NMR	Nuclear magnetic resonance
NO	Nitric oxide
OSC	Oxidosqualene cyclase
PARP	Poly-ADP-ribose polymerase
PBS	Phosphate Buffered Saline
PI	Propidium iodide
PI3-K	Phosphatidylinositol-3-kinase
PKC	Protein kinase C
PPAR	Peroxisome proliferator-activated receptor

PS	Phosphatidylserine
P/S	Penicillin/ streptomycin
PT	Pentacyclic triterpenoid
***p*-TSA**	*p*-Toluenesulfonic acid
PTEN	Phosphatase and tensin homologue deleted on chromosome ten
ROS	Reactive oxygen species
RPMI	Roswell Park Memorial Institute
r.t.	Room temperature
s	Singlet
SMAC	Second mitochondria-derived activator of caspases
Sp	Specificity protein
SQE	Squalene epoxidase
SQS	Squalene synthase
t	Triplet
TB	Trypan Blue
tBid	Truncated Bid
TGF	Transforming growth factor
TLC	Thin-layer chromatography
TNF	Tumor necrosis factor
TRADD	Tumor necrosis factor receptor-associated death domain
TRAIL	Tumor necrosis factor-related apoptosis-inducing ligand
VEGF	Vascular endothelial growth factor
XTT	2,3-Bis(2-methoxy-4-nitro-5-sulphophenyl)-2*H*-tetrazolium-5-carbonaxilide
δ	Chemical shift
~	Approximately

List of figures

List of tables

List of schemes

Thesis organization

This dissertation is divided in five chapters. The first section consists in a general introduction, the second and third chapters describe the work developed and the last two sections are dedicated to the concluding remarks and the supporting references used in this work.

The first chapter presents the theoretical background that supports the work developed and comprehends different sections. The first section includes cancer statistics and some details on its complex biology. The second section is related to the importance of natural products in the cancer treatment and in the discovery and development of new anticancer agents. The third section focus on the biosynthesis and on the multi-target therapeutic potential of the pentacyclic triterpenoids. The fourth section enunciates the different pharmacological activities of the glycyrrhetinic acid and focus essentially on its anticancer properties and its main reported derivatives. The last subsection describes the general objectives of the work developed, which is described in the following chapters.

Chapters 2 and 3 are dedicated to the description of the synthesis and biological evaluation of the new glycyrrhetinic acid derivatives, which include the experimental procedures used for their synthesis, structural elucidation and the biological studies, and the discussion of the results.

Chapter 4 outlines the concluding remarks of this work.

The last chapter provides the supporting references used in this dissertation.

In chapters 2 and 3, the glycyrrhetinic derivatives were numbered sequentially, with the first number identifying the chapter where they were included. The nomenclature of the new derivatives followed the guidelines established by the IUPAC Commission on the Nomenclature of Organic Chemistry. However, some compounds have been designated using their trivial name.

The main databases used for the bibliographic research were the Web of Science and the PubMed.

1. Introduction

1.1. Cancer

1.1.1. Cancer incidence and mortality

Cancer is a leading cause of death worldwide. According to GLOBOCAN 2020 an estimated 10.0 million cancer deaths and 19.3 million new cancer cases occurred in 2020. Considering both sexes, female breast cancer was the most diagnosed cancer followed by lung, colorectal, prostate and stomach cancers; lung cancer was the main cause of cancer death followed by colorectal, liver, stomach and female breast cancers (Fig. 1.1). Lung and female breast cancers were the most diagnosed cancers and leading causes of cancer death among men and women, respectively [1].

Global cancer incidence and mortality continue to rise due to the aging and growth of the world population and the increasing adoption of lifestyle choices associated with cancer in developed countries. In fact, cancer was the first or second leading cause of death before age 70 years in the countries with the highest levels of social and economic development, in 2019 [1].

In 2020, it was estimated that Europe had 22.8% of the total cancer cases and 19.6% of the cancer deaths, although it contains only 9.7% of the global population [1].

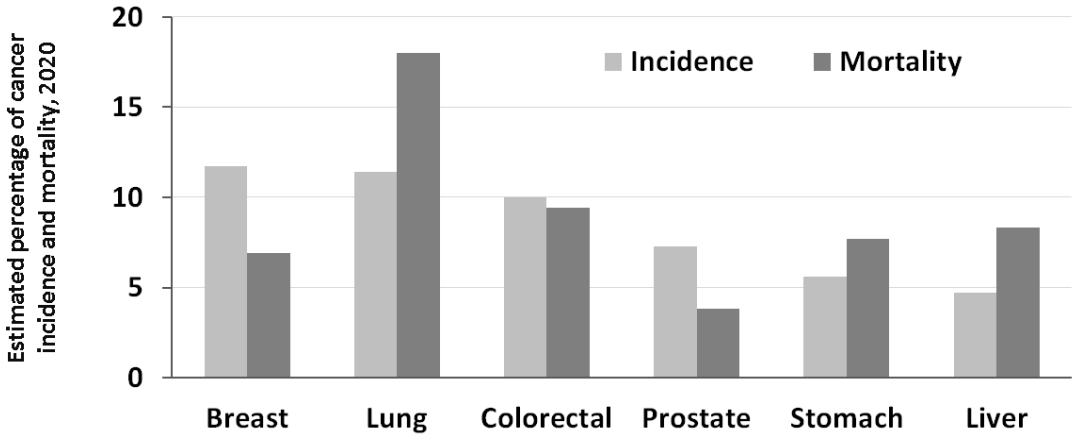

Figure 1.1 Estimated percentage of incidence and mortality of the major cancers worldwide in 2020.

1.1.2. Biology of cancer

Cancer is a group of diseases that results from unregulated proliferation of abnormal cells which have the potential to invade the adjacent tissues and spread to other parts of the body, creating new colonies called metastases [2].

The development of cancer is a multistep process involving mutation and selection for cells with progressively increasing ability to survive, proliferate and disseminate [3]. The mutant cells recruit and reprogram normal ones, as vascular or immune inflammatory cells, creating a microenvironment with signaling interactions between both. Mutant cells continue to evolve genetically and the reprogramed cells become active collaborators in the carcinogenic process. During this progressive transformation cells acquire the following hallmark capabilities: [4,5]

- **Sustaining proliferative signaling:** Cells become independent from external growth stimulation and acquire the ability to sustain chronic proliferation. The capability to sustain proliferative signaling is achieved in several ways:
    - Cells may produce their own growth factor ligands or induce their production by the surrounding cells;
    - Receptor signaling may be deregulated by elevation of the levels of receptors on the cell surface or by structural modifications of the receptors that enable ligand-independent firing;
    - Components of the signaling pathways operating downstream of receptors may be directly activated obviating the need of a ligand-receptor interaction.
- **Evading growth suppressors:** Cells acquire the ability to avoid antigrowth signals that often depend on tumor suppressor genes. This evasion is accomplished through the inactivation of those genes.
- **Resisting cell death:** The programmed cell death mechanisms of apoptosis, autophagy and programmed necrosis are a defense of the body that eliminates useless or abnormal cells [6]. Therefore, mutant cells need to become resistant to that mechanisms and they do so by deregulating their signaling pathways.
- **Enabling replicative immortality:** Normal cells pass through a finite number of replicative cycles. This limitation is due to the progressive erosion of telomeres which protect the ends of the chromosomes from deterioration or from fusion with

neighboring chromosomes. Since DNA polymerase is unable to completely replicate the 3' ends of DNA, small amounts of the terminal telomeric DNA sequence are lost during each doubling cycle. When telomere shortening reaches a critical point, cells are induced to become senescent; if that point is exceeded, the protection of the ends of chromosomal DNA is lost, end-to-end chromosomal fusions occur and the cells are induced to die. Mutant cells become capable to replicate unlimitedly through the maintenance of telomere length, which is achieved mostly through the upregulation of telomerase expression.

- **Evading immune destruction:** Cells become able to evade another defense of the body: the immune system. They manage to avoid their detection by the immune cells that would otherwise recognize them as abnormal cells and destroy them.
- **Reprogramming energy metabolism:** Cells switch their preferential source of energy from mitochondrial oxidative phosphorylation to glycolysis. Glycolysis allows the cells to proliferate under low oxygen conditions and provides metabolic substrates to the biosynthesis of macromolecules and organelles, required for the generation of new cells.
- **Inducing angiogenesis:** Cells become able to induce angiogenesis that generates the neovasculature required for tumor expansion. This induction is achieved through the upregulation of activators and the downregulation of inhibitors of angiogenesis [7].
- **Activating invasion and metastasis:** In the last stages of cancer development, cells acquire the ability to invade the adjacent tissues and spread to others parts of the body, creating new colonies called metastases. To accomplish that, cells modify their shape and their adhesion to other cells and to the extracellular matrix. Once detached from the primary tumor, they enter the blood and lymph vessels and are transported to new locations.

The acquisition of these functional abilities is possible thanks to two enabling characteristics: genome instability and tumor-promoting inflammation. Genome instability produces random mutations; some of those drive the development of the described hallmarks. Inflammation, caused by the immune cells of the microenvironment, promote tumor progression through several ways.

The knowledge provided by the study of the hallmarks is crucial for a better understanding of cancer development and for the discovery of targets for its treatment. Cancer treatment should be based on a combination of actions on different cellular targets, in order to avoid the development of adaptive resistance; cancer cells may use alternative signaling pathways within a hallmark or even become less dependent on a particular hallmark, improving their abilities on other(s).

1.1.2.1. Targeting cell cycle

The cell cycle is an ordered and regulated sequence of events that allows a cell to growth and divide, producing two daughter cells, genetically identical to itself. This cycle is divided into four phases: G1 (gap 1), S (DNA synthesis), G2 (gap 2) and M (mitosis). During the G1 phase, the cell grows and prepares for DNA replication that occurs in S phase. The S phase is followed by G2 phase, in which the cell get ready to enter mitosis (M phase). After a complete cell cycle, the daughter cells can undergo a new cell cycle or enter a quiescent state called G0 phase [8]. Quiescent cells can re-enter the cycle when stimulated by mitogenic growth factors.

Progression through the cell cycle is driven by cyclins and cyclin-dependent kinases (CDKs) (Fig. 1.2). CDK proteins alone are inactive and their levels remain constant along all the cycle. In contrast, their activating proteins, the cyclins, have an oscillatory pattern of expression. It is the sequence of synthesis and degradation of the different cyclins that drive the cell through the different phases of the cell cycle. The activity of CDKs can be negatively regulated by cyclin-dependent kinase inhibitors (CKIs). CKIs bind to the CDK-cyclin complexes and block their activity, which causes the arrest of the cell cycle [9-11].

Progression through each cell cycle phase and transition from one phase to the next are monitored by sensor mechanisms, called checkpoints. These checkpoints detect flaws in critical cell cycle events such as DNA replication and chromosome alignment on the mitotic spindle. When defects are detected, checkpoint pathways are activated inducing effectors, such as CKIs, to arrest the cell cycle. This halt allows the cell to repair the defect. After repair, progression through the cell cycle resumes. If the defect cannot be fixed, the cell is eliminated through apoptosis [12,13].

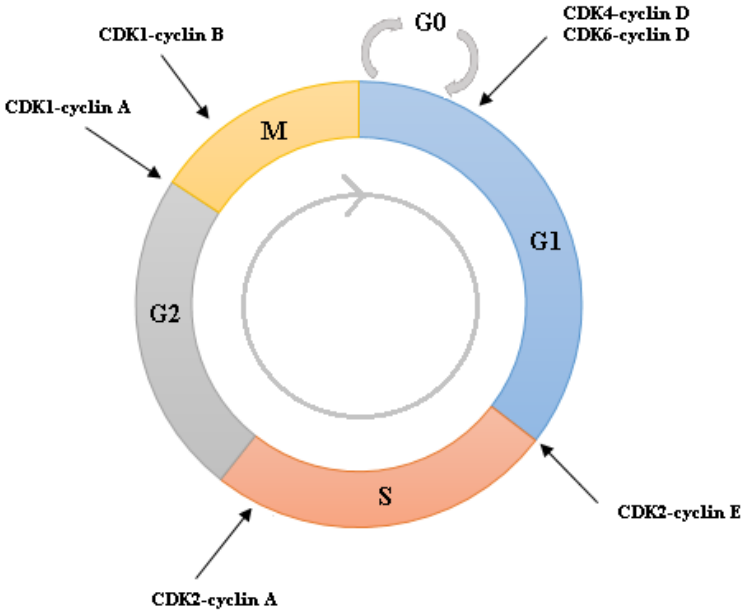

Figure 1.2 Simplified representation of cell cycle progression.

Deregulation of the cell cycle underlies the uncontrolled proliferation of tumor cells. In fact, many regulators that control the entry and progression through the cell cycle are altered by mutation or abnormalities in their expression, in cancer cells [13-15]. Tumorigenesis is frequently associated with:

- Alterations in upstream mitogenic pathways: Cells become independent of external growth signals to re-enter the cell cycle (as previously described, in the first hallmark of cancer) [5,13,16];
- Overexpression of CDKs and cyclins and loss of expression of CKIs [15,17];
- Loss of checkpoint control: Mutation or loss of the tumor suppressors that act as components of the cell cycle checkpoints leads to genomic and chromosomal instability. Cell cycle is not arrested in response to defects, which provide accumulation of further genetic alterations that contribute to tumor progression [8,13,14,16].

Since uncontrolled proliferation in cancer relies on altered cell cycle proteins, these regulators are considered attractive targets in cancer treatment. For instance, design of CDK inhibitors has become an area of great interest in oncology research [8,10,11,16,18].

1.1.2.2. Targeting apoptosis

Programmed cell death is a genetically regulated process of self-destruction that is crucial for morphogenesis, maintenance of tissue homeostasis and elimination of harmful cells. Apoptosis, autophagy and programmed necrosis are the three main types of programmed cell death, which are easily distinguished by their different morphological features [19-21].

Apoptosis is characterized by specific morphological and biochemical features. Morphologically, cells undergoing apoptosis present cell shrinkage, chromatin condensation, membrane blebbing and formation of apoptotic bodies. The main biochemical features of apoptosis are activation of a family of intracellular proteases called caspases, DNA and protein fragmentation, and phosphatidylserine externalization in the plasma membrane. The phosphatidylserine, moved to the outer layer of the cell membrane, functions as a recognition signal for neighbouring phagocytes to engulf apoptotic cells. During this process the plasma membrane remains intact and the rapid phagocytosis prevents secondary necrosis. Since apoptotic cells do not release their content, there is essentially no inflammatory reaction and therefore no damage is caused to the surrounding cells and tissues [19,22-25].

Apoptosis is a complex and regulated process that involves a cascade of events performed by caspases. These proteases are both the initiators and the executioners of the signaling pathways that lead to cell death. Caspases are synthesized as inactive proteins (procaspases). After an apoptotic stimuli, the initiator caspases auto-activate through proteolysis with the assistance of specific adapter molecules and once activated, they cleave the executioner caspases activating them in turn. It is the activity of these executioner caspases, on several cellular targets, that causes the morphological and biochemical changes observed in apoptotic cells and determines, ultimately, their death. The initiation of the apoptotic cascade involves two main pathways: the extrinsic or death receptor pathway that culminates in the activation of the initiator caspase 8 and the intrinsic or mitochondrial pathway that leads to the activation of the initiator caspase 9. Both pathways converge in the activation of the executioner caspases 3, 6 and 7 (Fig. 1.3) [22,23,26,27] .

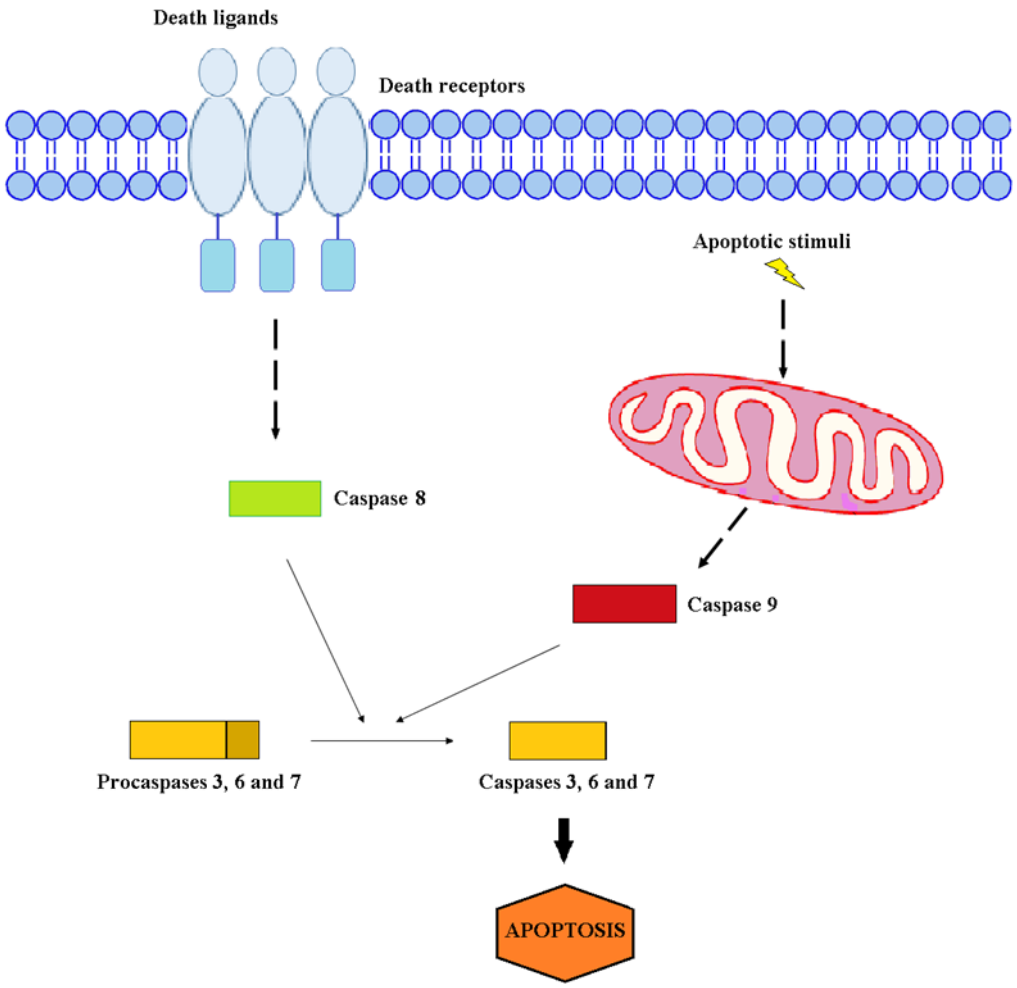

Figure 1.3 Simplified representation of the extrinsic and the intrinsic apoptotic pathways.

The intrinsic pathway is triggered by various intracellular stimuli, including hypoxia, severe oxidative stress, irreparable genetic damage and mitotic defects. All of these stimuli induce mitochondrial outer membrane permeabilization (MOMP); MOMP leads to the release of normally confined pro-apoptotic proteins, such as cytochrome c, second mitochondria-derived activator of caspases (SMAC) and Omi, from the mitochondrial intermembrane space to the cytoplasm. Once in the cytoplasm, cytochrome c binds to and activate an adapter protein, the apoptotic protease activating factor-1 (Apaf-1), which then recruits procaspase 9. Within this complex, called apoptosome, procaspase 9 is converted into caspase 9, which activates the executioner caspases. SMAC and Omi contribute to caspase activation by binding and neutralizing the inhibitors of apoptosis proteins (IAPs). Thereby, that pro-apoptotic proteins disrupt the inhibition of caspase 9 and executioner caspases by the IAPs (Fig. 1.4) [23,25,26,28-30].

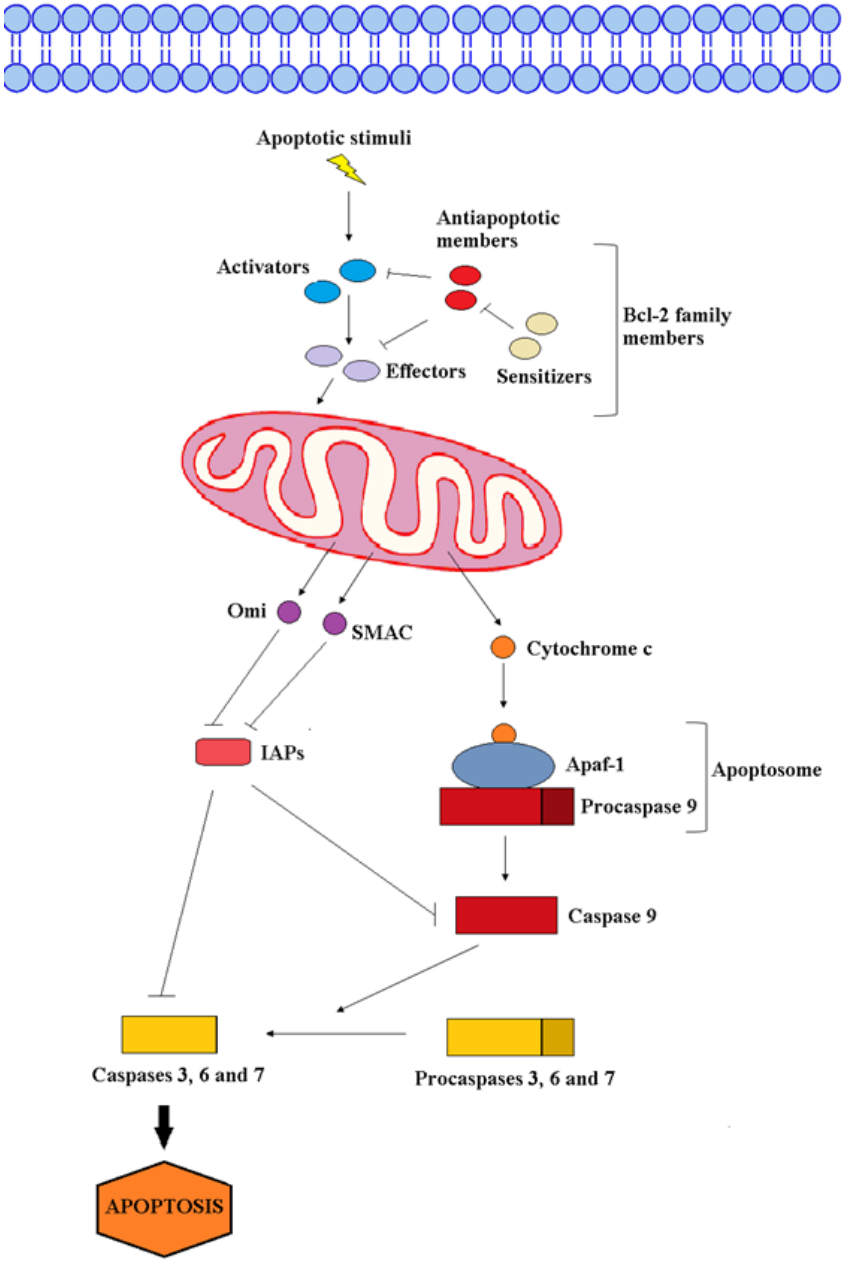

Figure 1.4 Representation of the intrinsic apoptotic pathway.

MOMP and consequent release of cytochrome c are regulated by the members of the B-cell lymphoma 2 (Bcl-2) family of proteins. These members can be divided into two groups: pro-apoptotic proteins and anti-apoptotic proteins. While pro-apoptotic proteins induce MOMP, the anti-apoptotic proteins prevent such alteration. The pro-apoptotic members can be further subdivided into three categories: effectors, activators and sensitizers. In response to an apoptotic stimulus, activator pro-apoptotic proteins,

such as Bid and Bim, induce the oligomerization of the effectors Bak and Bax within the outer mitochondrial membrane; these oligomers form pores that cause MOMP. The anti-apoptotic members, such as Bcl-2 and Bcl-xL, can interrupt this process in two ways: these proteins can sequestrate activators, preventing their interaction with the effectors, and can bind monomeric forms of effectors preventing their oligomerization. Sensitizer pro-apoptotic proteins can bind anti-apoptotic members inhibiting their binding to activators or effectors and can even displace them if they are already bound. It is the balance between the pro- and anti-apoptotic proteins that determines whether a cell undergoes cell survival or apoptosis (Fig. 1.4) [30,31].

The extrinsic pathway is activated by extracellular signals, the most common being those produced by immune cells, in response to cells that are infected or damaged. These signals are death ligands, such as Fas ligand (Fas-L), tumor necrosis factor alpha (TNFα) and TNF-related apoptosis-inducing ligand (TRAIL), which bind to and activate the TNF family of death receptors, present at the cell surface. Upon death receptor stimulation by its corresponding ligand, an adapter protein, such as Fas-associated death domain (FADD) and TNF receptor-associated death domain (TRADD), is recruited to the cytoplasmic domain of death receptor. Procaspase 8 then bind to the adapter protein, forming the death-inducing signaling complex (DISC). Within DISC, procaspase 8 is cleaved to initiator caspase 8, which in turn activate the executioner caspases. In some cells, caspase-8 also cleaves the pro-apoptotic activator Bid to its truncated form (tBid) to activate the mitochondrial intrinsic apoptotic pathway, thus amplifying the induction of apoptosis. The activation of caspase 8 can be inhibited by FADD-like interleukin-1β converting enzyme (FLICE) inhibitory protein (c-FLIP). This protein is an inactive procaspase 8 like molecule that can be recruited to the adapter protein, thereby inhibiting the binding and activation of caspase-8 (Fig. 1.5) [23,26,30,32].

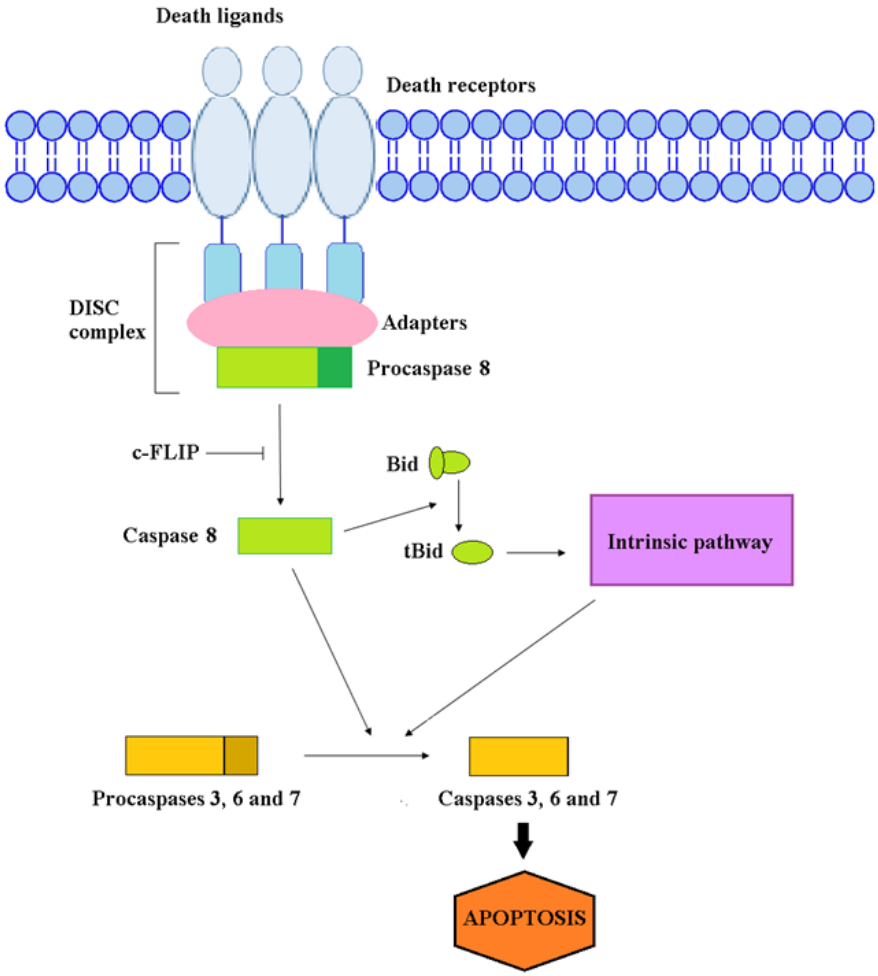

Figure 1.5 Representation of the extrinsic apoptotic pathway.

Defective apoptosis plays a central role in the development, progression and dissemination of cancer. In fact, the loss of apoptotic control leads to an unchecked proliferation of cells, allowing them to accumulate the genetic mutations that enable the multistep process of carcinogenesis [19,25,28,30,33]. Tumor cells suppress apoptosis through several mechanisms [25,26], including:

- Disruption in the balance between anti-apoptotic and pro-apoptotic members of the BCl-2 family (overexpression of anti-apoptotic proteins and/or downregulation of pro-apoptotic proteins);

- Impaired death receptor signaling: The extrinsic signaling can be impaired due to the downregulation or malfunction of death receptors, and the reduction of levels of death signals;
- Overexpression of IAP proteins;
- Downregulation of caspases or impairment of their function;
- Impaired p53 function: The p53 tumor suppressor protein is a critical DNA damage sensor that can engage apoptosis through both the extrinsic and intrinsic signaling pathways. The loss of its function is a common strategy employed by cancer cells to evade death. In fact, approximately 50% of human cancers bear P53 gene mutations and, in the majority of the remaining cases, its function is compromised by different mechanisms [5,34,35].

These mechanisms of evasion are also responsible for cancer resistance to many conventional anticancer drugs, as their action depends on an intact apoptotic machinery [26,30]. Despite that, targeting apoptosis remains a promising strategy for cancer treatment. The better understanding of the defects of the apoptotic pathways, provided by the intensive research in the last decades, is enabling a new approach in drug discovery: the development of new agents that aim to overcome those abnormalities and thus selectively restore apoptosis in cancer cells [21,25,26,30-32].

1.2. Natural products in cancer treatment

Nature has been a main source of healing products since ancient times [36]. Over the last century, natural products and their structural analogues have made a major contribution in drug discovery, especially in the treatment of cancer and infectious diseases [37,38]. Among all the approved drugs worldwide, between 1981 and 2019, approximately 50% were derived or inspired from nature. Over the same time frame, 63% of the new approved anticancer drugs were related to natural products and, if only the small molecules are considered, the percentage reaches to 84% [39].

Plants have been a prime source of highly effective anticancer drugs. Several isolated products from plants and/or their synthetically modified derivatives have become clinically useful agents for the treatment of different types of cancer. Currently, some of these drugs are still the mainstay of cancer therapy [40-43].

There are four major classes of plant-derived compounds in clinical use: vinca alkaloids, taxanes, podophyllotoxin derivatives and camptothecin derivatives (Table 1.1; Fig.s 1.6-1.9) [41-44].

Table 1.1 Approved drugs of the four major classes of plant-derived compounds for cancer therapy.

Anticancer agents	Plant source	Isolated product(s)	Year [39]	Derivatives	Year [39]	Mechanism of action
Vinca alkaloids	*Catharanthus roseus*	vincristine vinblastine	1963 1965	vindesine	1979	Tubulin-interactive agents: mitotic arrest
				vinorelbine	1989	
				vinflunine	2010	
Taxanes	*Taxus* species	paclitaxel	1993	docetaxel	1995	Tubulin-interactive agents: mitotic arrest
				cabazitaxel	2010	
Podophyllotoxin derivatives	*Podophyllum* species	podo--phyllotoxin	-	teniposide	1967	Topoisomerase II inhibitors: inhibition of DNA synthesis
				etoposide	1980	
				etoposide phosphate	1996	
Camptothecin derivatives	*Camptotheca acuminata*	camptothecin	-	irinotecan	1994	Topoisomerase I inhibitors: DNA damage
				topotecan	1996	

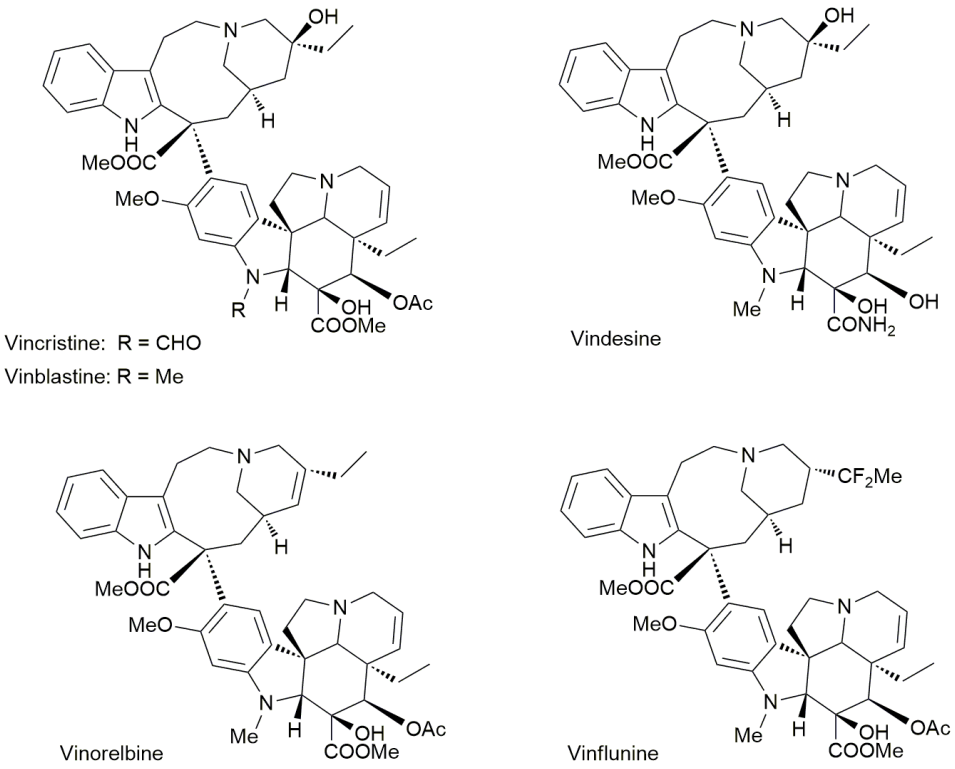

Figure 1.6 Chemical structures of vinca alkaloids.

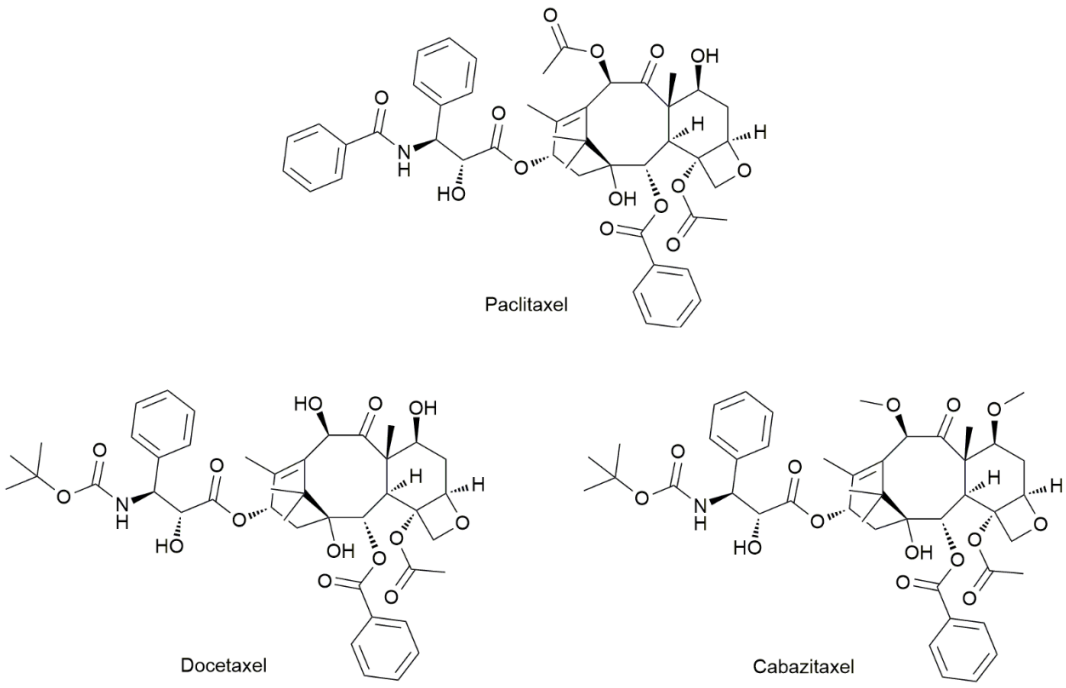

Figure 1.7 Chemical structures of taxanes.

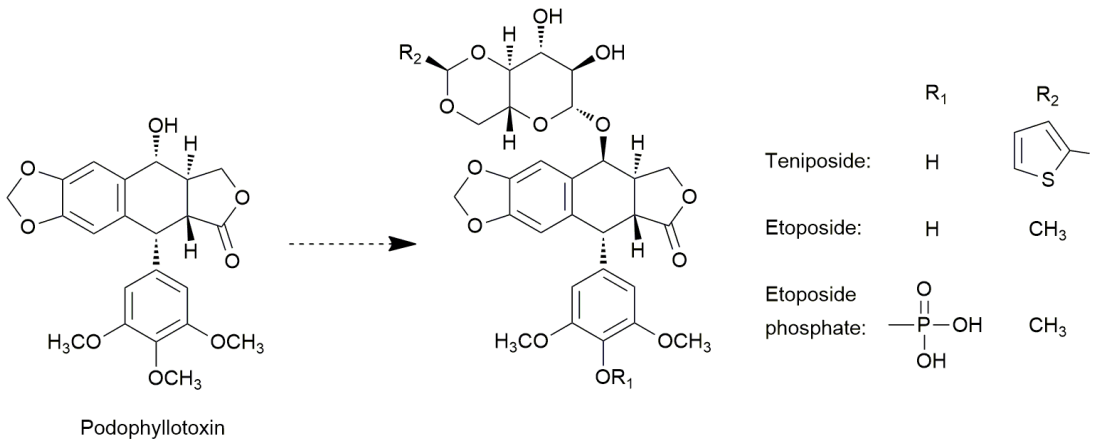

Figure 1.8 Chemical structures of podophyllotoxin and its derivatives.

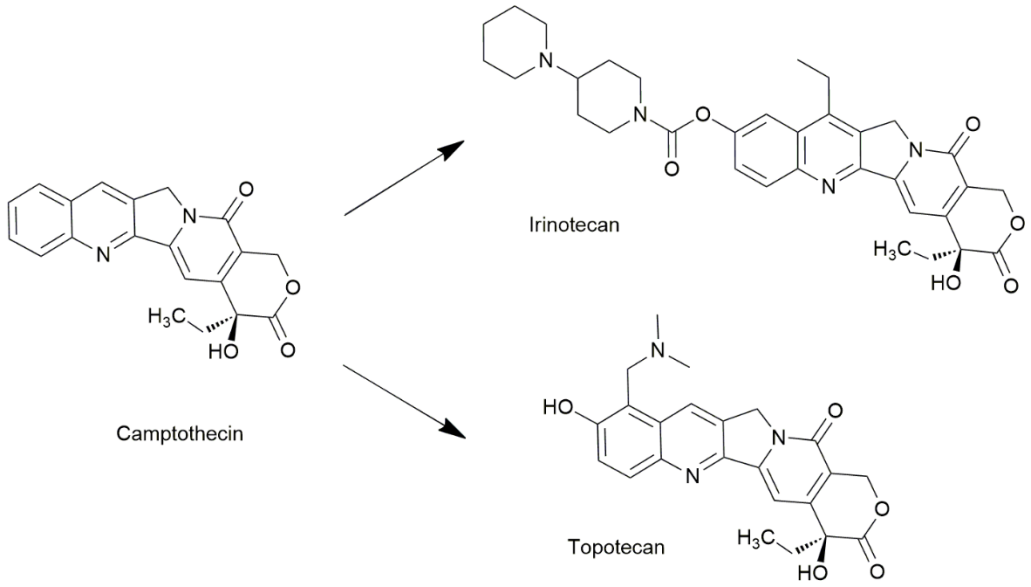

Figure 1.9 Chemical strutures of camptothecin and its derivatives.

Beside these, other plant-derived anticancer drugs from different classes, such as homoharringtonine (omacetaxine mepesuccinate) and ingenol mebutate, are also used clinically (Fig. 1.10) [43].

Many plant-based compounds are currently under preclinical and clinical trials, including new semisynthetic derivatives of the four major classes mentioned above. Some isolated products from plants, such as curcumin, epigallocatechin gallate and resveratrol, continue under evaluation, once they have shown a significant potential as anticancer agents in preclinical studies (Fig. 1.11) [30,42-44].

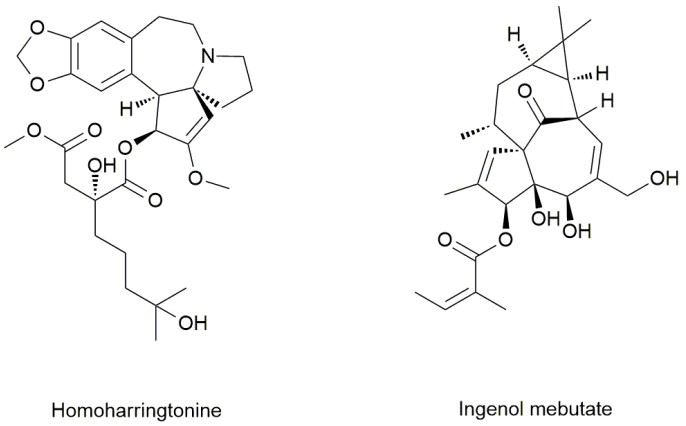

Figure 1.10 Chemical structures of homoharringtonine and ingenol mebutate.

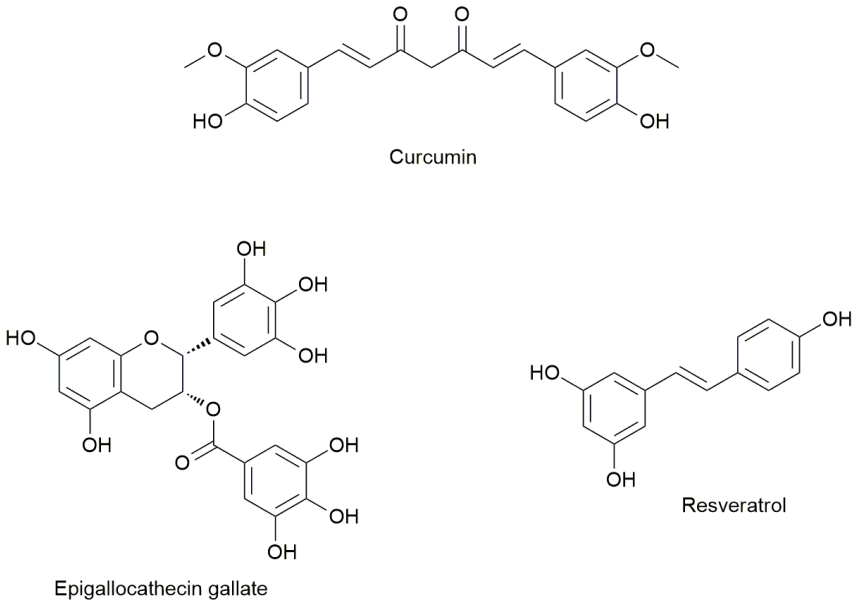

Figure 1.11 Chemical strucutures of curcumin, epigallocathecin gallate and resveratrol.

The interest of plant products in oncology extends beyond their innate anticancer activity. Several compounds exhibit promising properties as chemopreventive agents, sensitizers in multi-drug resistance and adjuvants in cancer treatment [43-45].

Natural product research for drug discovery reached a peak during the years 1970-1980. Its large success led to an increment of the patent activity, which created enthusiasm but also generated pressure to increase the number of new drug approvals.

Since investigation of natural products was associated with many inherent difficulties, pharmaceutical companies shifted its focus toward synthetic compounds. Through the 1990s, the development of combinatorial chemistry provided the synthesis of large libraries of compounds suitable for high throughput screening (HTS) platforms. Expectations that HTS screening of those vast libraries would prove to be more efficient and cost-effective than traditional approaches to drug discovery led to the abandonment or de-emphasis of natural product research. However, the efforts made in that direction have not resulted in the expected increment in the rate of discovery of new drugs. In fact, the declining numbers of new drug approvals revealed an opposite trend [37,46-49].

This scenario revitalized the interest in natural product-based drug discovery over the last decade. Although the reasons for the declining trend are complex, one important aspect is that the synthetic compound libraries lacked the diversity and complexity of the products synthesized by nature. Furthermore, the structures of these products have been optimized, through natural evolution, for specific biological functions, such as binding to specific target proteins or other biomolecules. The structural diversity and target specificity of natural products make them more likely to provide new leads for drug development, compared to synthetic compounds [36,37,46,48,50-52].

The target-based approach for drug discovery, adopted in the 1990s, did not yield the optimal outcomes that were expected in cancer therapy. Although targeted therapies greatly improved the treatment of a few forms of cancer, the benefit for the vast majority of cancers was disappointing. The complexity of their biology turn them not dependent on a single target. Additionally, most cancers were shown to activate multiple signaling pathway redundancies and adaptive mechanisms that either render them resistant to targeted therapies or facilitate acquired resistance after only few months of treatment. Therefore, a multi-target approach is needed to face the complexity of cancer diseases. In this context, the ability of natural compounds to impact on multiple signaling pathways has also contributed to the renaissance of their interest in drug discovery, for the development of multi-target agents [44,47,53].

The technical barriers to the investigation of natural products, which influenced pharmaceutical companies to withdraw from the field, are being addressed by technological advances. Natural products present challenges such as sustainable supply in adequate quantities, isolation, characterization and elucidation of the mechanisms of

action. However, several scientific and technological developments including improved analytical and screening tools, innovative biotechnology approaches, novel computational techniques, omics studies and automation are overcoming such hurdles and facilitating the identification of new leads for drug discovery [38,47,48,54-56].

Although isolated products are valuable lead compounds, they rarely can serve directly as drugs in clinical practice. Most natural products have limitations such as poor bioavailability or toxicity and need to be optimized. Semisynthesis is an essential strategy that provide structural analogues with a better profile. Semisynthetic processes are able to generate molecules with higher potency and selectivity, reduced toxicity and side effects, and improved physicochemical and pharmacokinetic properties [37,50,57-59].

Nature will remain a crucial source of new scaffolds for drug development. Together with the aspects described above, only a tiny portion of the huge biodiversity of the planet has been yet explored and the existing ethnopharmacological information is still poorly studied. Thus an integrated and interdisciplinary approach is required to harvest the full potential of natural products [38,43,48,60,61].

1.3. Pentacyclic triterpenoids

Terpenes are the largest and most diverse group of natural products. These compounds are widely distributed in plants and are an integral part of the human diet. Terpenes display a wide range of biological and pharmacological activities [62-64].

Terpenes are featured by the repetition of isoprene C_5H_8 units, resulting from condensation of two building blocks: isopentenyl diphosphate (IPP) and dimethylallyl diphosphate (DMAPP). These precursors can arise from two pathways: the mevalonic acid (MVA) pathway and the methylerythritol phosphate (MEP) pathway. Based upon the number of isoprene units, terpenes are commonly classified as monoterpenes (C10), sesquiterpenes (C15), diterpenes (C20), triterpenes (C30), tetraterpenes (C40) and polyterpenes (C > 40) [65-67].

Pentacyclic triterpenoids (PTs) are oxo-functionalized triterpenes derived from the intramolecular condensation reactions of oxidosqualene, which are promoted by the enzymes oxidosqualene cyclases. Lupeol synthase, α-amyrin synthase and β-amyrin synthase are the oxidosqualene cyclases that convert oxidosqualene into lupeol, α-amyrin and β-amyrin, respectively. Subsequent oxidations of these compounds afford the well-known PTs betulin, betulinic acid, ursolic acid, oleanolic acid and glycyrrhetinic acid (Fig. 1.12) [65,68,69].

PTs have been often reported to exhibit a wide spectrum of pharmacological activities such as anticancer, anti-inflammatory, antiviral, antibacterial, antidiabetic, cardiac- and hepatoprotective effects, among others [70-73]. Regarding to their anticancer activity, PTs have been shown to behave as multifunctional agents, impacting on multiple signaling pathways and molecular targets, which increase their interest as potential leads for the development of new anticancer drugs [74-77].

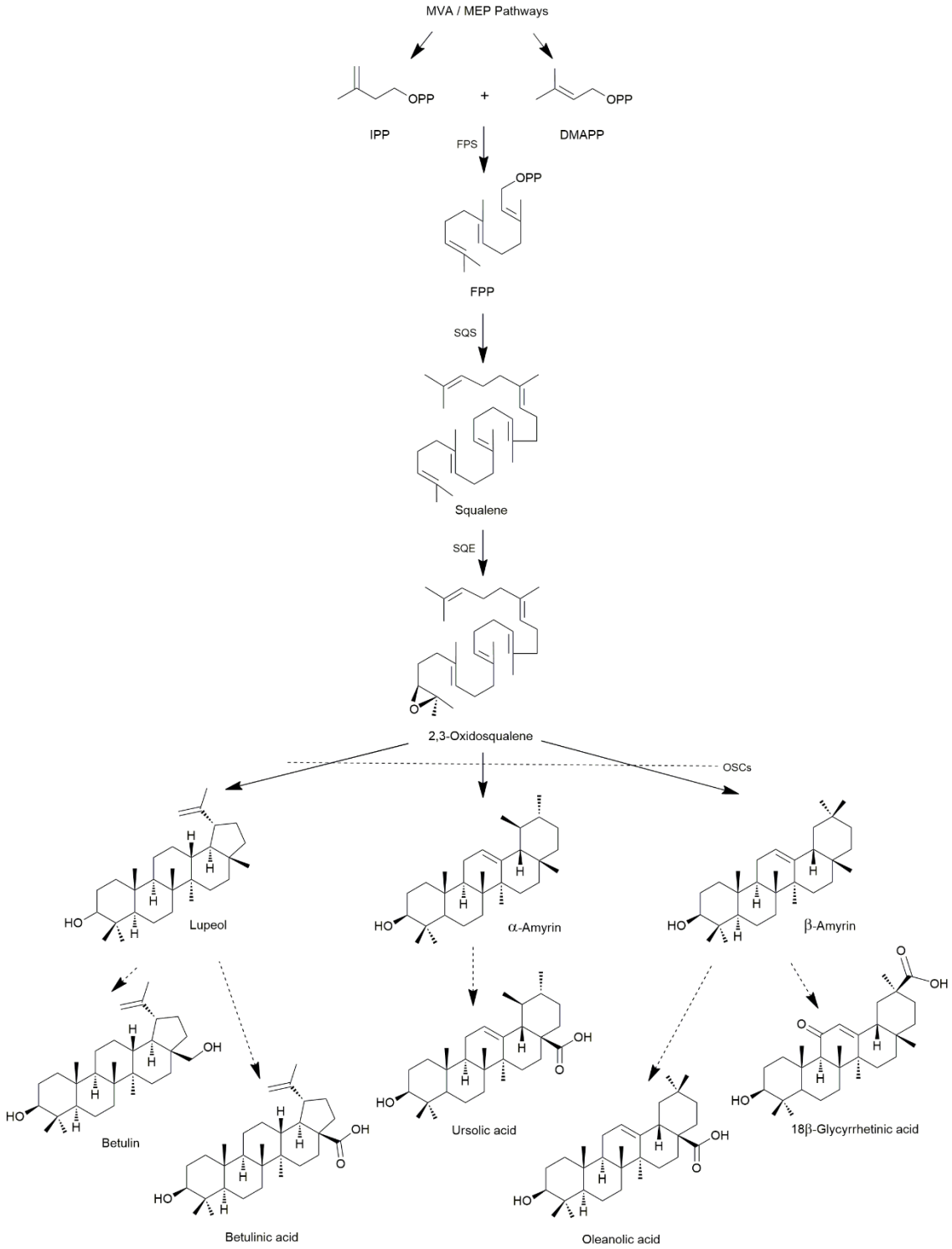

Figure 1.12 Simplified representation of biosynthetic pathways affording pentacyclic triterpenoids. Abbreviations: MVA, mevalonic acid; MVE, methylerythritol phosphate; IPP, isopentenyl diphosphate; DMAPP, dimethylallyl diphosphate; FPS, farnesyl diphosphate synthase; FPP, farnesyl diphosphate; SQS, squalene synthase; SQE, squalene epoxidase; OSCs, oxidosqualene cyclases.

1.4. Glycyrrhetinic acid

Glycyrrhetinic acid (3β-hydroxy-11-oxo-olean-12-en-30-oic acid) (**GA**) (Fig. 1.13) is the aglycone of glycyrrhizin, a major PT obtained from the roots of licorice (*Glycyrrhiza* species) in high yields up to 24%. Licorice roots have been used worldwide as an herbal remedy for many ailments, since at least 500 BCE [78-81].

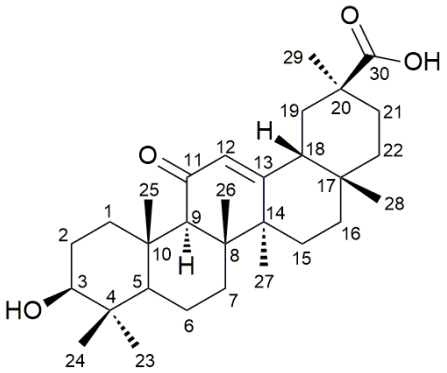

Figure 1.13 Chemical structure of 18β-glycyrrhetinic acid.

1.4.1. General activities

GA exhibits a broad range of pharmacological activities, such as anticancer, anti-inflammatory [82,83], antibacterial [84,85], antiviral [86,87], antiulcer [88] , antidiabetic [89,90], antimetabolic syndrome [73,91], hepatoprotector [92-97], antiallergic [98,99] and immunomodulatory [100-102] effects. **GA** has been found to exert anti-inflammatory effects in several conditions including skin disorders [103] , asthma [99,104] and cancer [105-107]. Immunomodulatory properties of **GA** have been also associated to its anticancer effects [100,102].

1.4.2. Anticancer activity

The anticancer activity of **GA** has been reported in several cancer cell lines and has also been observed in animal models [75,100,107-110]. This activity has been associated with several mechanisms of action including:

- **Chemoprevention**

  Chemoprevention of cancer is defined as the use of external agents to prevent, suppress or reverse the multistep carcinogenic process [111,112].

  GA has been shown to be a chemopreventive agent in several animal models, namely against oral, skin, liver and gastric cancers. **GA** showed to prevent tumor formation and to restore detoxification enzymes in a model of 7,12-dimethylbenz(a)anthracene (DMBA) induced hamster buccal pouch carcinogenesis [113]. **GA** also inhibited 12-*O*-tetradecanoylphorbol-13-acetate mediated oxidative stress and tumor promotion in DMBA-initiated skin of mice [114]. **GA** was tested in a model of 2-acetylaminofluorene-induced tumor formation and toxicity in the liver of Wistar rats; its protective effects against that hepatic carcinogen were exerted via attenuation of oxidative stress, inflammation and hyperproliferation [107]. **GA** was also studied in an orthotopic mice model of hepatocellular carcinoma (HCC); it was found that **GA** plays a protective role in HCC development by reversing hepatic stellate cell-mediated immunosuppression in the tumor microenvironment [100]. A model of transgenic mice, which develops inflammation-associated tumors in stomach, was used to assess the effects of **GA** on inflammation and gastric tumor growth; **GA** showed to exert protective effects against inflammation microenvironment in gastric tumorigenesis, targeting the prostaglandin E2-EP2 receptor-mediated arachidonic acid pathway [105]. In another transgenic mice model, **GA** also demonstrated to prevent gastric tumorigenesis by inhibiting the Toll-like receptor 2-accelerated energy metabolism [110].

- **Inhibition of cell proliferation**

  GA has a proven antiproliferative activity against many human cancer cells, including the breast cancer cell lines MCF7 and MDA-MB-231 [115-119], the lung cancer lines A549 and NCI-H460 [118,120,121], the colon and colorectal cancer lines DLD-1, HCT-116, HCT-8, SW480, SW620, LoVo and HT-29 [109,118], the prostate cancer cell lines DU-145 and LNCaP [116,122], the gastric cancer cell lines KATO III, BGC823 and SGC7901

[108,123,124], the liver cancer cell lines HepG2 and HLE [116,123,125], the cervix and uterus cancer cell lines SiHa and HeLa [126,127], the ovarian cancer cell lines OVCAR-3, SK-OV-3 and A2780 [118,128-130], the bladder cancer cell line NTUB1 [131] , the thyroid cancer cell lines 8505C and SW1736 [118], the melanoma cell line 518A2 [118], the leukemia cell line HL-60 [123,132,133], the salivary gland cancer cell A253 [118], the hypopharyngeal carcinoma cell line FaDu [118], the epidermal cancer cell line A431 [118] and the liposarcoma cell line LIPO [118].

- **Cell cycle arrest**

  GA induced G1 phase arrest in HepG2, A549, NCI-H460, HeLa and A2780 cells [125,127,134,135]. In A549 and NCI-H460 cells, the cell cycle arrest was induced through the endoplasmic reticulum (ER) stress pathway, with related upregulation of the CKIs p18, p16, p27 and p21 and inhibition of cyclins D1, D3 and E and CDKs 4, 6 and 2 [134]. In HeLa cells, the arrest was associated to an increment in reactive oxygen species (ROS) production [127]. In A2780 cells, it was observed a downregulation of cyclin D1 [135].

  GA triggered G2 phase arrest in BGC823 and SGC7901 by upregulation of p21 and downregulation of cdc2 and cyclin B1 [108] (Table 1.2).

- **Induction of apoptosis**

  GA induced apoptosis in several cancer cells, including MCF7 [117,119], SiHa [126], HeLa [127], LoVo, SW620 and SW480 [109], BGC823 and SGC7901 [108], KATO III [123], HL-60 [123], HepG2 [106,125], HLE [123], NCI-H460 [121] and A2780 [129,135] (Table 1.2).

  Apoptosis was achieved through modulation of various signaling pathways and molecular targets in the different cell lines. **GA** modulated the Akt/FOXO3 pathway [117] and suppressed the PI3K and STAT3 pathways [109], inhibited the prosurvival protein kinase C (PKC) α/βII [121], activated the pro-apoptotic proteins c-Jun NH_2-terminal kinase (JNK) [121,135] and p38 [135], upregulated Fas and FasL [129], increased the levels of the pro-apoptotic proteins Bim [117], Bax [106,126] and Bid [108],

decreased the levels of the anti-apoptotic proteins Bcl-2 [106,121,125,126], Bcl-xL [121,125], survivin [109] and cyclins D1 and E [121], increased the intracellular Ca^{2+} concentration [119], raised the production of reactive oxygen species (ROS) [106,126,127] and nitric oxide (NO) [106], depleted glutathione [126], promoted the loss of mitochondrial membrane potential [106,117,126,135], induced cytochrome c release [117,126] and activated caspases 9 [106,117,121,125,127,135], 8 [125] and 3 [106,121,126,127,135], and poly-ADP-ribose polymerase (PARP) [106,109,121,135].

Among the targets mentioned above, there are elements of both intrinsic and extrinsic pathways of apoptosis.

Table 1.2 Anticancer activity of GA, targeting cell cycle and apoptosis, in different cancer cell lines.

Cancer type	Cell line	Mechanism of action / Molecular targets	Ref.
Breast	MCF7	Inhibition of proliferation Induction of apoptosis: ↑ intracellular Ca^{2+} concentration	[119]
		Inhibition of proliferation Induction of apoptosis: ↓ Akt kinase, ↑ FOXO3a, ↑ Bim, loss of mitochondrial membrane potential, cytochrome c release, activation of caspase 9	[117]
Cervix and uterus	SiHa	Inhibition of proliferation Induction of apoptosis: ↑ Bax, ↓ Bcl-2, MOMP, cytochrome c release, activation of caspase 3 ↑ROS, ↓ glutathione	[126]
	HeLa	Inhibition of proliferation G1-phase arrest Induction of apoptosis: activation of caspases 9 and 3, ↑ ROS	[127]
Colorectal	LoVo SW620 SW480	Inhibition of proliferation Induction of apoptosis: suppression of PI3K and STAT3 pathways, ↓survivin, activation of PPAR Inhibition of invasion and migration	[109]

Cancer type	Cell line	Mechanism of action / Molecular targets	Ref.
Table 1.2 continued			
Gastric	BGC823 SGC7901	Inhibition of proliferation G2-phase arrest:↑ p21, ↓cdc2 and ↓cyclin B1 Induction of apoptosis: Bid translocation to mitochondria	[108]
	KATO III	Inhibition of proliferation Induction of apoptosis	[123]
Leukemia	HL-60	Inhibition of proliferation Induction of apoptosis	[123]
Liver	HepG2	Inhibition of proliferation G1-phase arrest Induction of apoptosis: activation of caspases 8 and 9, ↓Bcl-2 and Bcl-xL, = Bax and Bak	[125]
		Inhibition of proliferation Induction of apoptosis: ↑ROS, ↑NO, loss of mitochondrial membrane potential, ↓Bcl-2, ↑Bax, activation of caspases 9, 3 and PARP	[106]
	HLE	Inhibition of proliferation Induction of apoptosis	[123]
Lung	NCI-H460	Inhibition of proliferation. Induction of apoptosis: ↓ Bcl-2, Bcl-xL, cyclins D1 and E, inhibition of PKCα/βII and activation of JNK, caspases 9 and 3 and PARP	[121]
	A549 NCI-H460	Inhibition of proliferation G1-phase arrest: ER stress pathway, ↑p18, p16, p27 and p21, ↓ cyclins D1,D3 and E and ↓CDKs 4, 6 and 2	[134]
Ovarian	A2780	Inhibition of cell proliferation Induction of apoptosis: ↑ Fas and ↑ FasL	[129]
		Inhibition of cell proliferation G1-phase arrest: ↓cyclin D1 Induction of apoptosis: loss of mitochondrial membrane potential and activation of p38, JNK, caspases 9, 3and PARP	[135]

- **Suppression of angiogenesis**

  Li *et al* investigated the potential role of **GA** in angiogenesis through *in vitro*, *ex vivo* and *in vivo* studies. *In vitro* studies showed that **GA** inhibited proliferation, migration, invasion and tube formation in human umbilical vein endothelial cells (HUVECs). **GA** also inhibited the vascular endothelial growth factor (VEGF)-activation of major receptors and enzymes involved in angiogenesis such as VEGFR2, mTOR, Akt, ERK1/2, MEK1/2, p38 and JNK1/2 in HUVECs. *Ex vivo* experiments showed that **GA** inhibited microvessel sprouting in a rat aortic ring model. *In vivo* assays showed that **GA** inhibited the formation of new vessels in zebrafish and mouse Matrigel plug models. This work showed that **GA** has a promising antiangiogenic activity [135].

- **Inhibition of invasion and metastasis**

  GA inhibited the metastasis of LNCaP cells through downregulation of matrix metalloproteinase (MMP)-9 and VEGF via inhibition of PI3K/Akt-dependent NF-κB activity [136]. In MDA-MB-231 cells, **GA** inhibited MMP-2 and MMP-9 expression by impairing the p38-AP1 signaling axis [137]. **GA** showed to reduce migration and invasion of colorectal cancer cells through suppression of PI3K and STAT3 pathways [109]. **GA** also reduced migration and invasion of SGC-7901 cells through the ROS/PKCα/ERK signaling pathway and suppressed MMP-2 and 9 activities [124].

- **Reversal of multidrug resistance**

  GA showed to effectively inhibit P-glycoprotein and multidrug resistance protein 1 in cancer cell lines that overexpress those anticancer drug efflux transporters [138,139].

Considering its different anticancer effects, **GA** has shown to behave as a multifunctional agent. This feature has generated scientific interest in **GA** as a scaffold for the development of new derivatives for potential cancer treatment.

1.4.3. Semisynthetic derivatives with anticancer activity

Several structural modifications have been performed on the **GA** scaffold with the aim to improve its anticancer activity. Many of those were simple modifications on the C3-alcohol and on the C30-carboxylic acid; some derivatizations have also involved the positions C2 on A-ring and the positions C11 and C12 on C-ring. Some of the main derivatives that have been prepared are discussed below.

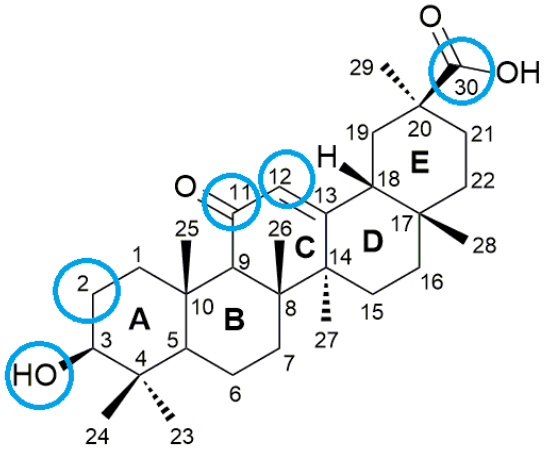

Figure 1.14 Main positions of the structural modifications performed on the **GA** scaffold.

Csuk *et al.* developed a series of works in which simple modifications at C3 and C30 produced **GA** derivatives with increased potency and enhanced ability to induce apoptosis [118,140-143] (Fig. 1.15). Chemical modifications at C30 have afforded compounds **1.1**-**1.3** with greater ability to induce apoptosis in the lung cancer cell line A549 than **GA**. These derivatives also showed higher cytotoxicity than **GA** against several tumor cell lines. However, cytotoxic assays against NIH3T3 cells (non-tumor mouse fibroblasts) demonstrated that compounds **1.2** and **1.3** displayed only slightly selectivity towards cancer cells [140]. Esters **1.4**-**1.6** with diverse modifications at C3 have also shown greater cytotoxicity and ability to induce apoptosis [118,141,142]. Compound **1.6**, in particular, has demonstrated an up to 140-fold better selectivity towards tumor cells than parent **GA** [142]. The combination of an ester group at C30 and an amino acid moiety at C3 provided derivatives with higher cytotoxicity and selectivity [143]. Within this group of derivatives, compounds **1.7** and **1.8** displayed the highest cytotoxicity against the studied tumor cell lines.

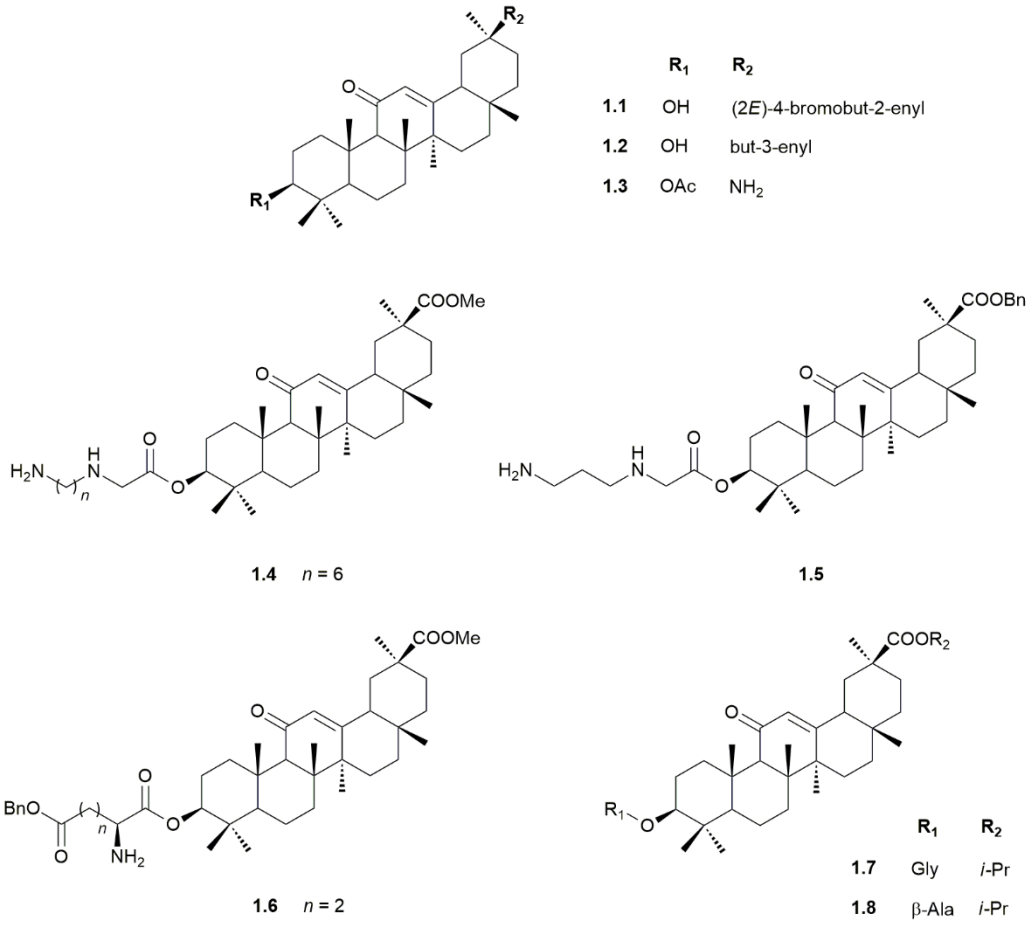

Figure 1.15 GA derivatives **1.1-1.8**.

Zhou and coworkers explored the effect of different bonding modes at C3 on the anticancer activity. In this study two series of derivatives have been prepared: a GA-OH series with esters and a GA-NH_2 series with amide linkages. The screening against various tumor cells showed that all derivatives **1.9-1.24** were more potent than **GA** and that all compounds of the GA-NH_2 series **1.17-1.24** were more potent than compounds of the GA-OH series **1.9-1.16**. Among all the prepared compounds, derivative **1.18** was the most active with an IC_{50} value of 2.11 μM against A549 cells (**GA**: IC_{50} > 40 μM). Compound **1.18** also showed to induce apoptosis and arrest cell cycle at S phase in those cells (Fig. 1.16) [144].

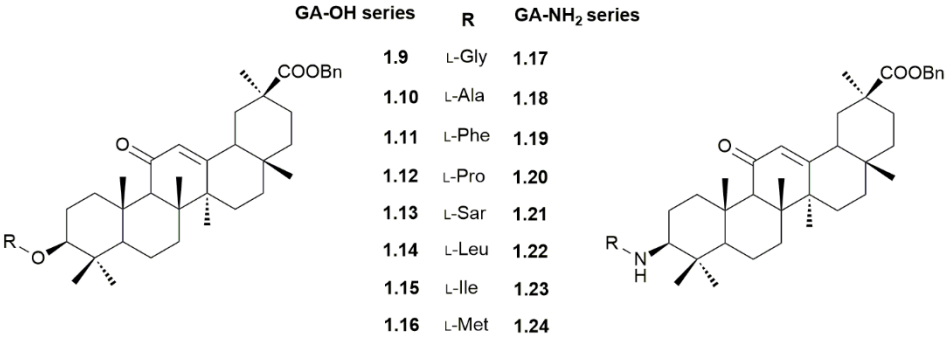

Figure 1.16 GA derivatives **1.9-1.24**.

Replacement of the C3 hydroxyl group of **GA** with an alkoxyimino group increased the antiproliferative activity in HL60 cells. Compounds **1.25** and **1.26** with an esterified carboxylic acid were the most potent inhibitors of HL60 cell growth, however, compounds **1.27** and **1.28** were the most effective inducers of apoptosis (Fig. 1.17) [133].

A series of furoxan-based NO-releasing derivatives of **GA** were prepared and tested against HCC cell lines. Derivatives **1.29-1.33** have proved to be highly cytotoxic (**1.29-1.33**: IC_{50}: 0.25–1.10 μM against BEL-7402 cells and 1.32–6.78 μM against HepG2 cells; **GA**: IC_{50} > 50 μM against both cell lines). The cytotoxicity of the compounds seems to be related with NO production (Fig. 1.17) [145].

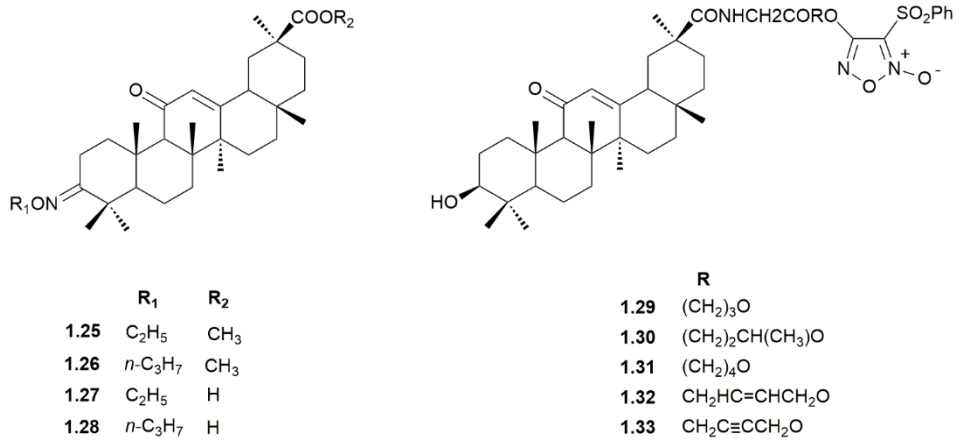

Figure 1.17 GA derivatives **1.25-1.33**.

Simple modifications performed on the **GA** scaffold also improved its anticancer activity as an inhibitor of the proteasome [146-148]. Compound **1.34**, glycyrrhetinic acid 3-*O*-isophthalate, was approximately 100-fold more potent than **GA** to inhibit the human 20S proteasome (Fig. 1.18) [146]. Spin-labeled **GA** derivatives were prepared and evaluated for their ability to inhibit the growth of four tumor cell lines. Among these, compound **1.35** bearing a tryptophan amino acid moiety and a piperidine nitroxyl radical, was the most active derivative in inhibiting the growth of cancer cells, being 5-fold more potent than **GA**. In a mechanistic study, compound **1.36** was proven to be a slightly better 20S proteasome inhibitor (Fig. 1.18) [147]. Lallemand *et al.* synthesized a series of **GA** amides by coupling **GA** with various amines. Compound **1.37** appeared to be the most potent derivative, with single-digit micromolarity IC_{50} values in a panel of eight cancer cell lines. This compound has also demonstrated marked anti-proteasome and anti-kinase activity (Fig. 1.18) [148].

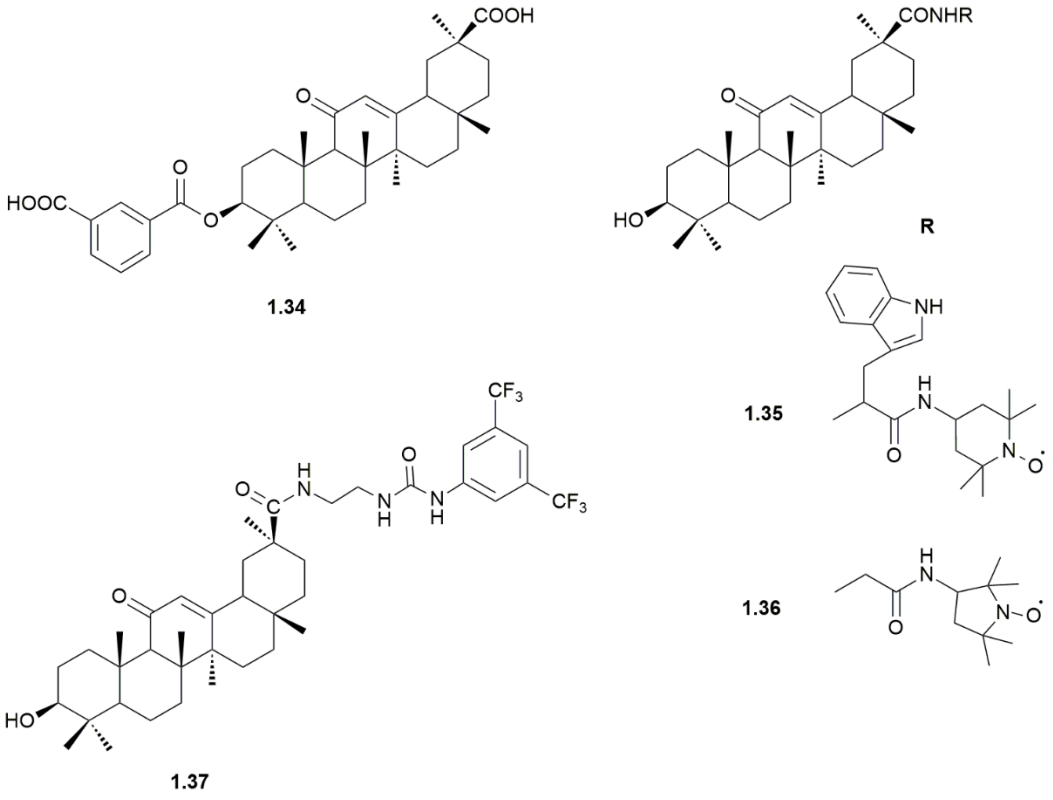

Figure 1.18 GA derivatives **1.34-1.37**.

Conjugation of two anticancer compounds is a drug design strategy that aim to produce a single agent with increased potency or reduced side effects and drug resistance development. Some simple hybrid entities have been prepared through the conjugation of **GA** with other bioactive compounds. Dehydrozingerone is a phenolic natural compound with antitumor-promoting activity. The esterification of **GA** with dehydrozingerone resulted in compound **1.38**, which demonstrated potent cytotoxic activity toward different cancer cell lines (Fig. 1.19) [149]. **GA** was also conjugated with paclitaxel affording compound **1.39** (Fig. 1.19). This conjugation, however, did not improve the antitumor activity [150]. The anticancer drug 5-fluorouracil, whose clinical usefulness is limited due to its adverse effects, was conjugated with PT's. Among the prepared hybrids, compound **1.40** (Fig. 1.19) showed increased potency and was the only hybrid that exhibited good antiproliferative activities against all the tested multidrug-resistant cancer cell lines. Furthermore, compound **1.40** showed to induce intracellular calcium influx, generate ROS, arrest the cell proliferation at the G1-phase, and activate caspase 8, in A549 cells [151].

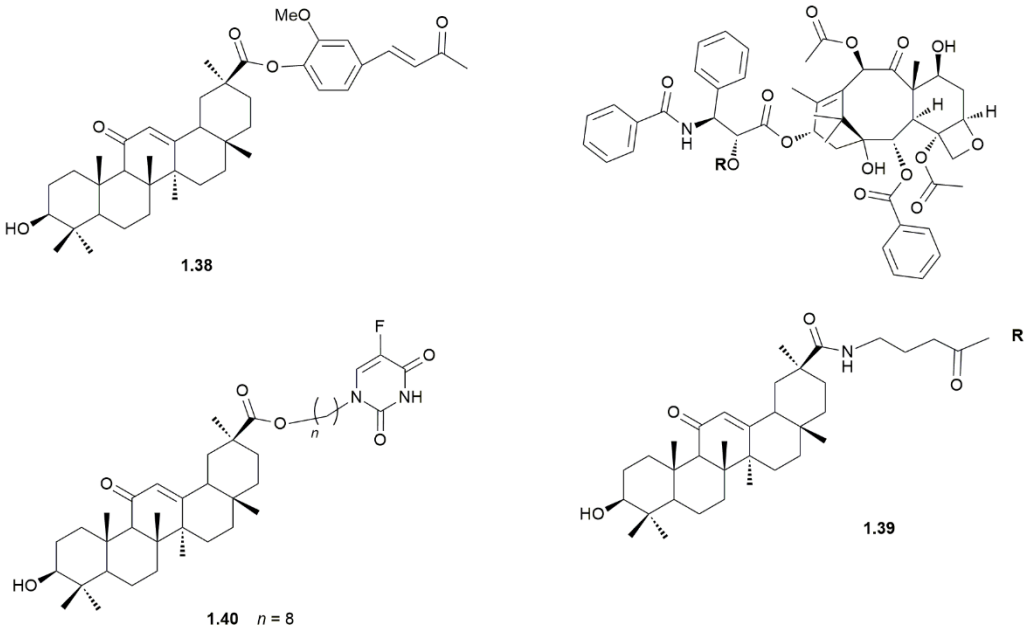

Figure 1.19 GA derivatives **1.38-1.40**.

Li *et al*. designed and synthesized a library of **GA** derivatives in which the C30-carboxyl group was attached to lipophilic fragments (ferulic acid analogues) and the C-3 hydroxyl was coupled to amino acids (L-methionine or L-selenomethionine). In addition to its lipophilic contribution, ferulic acid is itself a bioactive natural compound with anticancer properties. The cytotoxic activity of these derivatives was screened against two human breast cancer cell lines (MCF-7 and MDA-MB-231) and one non-tumor human retinal pigment epithelial cell line (hTERT-RPE1). Most of the compounds (**1.41-1.56**, Fig. 1.20) showed much stronger activity than **GA** against the two cancer cell lines, and relatively lower cytotoxic activity against the non-tumor cells. Of these, the most potent was compound **1.42**, which was obtained by the esterification at C30 with ferulic acid methyl ester, along with the coupling with the amino acid L-selenomethionine at C3 (**1.42**: IC_{50}: 1.88 μM against MCF-7cells and 1.37 μM against MDA-MB-231 cells; **GA**: IC_{50}: 75.66 μM against MCF-7cells and 84.70 μM against MDA-MB-231 cells) [115].

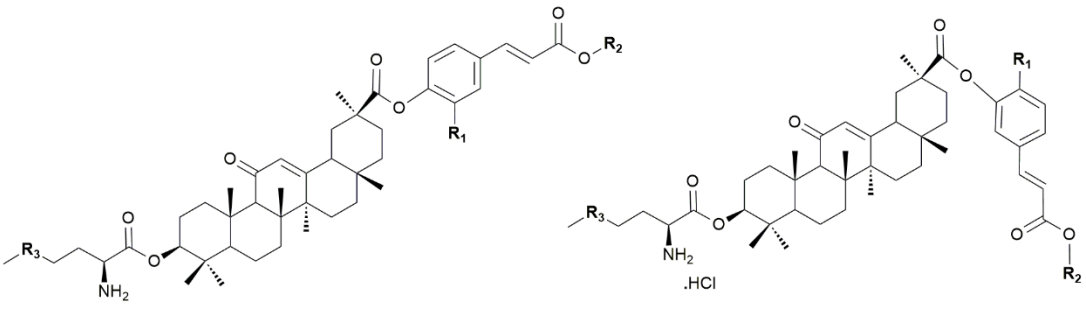

	R_1	R_2	R_3
1.41	OCH_3	CH_3	S
1.42	OCH_3	CH_3	Se
1.43	OCH_3	CH_2CH_3	S
1.44	OCH_3	CH_2CH_3	Se
1.45	H	CH_3	S
1.46	H	CH_3	Se
1.47	H	CH_2CH_3	S
1.48	H	CH_2CH_3	Se

	R_1	R_2	R_3
1.49	OCH_3	CH_3	S
1.50	OCH_3	CH_3	Se
1.51	OCH_3	CH_2CH_3	S
1.52	OCH_3	CH_2CH_3	Se
1.53	H	CH_3	S
1.54	H	CH_3	Se
1.55	H	CH_2CH_3	S
1.56	H	CH_2CH_3	Se

Figure 1.20 GA derivatives **1.41-1.56**.

Many of the current anticancer drugs contain a piperazine ring as part of their molecular structure. In this regard, Zhao and coworkers prepared a series of PTs derivatives bearing *O*-[4-(1-piperazinyl)-4-oxo-butiryl moiety, which was attached to **GA** at the C3 of its backbone (**1.57**, Fig. 1.21). The antiproliferative activity of these

compounds was evaluated against three cancer lines and the results revealed stronger anticancer effects compared with those of their respective parent compounds. Compound **1.57** and **GA** displayed IC_{50} lower than 19 μM and higher than 100 μM, respectively. The influence of the incorporation of piperazine ring on the enhanced activity could be explained by its ability to form hydrogen bonds, improve water solubility and adjust the molecular physicochemical properties [152].

The introduction of a piperazine moiety was also performed in other works found in the literature. A series of new **GA** derivatives, bearing different substituted piperazines at C30, was synthesized and evaluated for their VEGFR2 inhibitory activity and for their antiproliferative properties against four cancer cell lines. Compound **1.58** (Fig. 1.21) was the most active derivative with an IC_{50} value of 1.08 μM against MCF-7 cells. This derivative also showed to be a potent inhibitor of VEGFR2 tyrosine kinase [153]. Sun *et al.* prepared a series of **GA** derivatives as potential agonists of the peroxisome proliferator-activated receptor (PPAR) γ, which is a nuclear receptor and transcription factor that regulates the expression of several genes relevant to carcinogenesis. The derivatives were synthesized by the introduction of different substituted piperazines at C3. In the essays performed, compounds **1.59** and **1.60** inhibited the cell proliferation of MCF-7 and HepG2 cells, showed to be highly efficient PPAR γ agonists and displayed low toxicity [154].

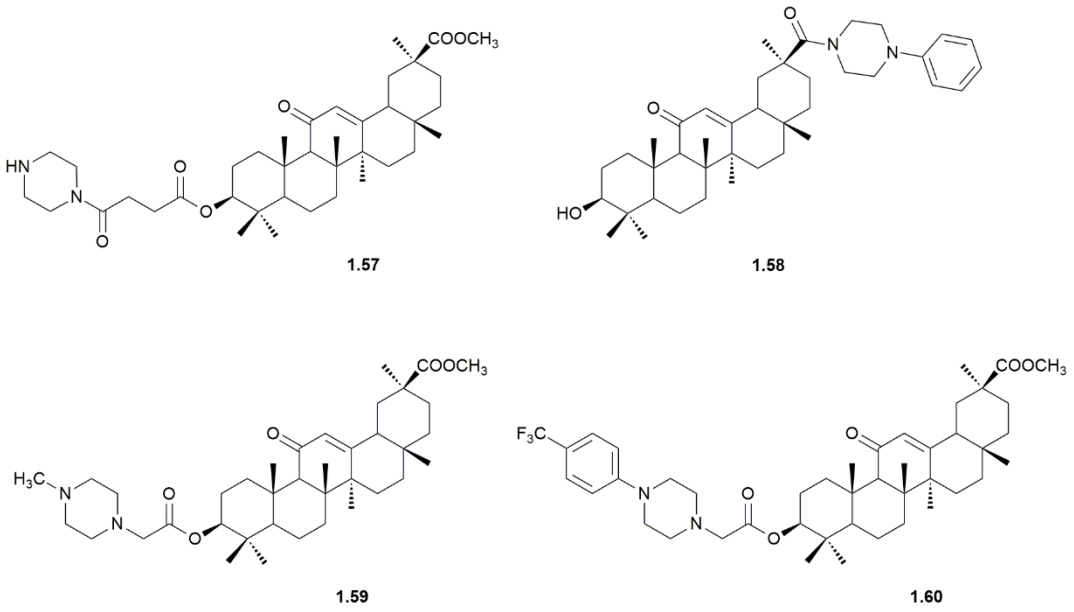

Figure 1.21 GA derivatives **1.57-1.60**.

Guo and coworkers developed **GA**-cinnamoyl hybrids based on the knowledge that both **GA** and cinnamic acid (CA) exhibit cytotoxic activity. Moreover, the presence of a CA fragment could provide selectivity for cancer cells. Therefore, a series of hybrids was synthesized combining **GA** and CA or CA-derivatives fragments through an ester bond at C3. The antiproliferative activity of these compounds was evaluated against three tumor cell lines and three non-tumor cell lines. The results demonstrated that the new hybrids **1.61**-**1.69** (Fig. 1.22) exhibited higher potency than **GA** against the three tumor cell lines. Within these, the most active was compound **1.68**, which revealed selective toxicity towards HeLa cells (**1.68**: IC_{50} = 8.54 μM; **GA**: IC_{50} > 50 μM). Additional assays indicated that compound **1.68** could induce cell damage, nuclei lysis, blockage of intercellular contact and apoptosis in these cells [155].

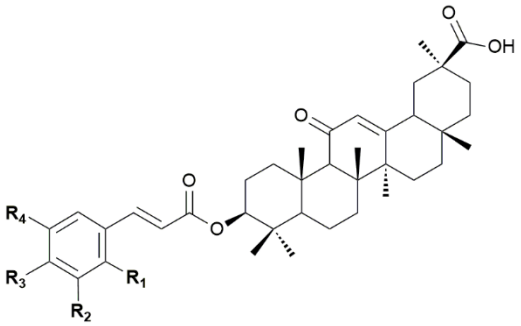

	R_1	R_2	R_3	R_4
1.61	H	H	H	H
1.62	H	H	CH_3	H
1.63	OCH_3	H	H	H
1.64	H	OCH_3	H	H
1.65	H	H	OCH_3	H
1.66	OCH_3	OCH_3	H	H
1.67	OCH_3	H	H	OCH_3
1.68	OCH_3	OCH_3	OCH_3	H
1.69	H	OCH_3	OCH_3	OCH_3

Figure 1.22 GA derivatives **1.61-1.69**.

Li *et al.* also prepared a series of **GA** derivatives containing a CA moiety. Different CA fragments were attached to **GA** at C30, through a linker of piperazine or ethylenediamine. The resulting compounds **1.70-1.87** (Fig. 1.23) were screened for their antiproliferative activity against SK-OV-3 and OVCAR-3 cells. The majority of the derivatives exhibited stronger antiproliferative activities than **GA** against both cancer cell lines and compounds **1.79-1.87** with an etylenediamine linker were more potent than compounds **1.70-1.78** with a piperazine linker. Among all the prepared derivatives, compound **1.72** was the most active with IC_{50} values of 27.9 μM and 33.9 μM against SK-OV-3 and OVCAR-3 cells, respectively (**GA**: IC_{50} (SK-OV-3) = 98.5 μM; IC_{50}

(OVCAR-3) = 72.4 μM)), and showed selective activity towards those ovarian cancer cell lines. Further experiments demonstrated that compound **1.72** could induce apoptosis, suppress migration and significantly reduce the subpopulation of cancer stem cells in both cancer cell lines [156].

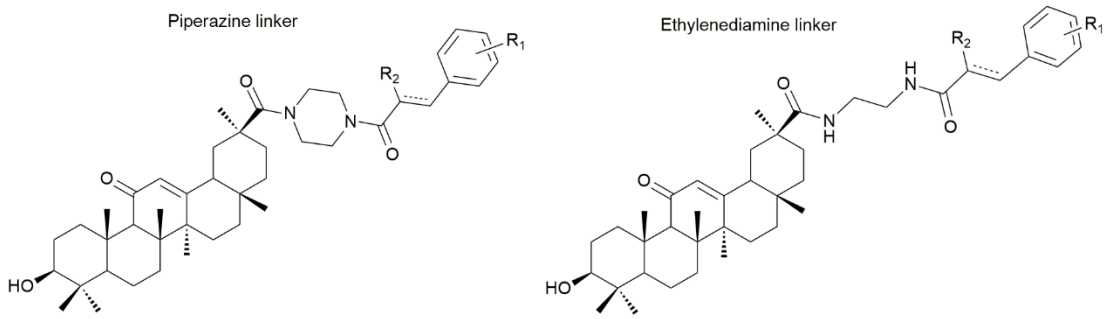

	R_1	R_2	Bond	
1.70	H	H	Double	**1.79**
1.71	4-F	H	Double	**1.80**
1.72	4-Cl	H	Double	**1.81**
1.73	4-CH_3	H	Double	**1.82**
1.74	4-CF_3	H	Double	**1.83**
1.75	4-OCH_3	H	Double	**1.84**
1.76	3,4,5-triOCH_3	H	Double	**1.85**
1.77	H	CH_3	Double	**1.86**
1.78	H	H	Single	**1.87**

Figure 1.23 GA derivatives **1.70-1.87**.

Rhodamine B is a cationic compound that belongs to a group of molecules that target mitochondria, called mitocans. The increased mitochondrial membrane potential in tumor cells compared to non-tumor cells leads to a greater accumulation of this mitocan in cancer cells. Thus it is expected that this compound will have a higher selectivity for tumor cells. In this regard, Csuk and coworkers developed a series of works in which rhodamine B was conjugated to **GA** and other PTs, through different linkers and at different positions. The first group of compounds synthesized were triterpenoid piperazine-spacered rhodamine B derivatives. These conjugates were evaluated for their antiproliferative activity against a panel of cancer cell lines and against non-tumor mouse fibroblasts (NIH3T3). While rhodamine is not cytotoxic and PTs showed very low cytotoxicity (**GA**: IC_{50} > 30 μM), the rhodamine conjugates were active in nanomolar

concentrations (**1.88**: IC_{50}: 0.083-0.175 μM, Fig. 1.24). However, no gain in selectivity was achieved for these derivatives [157]. In a second study, a homopiperazinyl moiety was used as linker instead of a piperazinyl group. The new **GA**-derived compound **1.89** (Fig. 1.24) did not show a better cytotoxicity or selectivity profile compared to the previously prepared piperazinyl analogue [158]. A different series of conjugates was prepared by the coupling of rhodamine B directly at the C3 position. Along with this conjugation, the carboxylic acids of the different PTs were converted to methyl and benzyl esters or benzyl amides. The **GA** rhodamine B benzyl amide **1.90** (Fig. 1.24) was the most potent derivative of this series, with IC_{50} values ranging from 0.02 to 0.06 μM, against the cancer cell lines tested. However, selectivity remained without improvement [159].

GA was also coupled to another mitocan, the triphenylphosponium cation. Among the new series of **GA** conjugates with a triphenylphosponium moiety, compound **1.91** (Fig. 1.24) was the most active against the proliferation of the tested cancer cell lines (IC_{50}: 5.25-9.22 μM) and exhibited better selectivity than **GA**. Derivative **1.91** also revealed to arrest cell cycle at G2 phase, induce apoptosis and inhibit migration, in A549 cells [160].

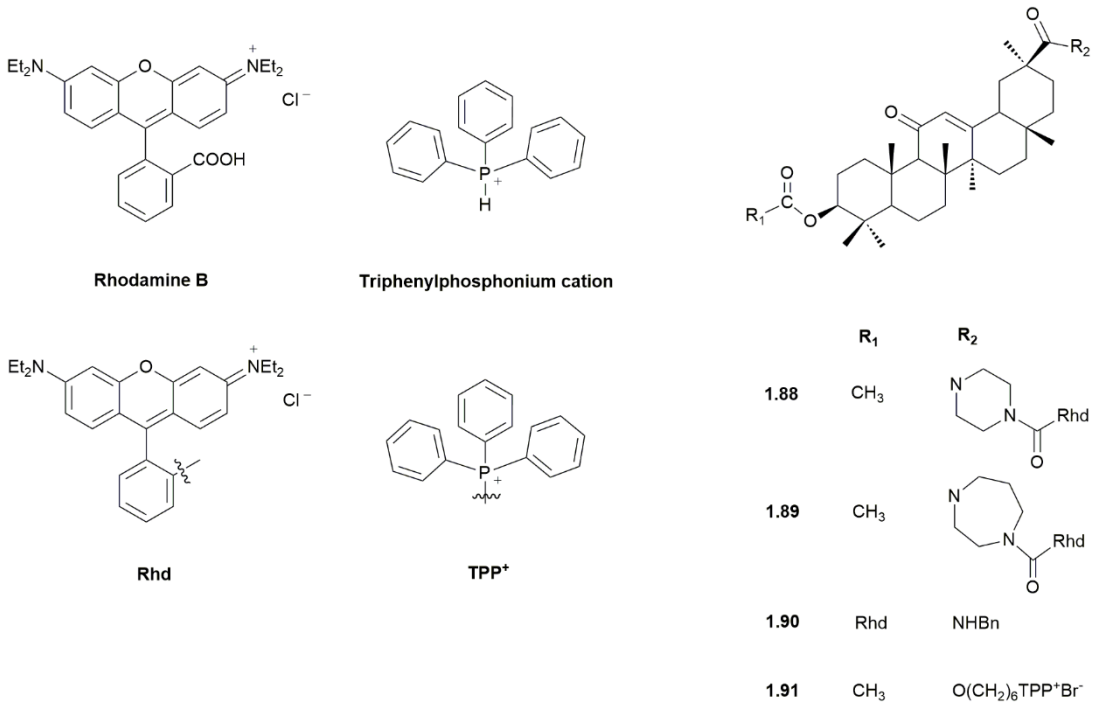

Figure 1.24 GA derivatives **1.88-1.91**.

Beyond the modifications performed at positions C3 and C30 of the **GA** backbone, some derivatizations have involved modifications on the A-ring. A series of **GA** derivatives with an open ring A were prepared [131,161] and evaluated for their antiproliferative activity against the human bladder cancer line NTUB1 [131]. Compounds **1.92-1.94** (Fig. 1.25) were the most potent derivatives of this series, with IC_{50} values of 2.34, 4.76 and 3.31 μM, respectively. Compound **1.94** showed to induce ROS production which led to the activation of p53 and consequent induction of apoptosis.

A library of five-membered heterocyclic ring-fused **GA** derivatives at positions C2 and C3 was synthesized and their cytotoxic activity was screened against eight cancer cell lines. Among the heterocyclic rings fused at ring A, pyrazole and its derivatives afforded the most potent compounds (**1.95-1.98**, Fig. 1.25). Compound **1.95** was further modified to produce compounds **1.99-1.105** (Fig. 1.25). Migration assays with **GA** (IC_{50}: 70.48-136.40 μM) and the most active derivative **1.105** (IC_{50}: 5.19-11.72 μM) revealed an important increment in the antimetastatic activity, in which compound **1.105** was about 20-fold more potent than **GA**.

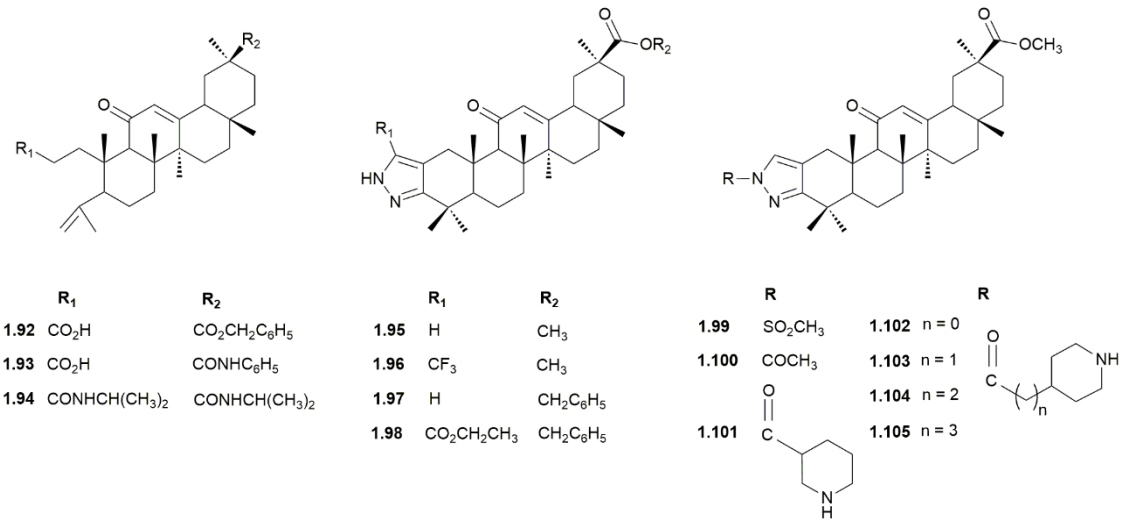

	R_1	R_2
1.92	CO_2H	$CO_2CH_2C_6H_5$
1.93	CO_2H	$CONHC_6H_5$
1.94	$CONHCH(CH_3)_2$	$CONHCH(CH_3)_2$

	R_1	R_2
1.95	H	CH_3
1.96	CF_3	CH_3
1.97	H	$CH_2C_6H_5$
1.98	$CO_2CH_2CH_3$	$CH_2C_6H_5$

	R		R
1.99	SO_2CH_3	**1.102**	n = 0
1.100	$COCH_3$	**1.103**	n = 1
1.101		**1.104**	n = 2
		1.105	n = 3

Figure 1.25 GA derivatives **1.92-1.105**.

Derivatizations involving more profound modifications on the **GA** scaffold were also performed. The introduction of Michael acceptors in its structure has been a drug design strategy that resulted in **GA** derivatives with remarkable improvement of the anticancer activity. The knowledge that the introduction of an electron-withdrawing group at C2 in ring A with a 1-en-3-one system increase the antiproliferative and anti-inflammatory activities of PTs [162-164], led to the design and preparation of compounds **1.106-1.113** (Fig. 1.26) [165]. These derivatives were tested for their cytotoxic activity against four cancer cell lines. The results showed that the 2-cyano and 2-trifluoromethyl derivatives **1.107**, **1.108**, **1.112** and **1.113** were the most potent compounds, with IC_{50} values ranging from 0.05 to 1.80 μM over the four cell lines. Moreover, rearrangement of ring C to the 9(11)-en-12-one isomer afforded derivatives with higher cytotoxicity (**1.111-1.113**). Further studies were carried out, focused on chemical modifications at ring C of compound **1.107** [166,167]. Those experiments confirmed that derivative **1.112** was the most potent compound of this series. Despite the higher potency of **1.112**, derivative **1.115** (Fig. 1.26) has proven to be more selective towards cancer cells [167]. The interest in this drug design strategy has been reflected in the large number of scientific papers that report the synthesis of new **GA** derivatives with Michael acceptors in their structures (e.g., **1.116** and **1.117**, Fig. 1.26) [166,168-170], and the studies for the elucidation of their mechanisms of action. Table 1.3 shows some of the main mechanistic studies performed for this group of compounds.

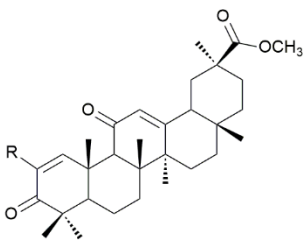

	R
1.106	I
1.107	CN
1.108	CF_3
1.109	SO_2CH_3
1.110	$PO(OCH_3)_2$

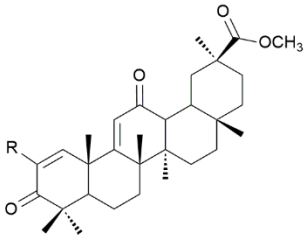

	R
1.111	I
1.112	CN
1.113	CF_3

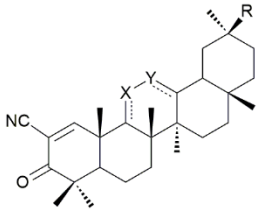

	X	Y	R
1.114	CH_2	CH	$COOCH_3$
1.115	CH_2	C=O	$COOCH_3$
1.116	CH	CH	$COOCH_3$
1.117	CH	CH	CN

Figure 1.26 GA derivatives **1.106-1.117**.

Table 1.3 Mechanisms of action of **GA** derivatives presenting Michael acceptors in their structures.

GA derivative	Cancer type	Model	Mechanism of action/ Molecular targets	Ref.
1.107	Bladder	*In vitro:* J82 RT4P 253JB-V	Induction of ROS production which downregulated specificity protein (Sp) transcription factors and Sp-regulated proteins survivin and VEFGR2.	[171]
	Colorectal	*In vitro:* SW480 HT-29 HCT-15	PPARγ agonist: induction of expression of pro-apoptotic proteins: caveolin-1 and tumor-suppressor gene Krüppel-like factor-4.	[172]
		In vitro: SW480 RKO	Repression of oncogenic microRNA-27a: ↓ expression of Sp transcription factors and Sp-dependent gene expression of survivin, VEFG and VEFGR1. Induction of apoptosis and cell cycle arrest at G2 phase.	[173]
	Pancreatic	*In vitro:* Panc1 Panc28	PPARγ agonist. Activation of phosphatidylinositol-3-kinase (PI3-K) and/or p42 and p38 mitogen-activated protein kinase (MAPK) pathways: induction of the pro-apoptotic proteins early growth response-1 (Egr-1), nonsteroidal anti-inflammatory drug-activated gene-1 (NAG-1), and activating transcription factor-3 (ATF-3).	[174]
	Prostate	*In vitro:* LNCaP	PPARγ agonist. Activation of PI3-K, MAPK and JNK: induction of p21 and p27, downregulation of cyclin D1 protein expression, induction of pro-apoptotic proteins NAG-1 and ATF-3. ↓androgen receptor and prostate-specific antigen mRNA and protein levels through kinase-independent pathways.	[175]
	-	*In vitro:* HUVECs *Ex vivo:* Rat aortic ring *In vivo:* Mice Matrigel plug	*HUVECs:* inhibition of proliferation, migration, invasion and lamellipodium and capillary-like structure formation by inhibiting VEGF/ VEGFR2 and mTOR signaling pathways. *Rat aortic ring:* abrogation of VEGF induced sprouting of microvessels. *Mice Matrigel plug:* inhibition of the formation of new vessels.	[176]
1.107 and 1.112	Leukemia	*In vitro:* HL-60	Induction of apoptosis. Downregulation of the anti-apoptotic proteins c-FLIP, XIAP and Mcl-1. Depletion of glutathione (GSH).	[177]
1.107 and 1.108	Thyroid	*In vitro:* ARO,DRO K-18 HTh-74	Downregulation of Sp transcription factors and Sp-dependent genes survivin, VEGF and pituitary tumor-transforming gene-1.	[178]

GA derivative	Cancer type	Model	Mechanism of action/ Molecular targets	Ref.
Table 1.3 continued				
1.108	Bladder	*In vitro:* RT4P	Induction of apoptosis. Blockade of the blebbishield emergency program through degradation of Sp1and inhibition of VEGF, VEGFR2, N-Myc, and p70S6K and inhibition of ROS production and K-Ras activation.	[179]
	Rhabdo--myo--sarcoma	*In vitro:* RD Rh30	Induction of apoptosis and inhibition of invasion. Induction of ROS-dependent downregulation of Sp transcription factor and pro-oncogenic Sp-regulated genes including PAX3-FOXO1.	[180]
1.117	Liver	*In vitro:* Bel-7402	Induction of apoptosis: depletion of intracellular GSH, increased levels of ROS and consequent induction of MOMP; activation of JNK and p38-MAPK pathways.	[181]
			PPARγ agonist. Modulation of the phosphatase and tensin homologue deleted on chromosome ten (PTEN)-PI3K/Akt pathway. Induction of apoptosis and cell cycle arrest at G1phase.	[182]
1.112 and 1.116	Leukemia	*In vitro:* HL-60	**1.112 and 1.116:** Induction of apoptosis. **1.112**: Downregulation of the anti-apoptotic proteins c-FLIP, XIAP and Mcl-1. Depletion of GSH. **1.116:** Downregulation of c-FLIP. Less depletion of GSH.	[166]
1.116	Leukemia	*In vitro:* HL-60 THP-1 MOLM13 NB4 U937 KG-1	Induction of apoptosis. Upregulation of the pro-apoptotic protein Noxa, downregulation of c-FLIP and activation of the apoptotic effectors Bax and Bak. Modulation of the histone deacetylase (HDAC)3/HDAC6 and Ku70 axis	[183]
1.112	Breast	*In vitro:* MCF-7 MDA-MBA-231	Induction of apoptosis. MDA-MBA-231: apoptosis triggered by ER stress.	[184]
	Lung and Melanoma	*In vitro:* A549 *In vivo:* Metastatic murine melanoma B16	*A549*: Blockade of the transforming growth factor (TGF) -induced epithelial-mesenchymal transition (EMT): inhibition of motility and invasion and loss of epithelial characteristics. Modulation of MMP-2/-9 and JNK 1. *Murine melanoma B16*: blockade of metastatic dissemination, ↑ expression of E-cadherin and ↓expression of MMP-9.	[185]

1.5. General objectives of this work

Cancer is a leading cause of death worldwide and its burden is expected to continue to rise in the coming years. Despite the scientific progress in cancer research, the biological complexity of the disease and the drug resistance and side effects of the current chemotherapeutic armamentarium, demand for the discovery of new anticancer drugs.

PTs have been reported to possess interesting pharmacological activities. Regarding to their antitumor properties, these natural compounds show to behave as multifunctional agents, which increased their interest as potential leads for cancer drug development. **GA** is a PT with a promising multi-target anticancer profile that can be extracted from its natural sources in high yields, which make it an available and affordable lead.

Given these considerations, the aim of this work is the development of new **GA** derivatives and the evaluation of their antiproliferative activity against several cancer lines.

With the goal to obtain new **GA** derivatives with improved anticancer activity, two synthetic strategies were projected:

a) the introduction of different heterocyclic rings conjugated with an α,β-unsaturated ketone in its ring A;

b) the opening of its ring A along with the coupling with an amino acid.

The structural elucidation of the new prepared compounds should be achieved through different analytical techniques, such as infrared spectroscopy, mass spectrometry and nuclear magnetic resonance.

The antiproliferative activity of the new derivatives should be evaluated against a panel of several cancer cell lines and the IC_{50} values should be determined. The most potent compound of each series should be further tested for its biological activity in the cancer cell line that yields the best results. These two selected derivatives should be tested against a nontumor cell line, to assess selectivity. Cell cycle perturbations and induction of apoptosis should be investigated through different biological assays, using techniques such as fluorescence-activated cell sorting and western-blotting, in order to shed some light in their mechanisms of action.

2. Heterocyclic Glycyrrhetinic Acid Derivatives

2.1. Introduction

Heteroaryl groups are present in diverse pharmacological active compounds, including several derivatives with anticancer properties [186-191].

In previous studies performed by our research group, introduction of imidazole, methyl-imidazole and triazole heterocyclic rings was achieved in several positions of betulinic and ursolic acids, affording several derivatives with better antiproliferative activity compared with the parent compounds. The structure-activity relationship analysis revealed that the introduction of a heterocyclic ring conjugated to an α,β-unsaturated ketone in the ring A of the backbone seems to provide the most potent derivatives [192,193].

Cycloaddition of azides and alkynes, commonly referred to as "click chemistry", has acquired great interest in the development of novel heterocyclic compounds with varied biological activities [194-197]. This simple and efficient process has been successfully used in the synthesis of PTs derivatives with improved anticancer activity [198-201]. The strategy of synthesis used in this work was the Cu (I)-catalysed azide-alkyne cycloaddition (CuAAc) with terminal alkynes, which yields regioselectively 1,4-substituted-triazolyl derivatives [202-204].

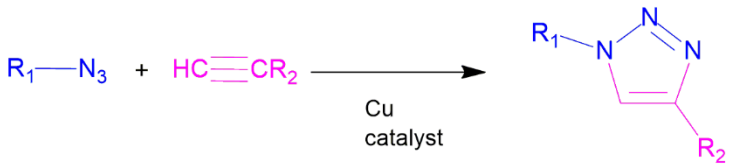

Figure 2.1 The synthesis of triazoles through CuAAc with terminal alkynes.

The mentioned information prompted us to synthesize new **GA** derivatives via the introduction of different heterocyclic rings conjugated with an α,β-unsaturated ketone in its ring A, which would behave as Michael acceptors [205]. These derivatives were tested for their antiproliferative activity against a panel of nine human cancer lines. Further biological assays were performed for the most active compound **2.9** (Scheme 2.1) in the leukemia Jurkat cancer cell line, which yielded the best results, to elucidate its mechanism of action.

2.2. Results and discussion

2.2.1. Chemistry

The synthesis of the **GA** derivatives is outlined in Schemes 2.1-2.3. The structures of the newly synthesized compounds were fully elucidated by nuclear magnetic resonance (NMR), mass spectrometry (MS) and infrared (IR) techniques, and elemental analysis. The analytical data obtained for the known compounds **2.1**-**2.7**, were in good agreement with those reported in the literature [143,166,206].

The preparation of three pairs of novel **GA** heterocyclic derivatives is summarized in Scheme 2.1. In addition to the intention to prepare heterocyclic derivatives with improved cytotoxicity, compounds **2.8**-**2.13** were synthesized to explore the effect of the keto group in position C-11 on the antiproliferative activity. Therefore, the first step performed in this sequence of reactions was the removal of the keto group via Clemmensen reduction with zinc dust and concentrated HCl in dioxane at room temperature (r.t.), to afford **2.1** [166]. The following steps were executed in both original and reduced structures, providing successive pairs of derivatives. Methyl esters **2.2** and **2.3** were obtained from the reactions of **GA** and **2.1** with methyl iodide in the presence of potassium carbonate [143]. The 3β-hydroxyl group of these esters was oxidized using the Jones reagent [206], to give the 3-keto derivatives **2.4** and **2.5**. The reaction of this derivatives with ethyl formate and sodium methoxide allowed the preparation of the 2-hydroxyvinyl-3-keto compounds **2.6** and **2.7** [206]. The heterocyclic derivatives **2.8**-**2.13** were prepared via the reaction of the vinyl alcohol at C-2 with the appropriate heterocyclic reagent, 1,1'-carbonyldiimidazole (CDI), 1,1'-carbonylbis(2'-methylimidazole) (CBMI) or 1,1'-carbonyl-di(1,2,4-triazole) (CDT) in reflux of THF under inert atmosphere [193], in yields ranging from 41% to 70%.

Compounds **2.16** and **2.17** were synthesized as depicted in Scheme 2.2. These derivatives were prepared to evaluate if the presence of another heterocyclic ring at C-30 would benefit the antiproliferative activity. The steps of this sequence of reactions were performed using the same methods of oxidation, reaction with ethyl formate and introduction of heterocyclic rings described in Scheme 2.1. These novel heterocyclic derivatives, **2.16** and **2.17**, were obtained in yields of 56% and 38%, respectively.

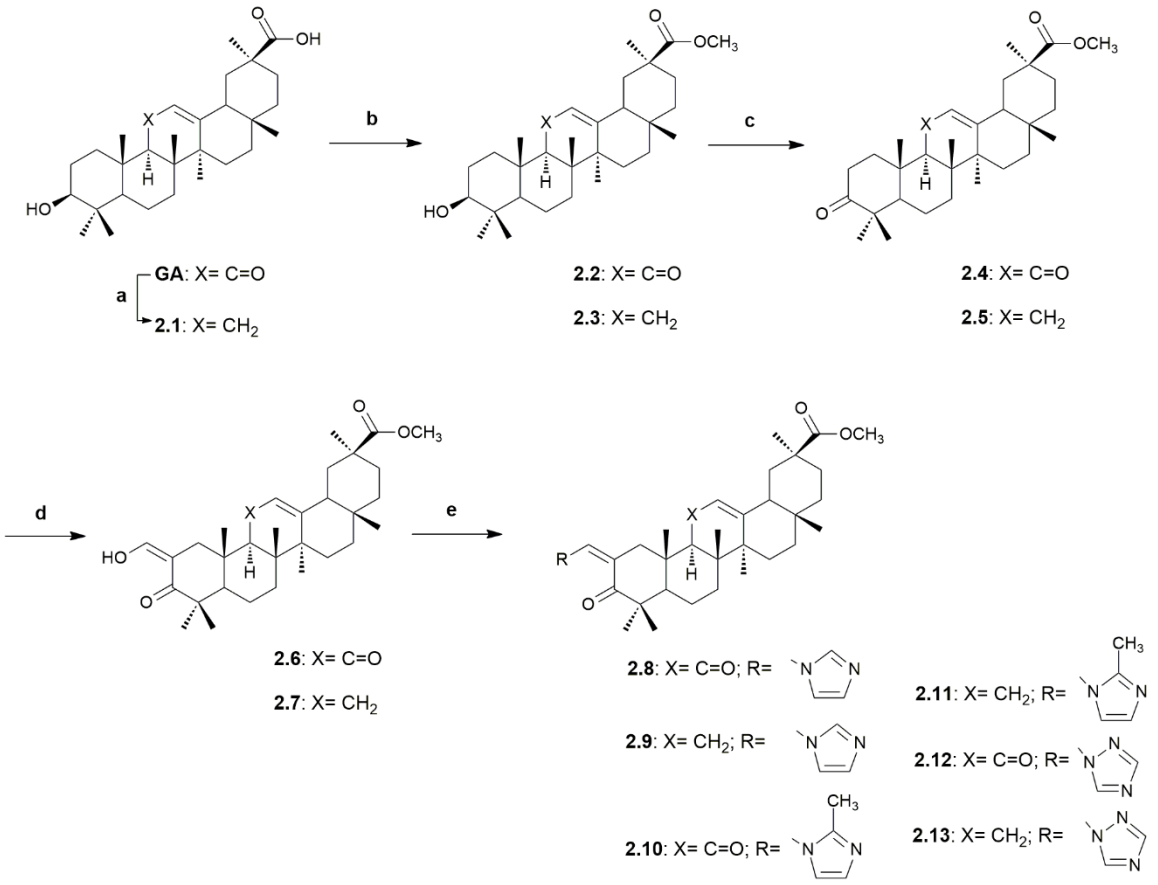

Scheme 2.1 Synthesis of derivatives **2.1**-**2.13**. Reagents and conditions: (a) zinc dust, concentrated HCl, dioxane, r.t.; (b) CH_3I, K_2CO_3, DMF, r.t.; (c) Jones reagent, acetone, 0ºC; (d) ethyl formate, NaOMe, benzene, r.t. N_2; and (e) CDI, CBMI or CDT, dry THF, reflux, N_2.

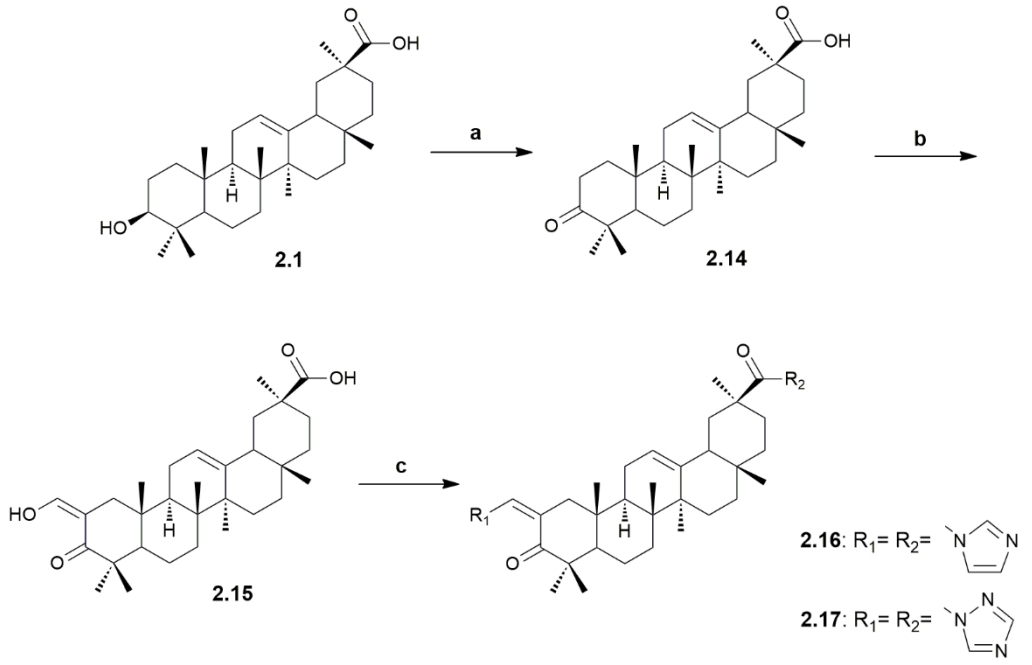

Scheme 2.2 Synthesis of derivatives **2.14**-**2.17**. Reagents and conditions: (a) Jones reagent, acetone, 0ºC; (b) ethylformate, NaOMe, benzene, r.t., N_2; and (c) CDI or CDT, dry THF, reflux, N_2.

The preparation of compound **2.15** was confirmed by the presence of a δ signal at ~8.6 ppm in the ^{1}H NMR spectrum, corresponding to the proton in the exocyclic double bond at C-2 (Fig. 2.2). On the ^{13}C NMR spectrum, the presence of this moiety was confirmed by the observation of a δ signal at ~188 ppm, corresponding to the exocyclic carbon, and a δ signal at ~106 ppm, corresponding to the C-2 carbon (Fig. 2.3).

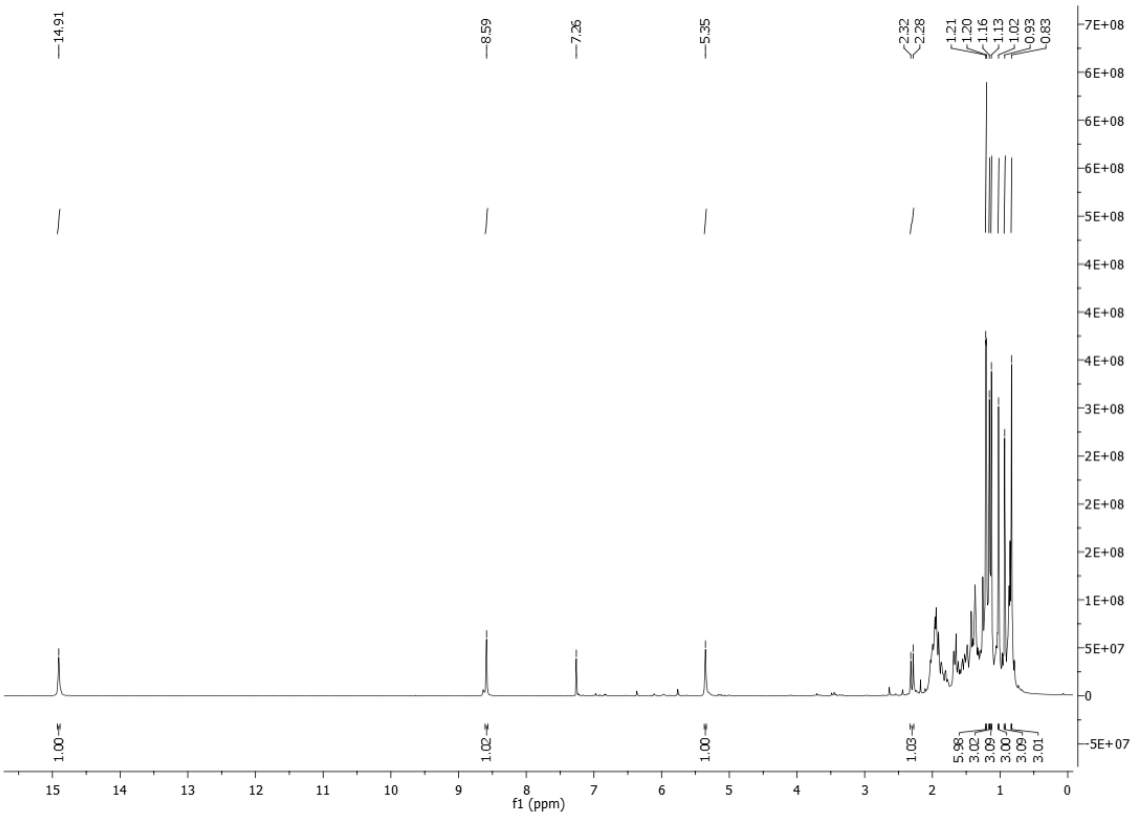

Figure 2.2 ^{1}H NMR spectrum of compound **2.15**.

Click chemistry was handled as shown in Scheme 2.3. We prepared the azido derivatives **2.18** (62%) and **2.19** (57%) by tosylation of the vinyl alcohol at C-2 and subsequent replacement by azide. The triazolyl derivatives **2.20** and **2.21** were obtained via the "click chemistry" of those compounds with methyl propiolate, catalysed by CuI, in THF, at 65ºC (which were the best reaction conditions observed here), in yields of 42% and 44%, respectively.

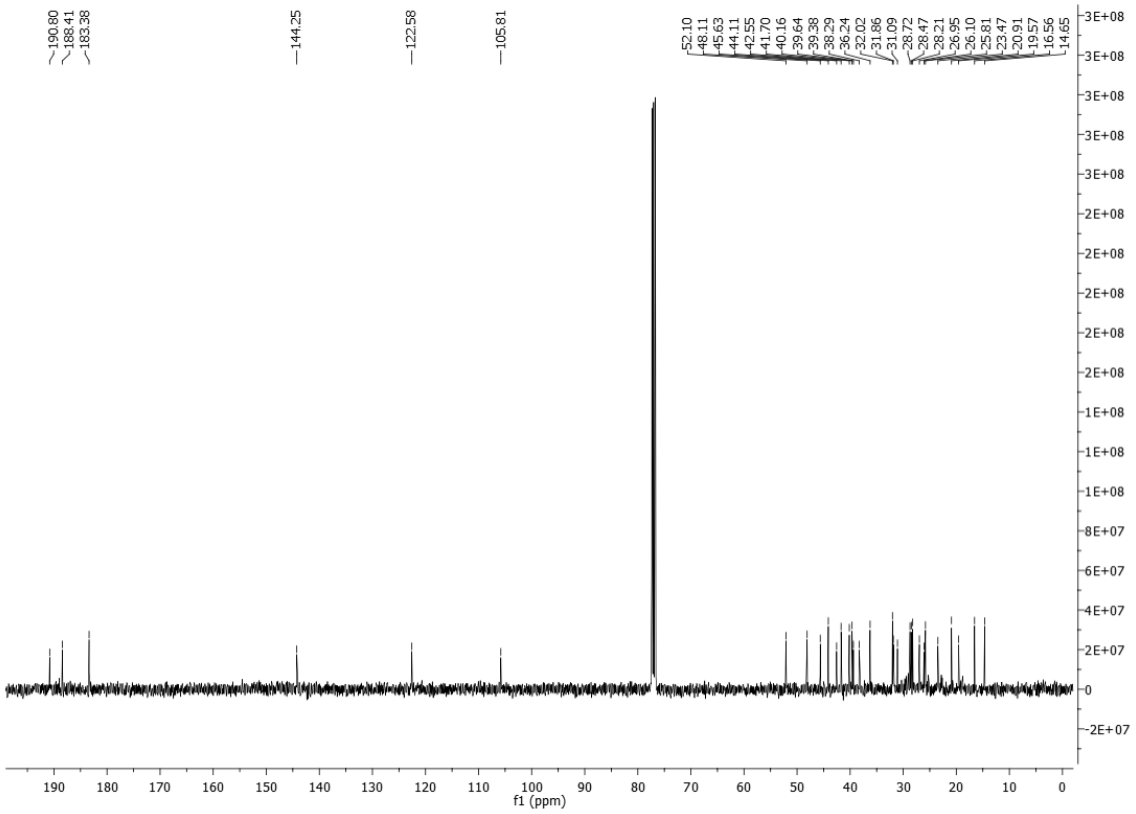

Figure 2.3 ^{13}C NMR spectrum of compound **2.15**.

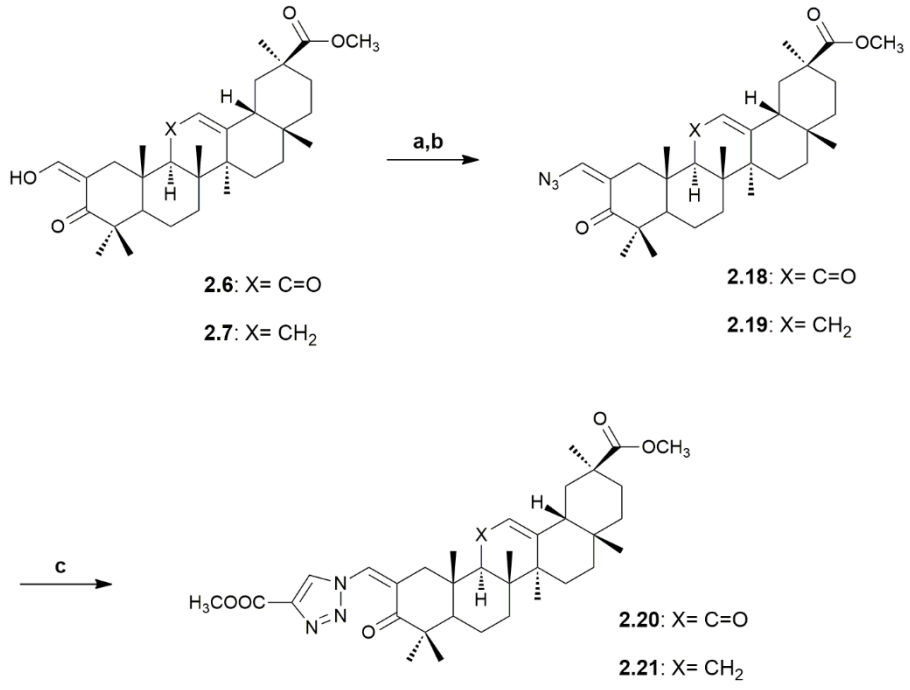

Scheme 2.3 Synthesis of derivatives **2.18**-**2.21**. Reagents and conditions: (a) TsCl, Et_3N, CH_2Cl_2, r.t.; (b) NaN_3, acetone, r.t.; and (c) methyl propiolate, CuI, THF, 65ºC.

The introduction of an azide group was confirmed by the presence of a band observed at around 2120 cm^{-1} in the IR spectrum (Fig. 2.4).

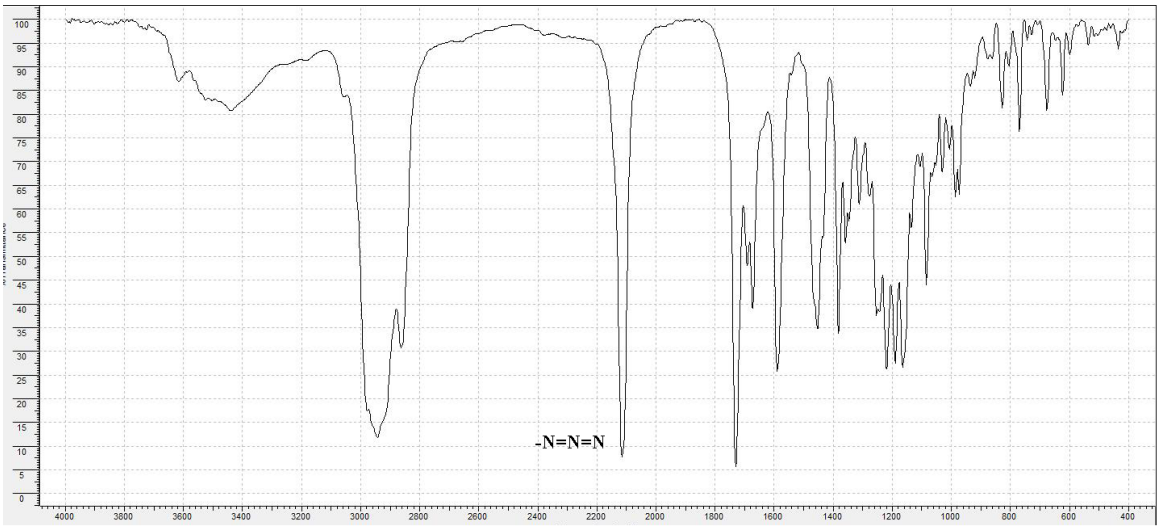

Figure 2.4 IR spectrum of compound **2.19.**

The successful preparation of the heterocyclic derivatives **2.8**-**2.13**, **2.16** and **2.17**, and **2.20** and **2.21**, was confirmed by the presence of a δ signal at ~7.7-8.0 ppm, corresponding to the proton of the exocyclic double bound at C-2 in the ^{1}H NMR spectra. On the 13C spectra the presence of this moiety was confirmed by the presence of a δ signal at ~127-131 ppm, corresponding to the exocyclic carbon.

The presence of heterocyclic ring(s) can be detected by the presence of extra δ signals in ^{1}H and ^{13}C NMR spectra. On the ^{1}H NMR spectra, the imidazole group had three specific protons that appeared at values higher than 7 ppm, the methyl-imidazole group had two protons ranging from 6.9 to 7.7 ppm, the triazole group had two proton signals with a δ higher than 8 ppm, and the triazole group on compounds **2.20** and **2.21** had only one proton at ~8.3-8.4 ppm. In the ^{13}C NMR spectra, the δ signals of the carbons of heterocyclic rings were present at values ranging from 118 to 153 ppm, varying in accordance with the different heterocyclic rings.

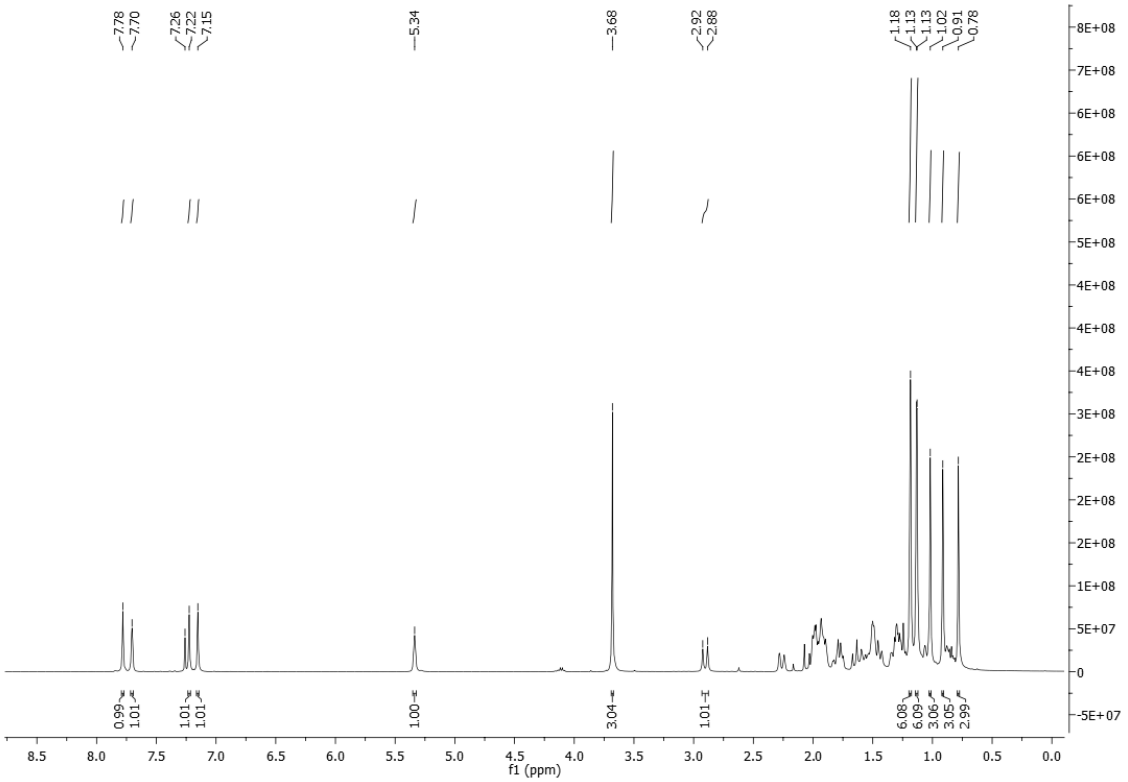

Figure 2.5 ^{1}H NMR spectrum of compound **2.9**.

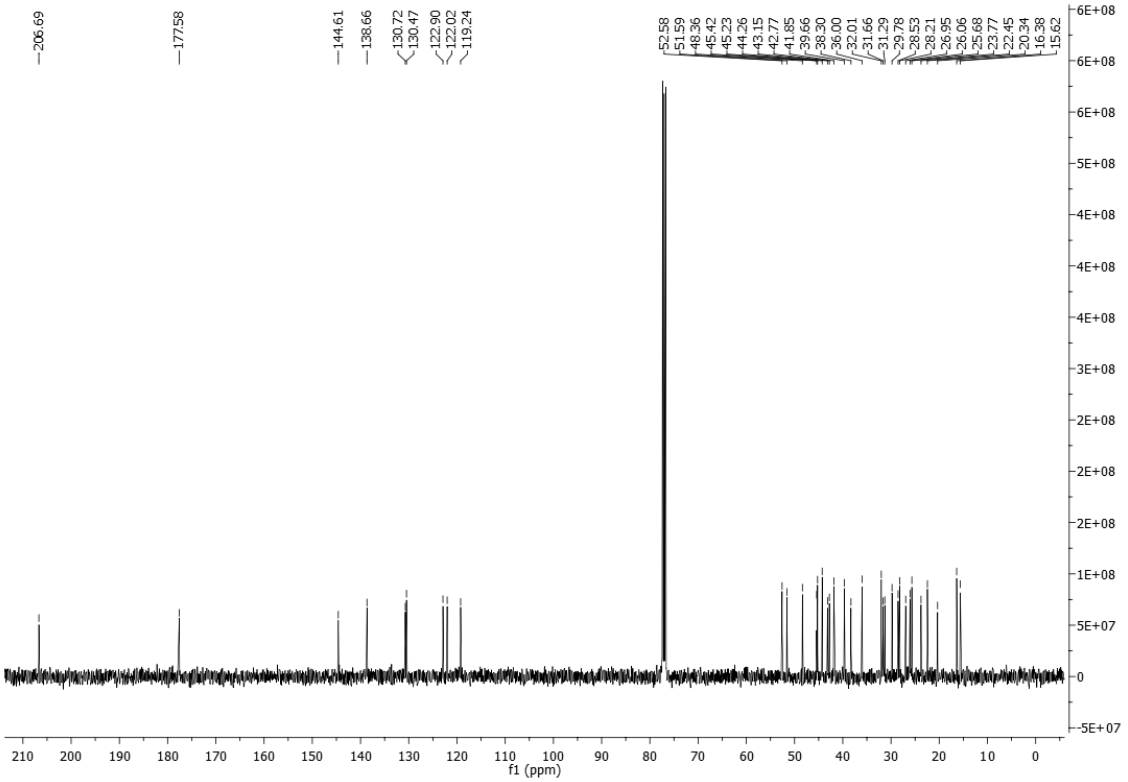

Figure 2.6 ^{13}C NMR spectrum of compound **2.9**.

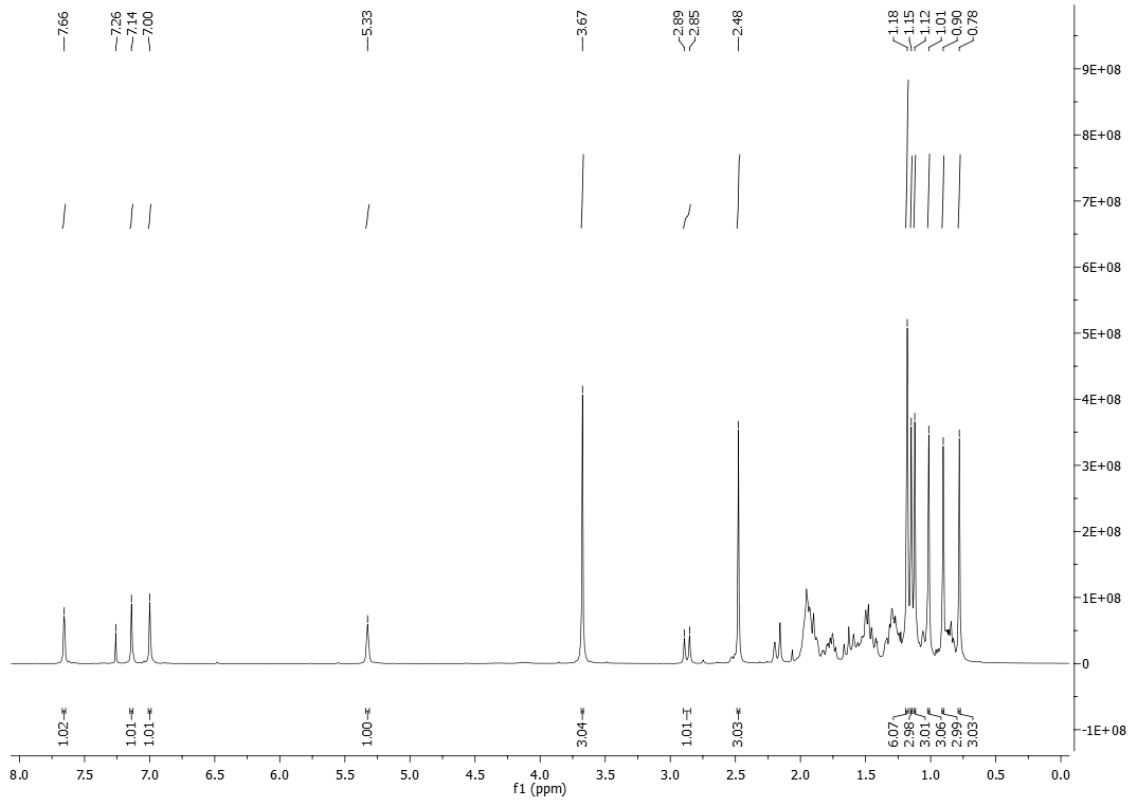

Figure 2.7 ^{1}H NMR spectrum of compound **2.11**.

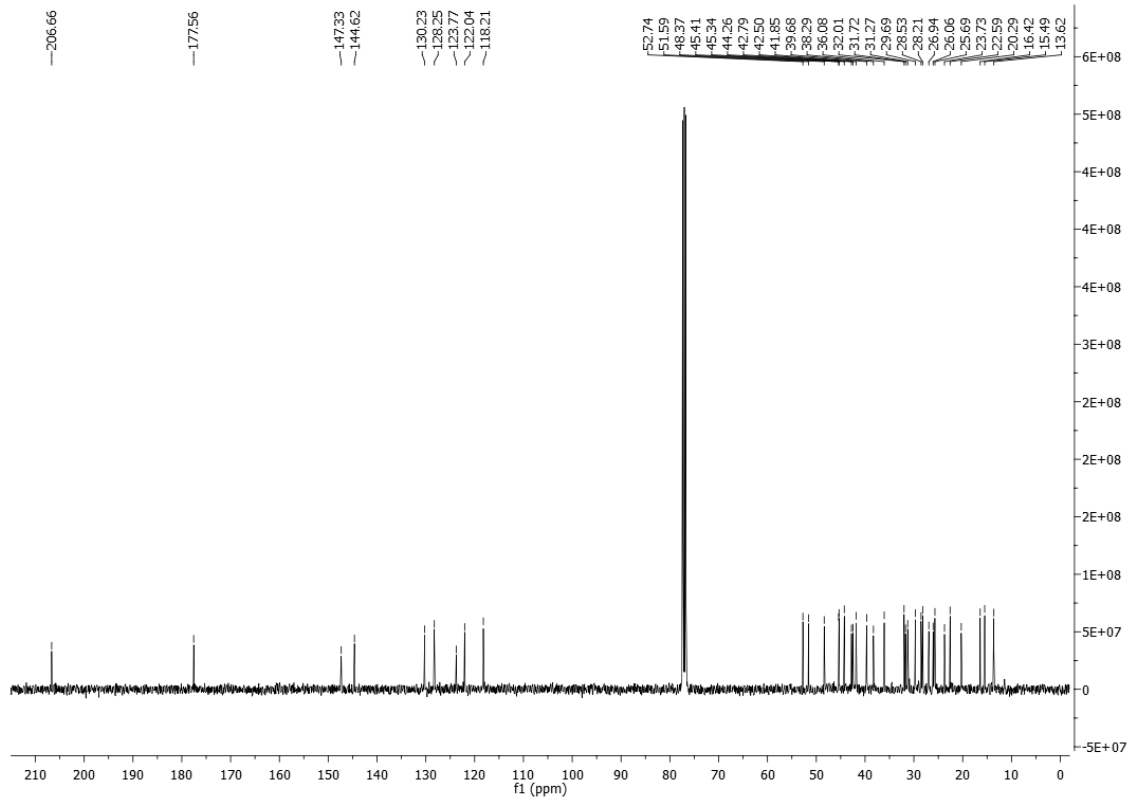

Figure 2.8 ^{13}C NMR spectrum of compound **2.11**.

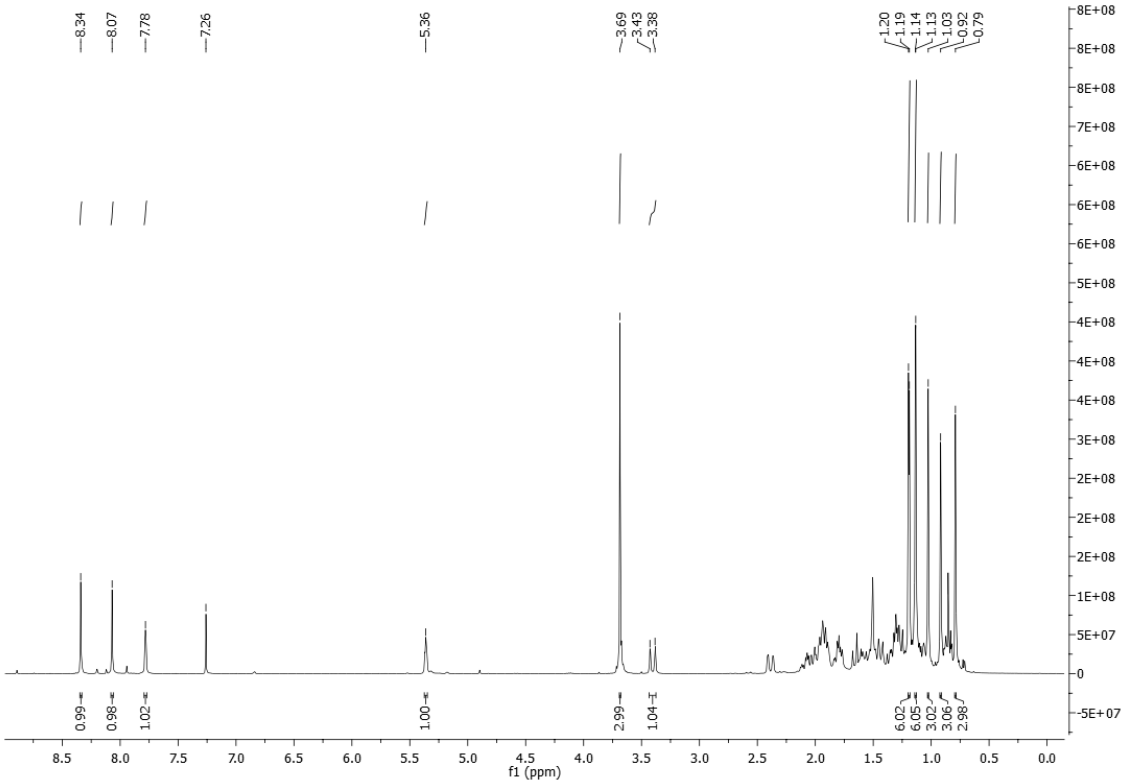

Figure 2.9 ^{1}H NMR spectrum of compound **2.13**.

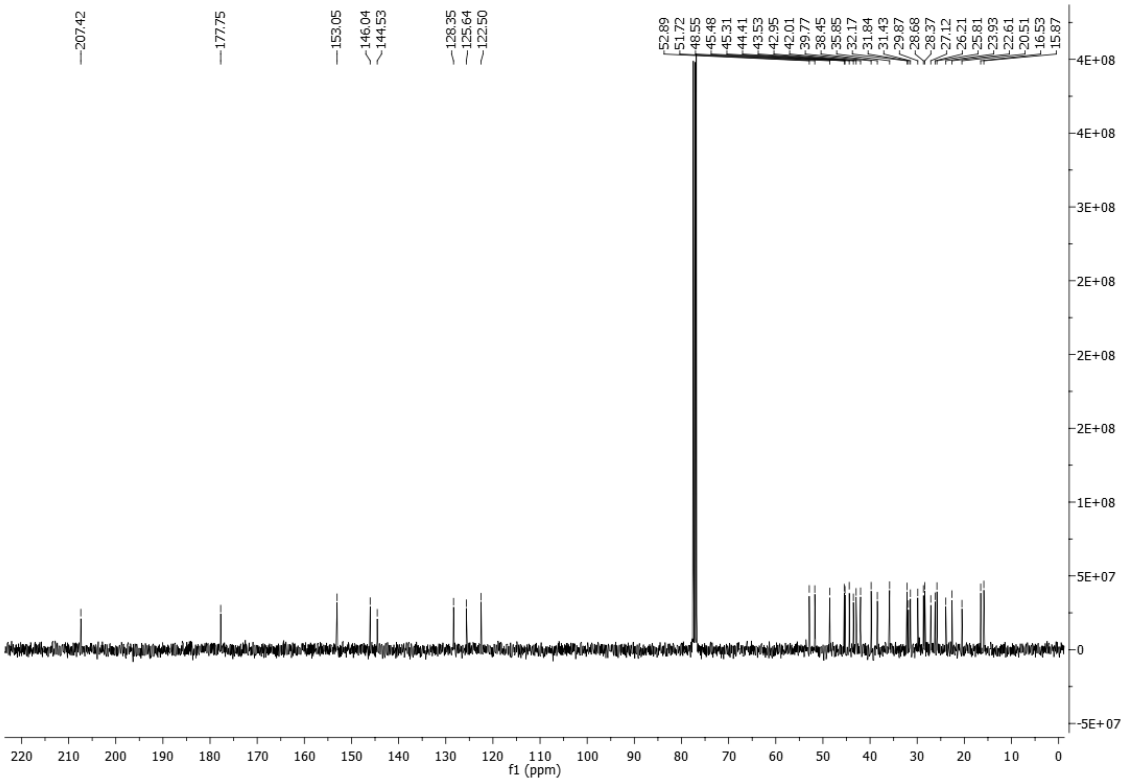

Figure 2.10 ^{13}C NMR spectrum of compound **2.13**.

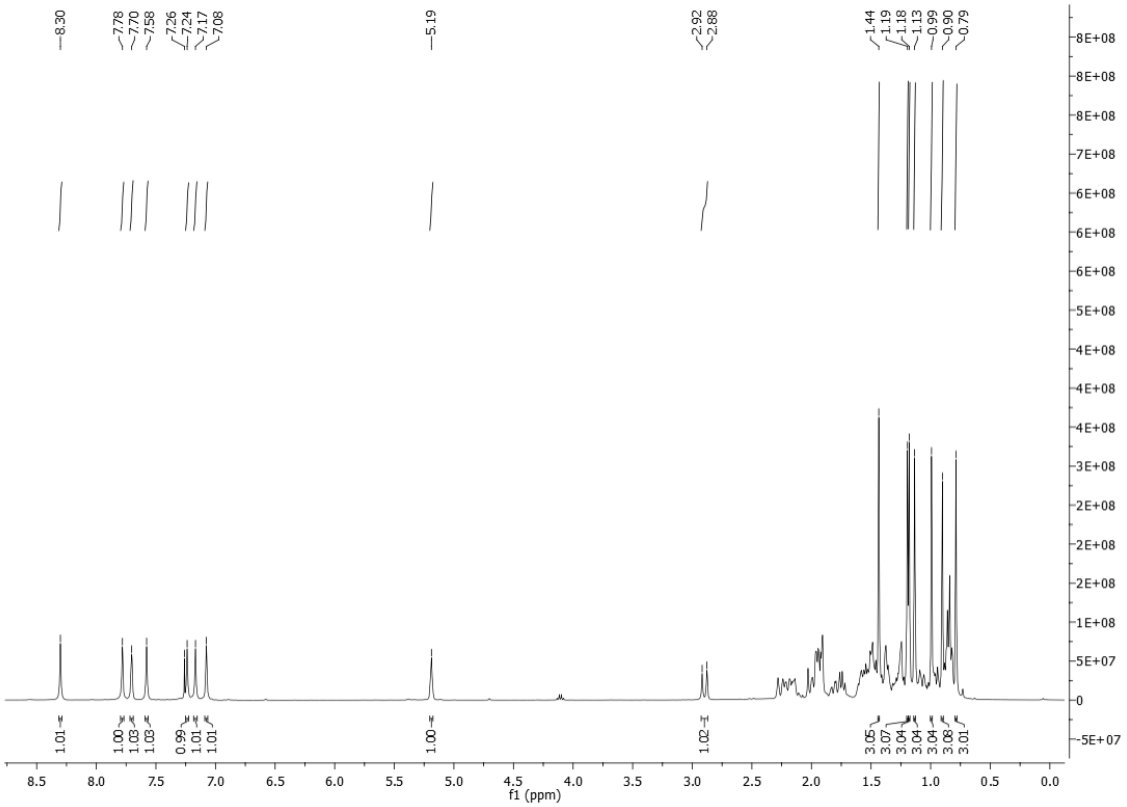

Figure 2.11 ^{1}H NMR spectrum of compound **2.16**.

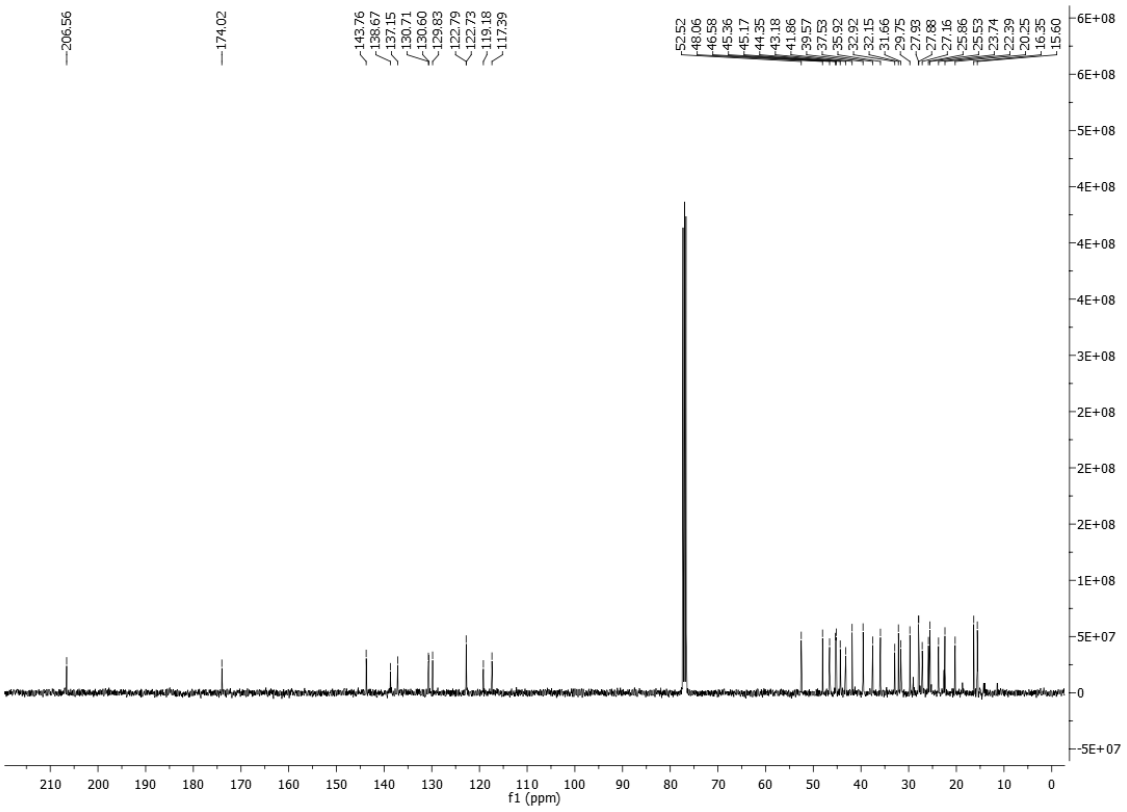

Figure 2.12 ^{13}C NMR spectrum of compound **2.16**.

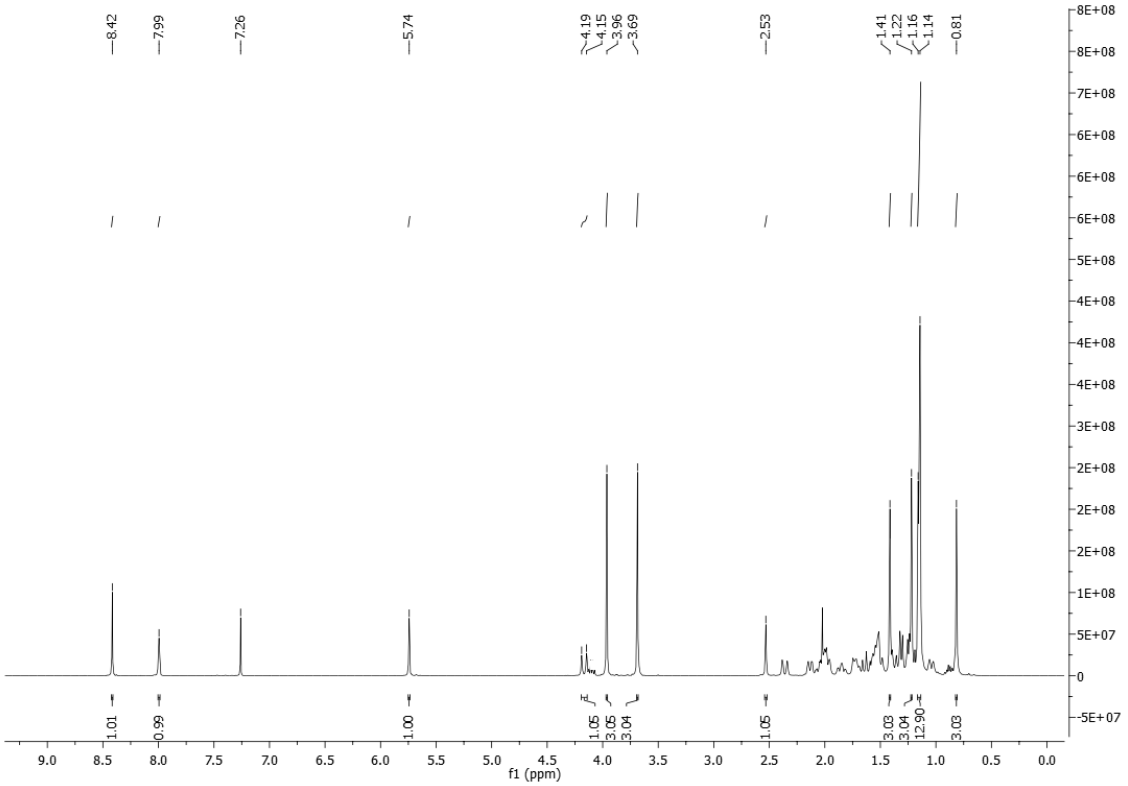

Figure 2.13 ^{1}H NMR spectrum of compound **2.20**.

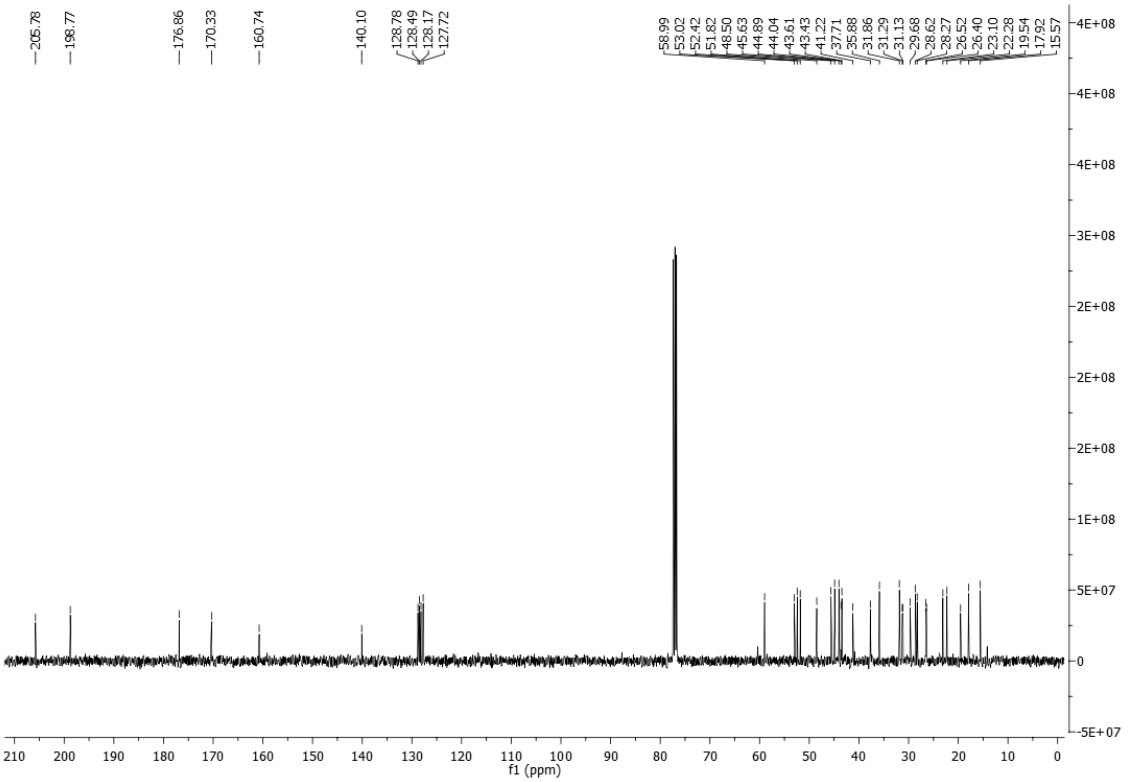

Figure 2.14 ^{13}C NMR spectrum of compound **2.20**.

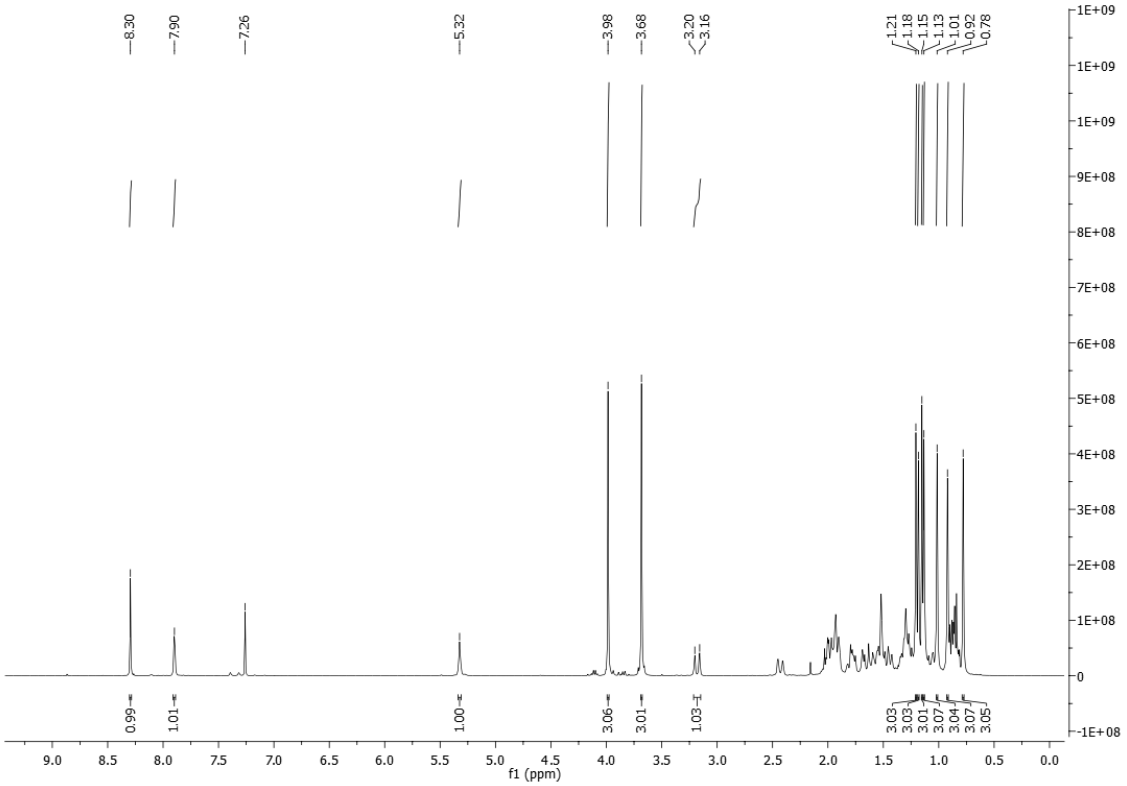

Figure 2.15 ^{1}H NMR spectrum of compound **2.21**.

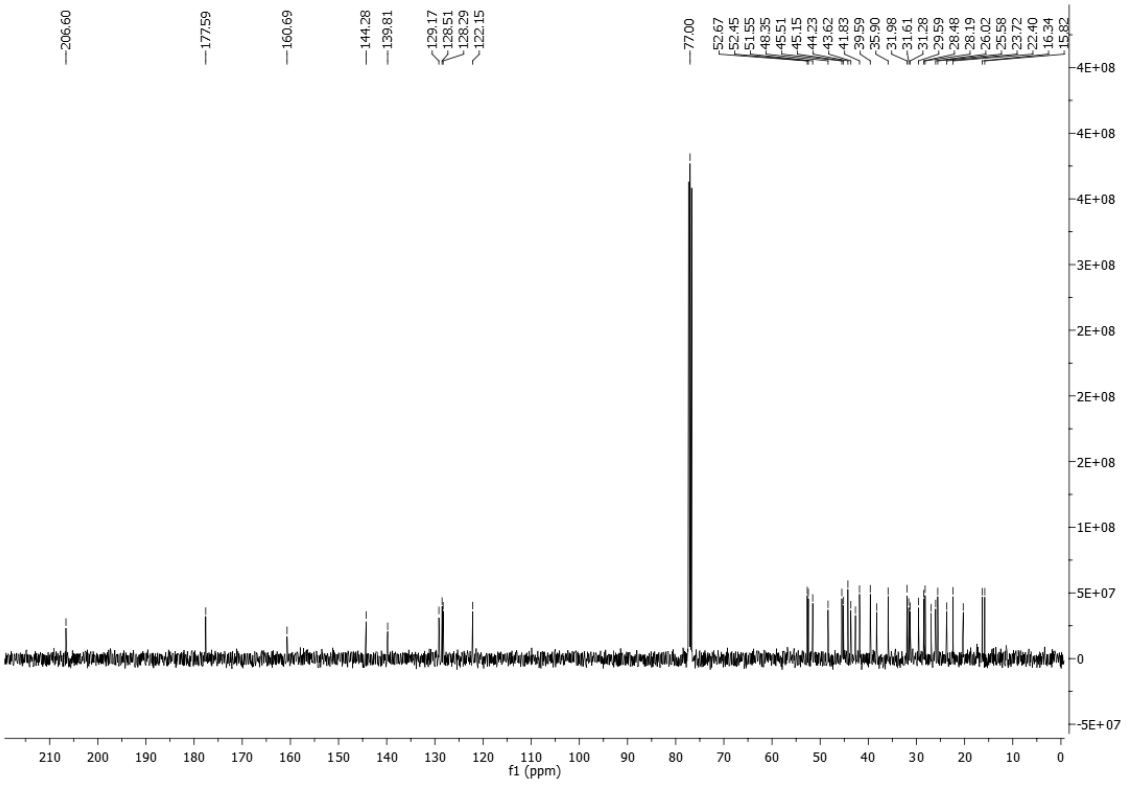

Figure 2.16 ^{13}C NMR spectrum of compound **2.21**.

2.2.2. Biological activity

2.2.2.1. Antiproliferative Activity

Several cancer lines were cultured and used in experiments aimed to evaluating the potential cytotoxicity of the synthesized compounds against human cancers. This evaluation was based on the determination of IC_{50} values using 3-(4,5-dimethylthiazol-2-yl)-3,5-diphenyltetrazolium bromide (MTT) or 2,3-bis(2-methoxy-4-nitro-5-sulphophenyl)-2*H*-tetrazolium-5-carbonaxilide (XTT) assays after 72h of treatment with the compounds.

All compounds were screened for their antiproliferative activity on the colon adenocarcinoma HT-29 cell line. As shown in Table 2.1, most of the novel heterocyclic derivatives (**2.8**-**2.13**, **2.16**, **2.17**, **2.20** and **2.21**) showed improved cytotoxicity compared with the parent compound **GA** and the intermediate compounds.

Table 2.1 Antiproliferative activities of **GA**, its derivatives and cisplatin against HT-29 and A549 cell lines.

Compound	Cell line (IC50, μM) [1]	
	HT-29	A549
GA	115.7 ± 1.6	110.5 ± 3.9
2.1	88.1 ± 1.4	N.D.
2.2	19.6 ± 0.6	N.D.
2.3	18.5 ± 0.9	N.D.
2.4	46.3 ± 2.3	N.D.
2.5	63.9 ± 1.1	N.D.
2.6	14.3 ± 0.3	18.5 ± 1.5
2.7	14.0 ± 0.2	17.0 ± 0.6
2.8	11.5 ± 0.5	11.1 ± 0.1
2.9	3.3 ± 0.2	2.8 ± 0.2
2.10	9.4 ± 0.7	10.3 ± 0.6
2.11	3.6 ± 0.1	3.1 ± 0.1
2.12	31.2 ± 1.5	24.7 ± 0.9
2.13	12.1 ± 0.2	12.3 ± 0.6
2.14	92.3 ± 1.5	N.D.
2.15	60.3 ± 2.0	54.4 ± 2.6
2.16	22.4 ± 0.5	23.1 ± 0.8
2.17	21.8 ± 1.6	24.5 ± 0.6
2.18	38.5 ± 0.6	48.5 ± 0.8
2.19	36.3 ± 1.4	44.3 ± 3.6
2.20	11.0 ± 0.8	10.6 ± 0.1
2.21	8.9 ± 0.5	7.9 ± 0.4
Cisplatin	6.1[207]	12.6 ± 0.8 [208]

[1] The cell lines were treated with different concentrations of each compound for 72 h. IC_{50} values were determined by MTT assay and are expressed as means ± SD (standard deviation) of three independent experiments. IC_{50} is the concentration that inhibits 50% of cellular growth. N.D.: not determined.

The methylation of compounds **GA** and **2.1** provided the derivatives **2.2** and **2.3**, which exhibited an important increment in the antiproliferative activity, but lacked selectivity towards tumor cells [143]. The intermediates **2.6**, **2.7**, **2.15**, **2.18** and **2.19**, which preceded the final heterocyclic derivatives, were also tested on the lung carcinoma A549 cell line. Analysis of the IC_{50} values of the heterocyclic derivatives with respect to their substrates in the two cancer cell lines showed that the introduction of a heterocyclic ring provided more potent compounds, with the exception of compound **2.12**.

The novel compounds **2.8**-**2.13**, **2.16**, **2.17**, **2.20** and **2.21**, and the parent compound **GA** were further tested in seven additional human cancer cell lines: MIAPaCa2 (pancreas adenocarcinoma), HeLa (cervix adenocarcinoma), A375 (melanoma), MCF7 (breast adenocarcinoma), HepG2 (hepatocellular carcinoma), SH-SY5Y (neuroblastoma), and Jurkat (acute T cell leukemia) cells (Tables 2.2 and 2.3). The synthesis of compounds **2.16** and **2.17** was performed to investigate the effect of the combined introduction of heterocyclic rings at the vinyl alcohol at the C-2 and at C-30 positions. This combination resulted in a loss of cytotoxicity in all tested lines compared with compounds **2.9** and **2.13**, respectively. The preparation of the four pairs of derivatives **2.8**-**2.13**, **2.20** and **2.21** allowed us to evaluate the effect of the keto group at position C-11 on the antiproliferative activity. The results of the assays in all tested cell lines were consistent and revealed that the compounds from which the keto group was removed from ring C were more potent. The type of heterocyclic ring conjugated with the α,β-unsaturated ketone in ring A also influenced the antiproliferative activity. Within the group of heterocyclic derivatives with a reduced ring C, compound **2.9,** which bears an imidazole ring, was the most active derivative in all tested cell lines. This compound was 31- to 96-fold more potent than **GA**, depending on the cancer cell line. Moreover, with the exception of SH-SY5Y cells, compound **2.9** showed a similar or slightly improved antiproliferative activity against all cancer cell lines compared to the chemotherapy agent cisplatin [207-212] (Tables 2.1-2.3).

The selectivity towards cancer cells was studied for **GA** and compound **2.9** by incubating them with a human nontumoral cell line (BJ) (Table 2.3). Compound **2.9** and **GA** showed IC_{50} values that were 6.3 and 1.6 times lower on Jurkat cells than on the nontumoral BJ cells, respectively. Therefore, the heterocyclic derivative **2.9** was more selective towards malignant cells than its parent compound **GA**.

Table 2.2 Antiproliferative activities of **GA**, its heterocyclic derivatives, and cisplatin against MIAPaCa2, HeLa, A375 and MCF7 cell lines.

Compound	Cell line (IC50, μM) [1]			
	MIAPaCa2	**HeLa**	**A375**	**MCF7**
GA	101.6 ± 1.6	107.2 ± 2.5	112.2 ± 2.6	97.8 ± 3.9
2.8	14.2 ± 0.9	12.4 ± 1.2	10.4 ± 1.0	6.4 ± 0.3
2.9	3.3 ± 0.2	2.2 ± 0.1	2.0 ± 0.2	3.0 ± 0.2
2.10	10.8 ± 0.2	10.9 ± 1.0	7.1 ± 0.3	5.6 ± 0.3
2.11	3.3 ± 0.2	2.6 ± 0.2	2.3 ± 0.2	3.2 ± 0.3
2.12	28.7 ± 2.6	28.9 ± 1.7	26.5 ± 0.9	N.D.
2.13	13.4 ± 0.5	11.8 ± 0.7	10.3 ± 1.0	N.D.
2.16	17.8 ± 1.1	22.2 ± 0.8	17.9 ± 0.2	N.D.
2.17	15.2 ± 0.5	17.9 ± 0.6	13.4 ± 1.0	N.D.
2.20	12.0 ± 1.0	10.6 ± 0.1	7.2 ± 0.5	6.0 ± 0.3
2.21	6.9 ± 0.3	5.4 ± 0.3	4.9 ± 0.1	5.2 ± 0.2
Cisplatin	5.0 ± 1.0 [212]	2.3 ± 0.3 [209]	3.1 ± 1.0 [208]	19.1 ± 4.5 [209]

[1] The cell lines were treated with different concentrations of each compound for 72 h. IC_{50} values were determined by by MTT assay. Results are expressed as means ± SD of three independent experiments. IC_{50} is the concentration that inhibits 50% of cellular growth. N.D.: not determined.

Table 2.3 Antiproliferative activities of GA, its heterocyclic derivatives, and cisplatin against HepG2, SH-SY5Y and Jurkat cancer cell lines, and the nontumoral BJ cell line.

Compound	Cell line (IC50, μM) [1]			
	HepG2	**SH-SY5Y**	**Jurkat**	**BJ**
GA	125.1 ± 9.1	109.7 ± 2.5	105.8 ± 5.0	165.0 ± 7.1
2.8	14.3 ± 0.3	6.0 ± 0.2	3.2 ± 0.1	N.D.
2.9	3.1 ± 0.1	1.7 ± 0.15	1.1 ± 0.06	6.9 ± 0.07
2.10	13.5 ± 0.4	5.6 ± 0.2	2.4 ± 0.1	N.D.
2.11	3.5 ± 0.2	2.2 ± 0.2	1.3 ± 0.12	N.D.
2.12	N.D.	N.D.	N.D.	N.D.
2.13	N.D.	N.D.	N.D.	N.D.
2.16	N.D.	N.D.	N.D.	N.D.
2.17	N.D.	N.D.	N.D.	N.D.
2.20	11.8 ± 0.4	3.7 ± 0.1	1.7 ± 0.10	N.D.
2.21	9.0 ± 0.1	3.2 ± 0.1	1.5 ± 0.12	N.D.
Cisplatin	2.9 [207]	0.7 ± 0.1[210]	1.9 [211]	10.01 ± 2.0 [209]

[1] The cell lines were treated with different concentrations of each compound for 72 h. IC_{50} values were determined by XTT assay in Jurkat and SH-SY5Y cells and by MTT assay in HepG2 and BJ cells. Results are expressed as means ± SD of three independent experiments. IC_{50} is the concentration that inhibits 50% of cellular growth. N.D.: not determined.

2.2.2.2. Cell viability over Time

The Jurkat cell line, which exhibited the best results regarding antiproliferative activity among the tested cancer cell lines, was used to study the mechanism of action of the most potent compound synthesized here, the heterocyclic derivative **2.9**. Trypan blue cell-counting assays were conducted to assess the antiproliferative profile of this compound over time. The counting of viable cells was performed after incubation of Jurkat cells with compound **2.9**, at a concentration corresponding to its IC_{50} value at 72 h of treatment, or with only the vehicle (control with DMSO). As shown in Figure 2.17, compound **2.9** affected the cell growth of Jurkat cells as early as at 6 h of treatment. At this incubation time, a reduction of 18% of cell viability was observed in cells treated with compound **2.9** compared with cells that were not treated with the same compound. This effect on cell viability increased during next hours, until cell viability was 45% lower than it was in control cells at 24 h, and reached the value of 50% at 72 h of treatment. Based on the antiproliferative profile obtained in these Trypan Blue counting experiments, we established the incubation times for the subsequent biological studies that were performed in this study.

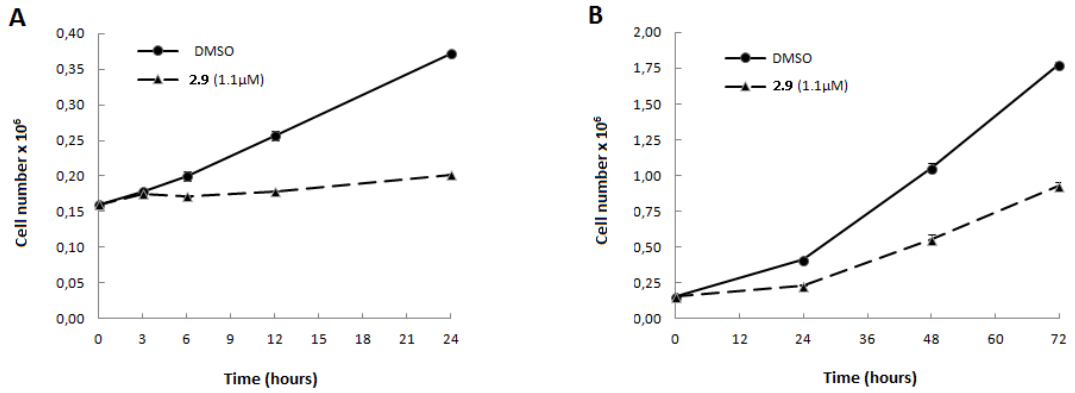

Figure 2.17 Effect of compound **2.9** on cell viability. Jurkat cells were treated with 1.1 µM compound **2.9** for different time periods ((**A**): 3, 6, 12 and 24 h; (**B**): 24, 48 and 72 h). Cell numbers were determined by Trypan Blue counting assays. Results are presented as means ± SD of three independent experiments.

2.2.2.3. Analysis of Cell Cycle Distribution and Apoptosis

Cell cycle and apoptosis assays were performed to elucidate the underlying antiproliferative mechanisms of compound **2.9**. To examine the effects on the cell cycle pattern, Jurkat cells were treated with compound **2.9**, at a concentration corresponding to its IC_{50} value at 72 h of treatment, for 3, 6 and 24 h. The study was performed using flow cytometry, and the calculation of the fraction of cells in phases G0/G1, S and G2/M was executed using the fraction of live cells. No significant changes on the cell cycle distribution were detected after 3 and 6 h of exposure; treatment for 24 h increased the population at the G0/G1 phase, with a concomitant decrease in the populations of cells at the S and the G2/M phases with respect to the untreated cells (Fig. 2.18).

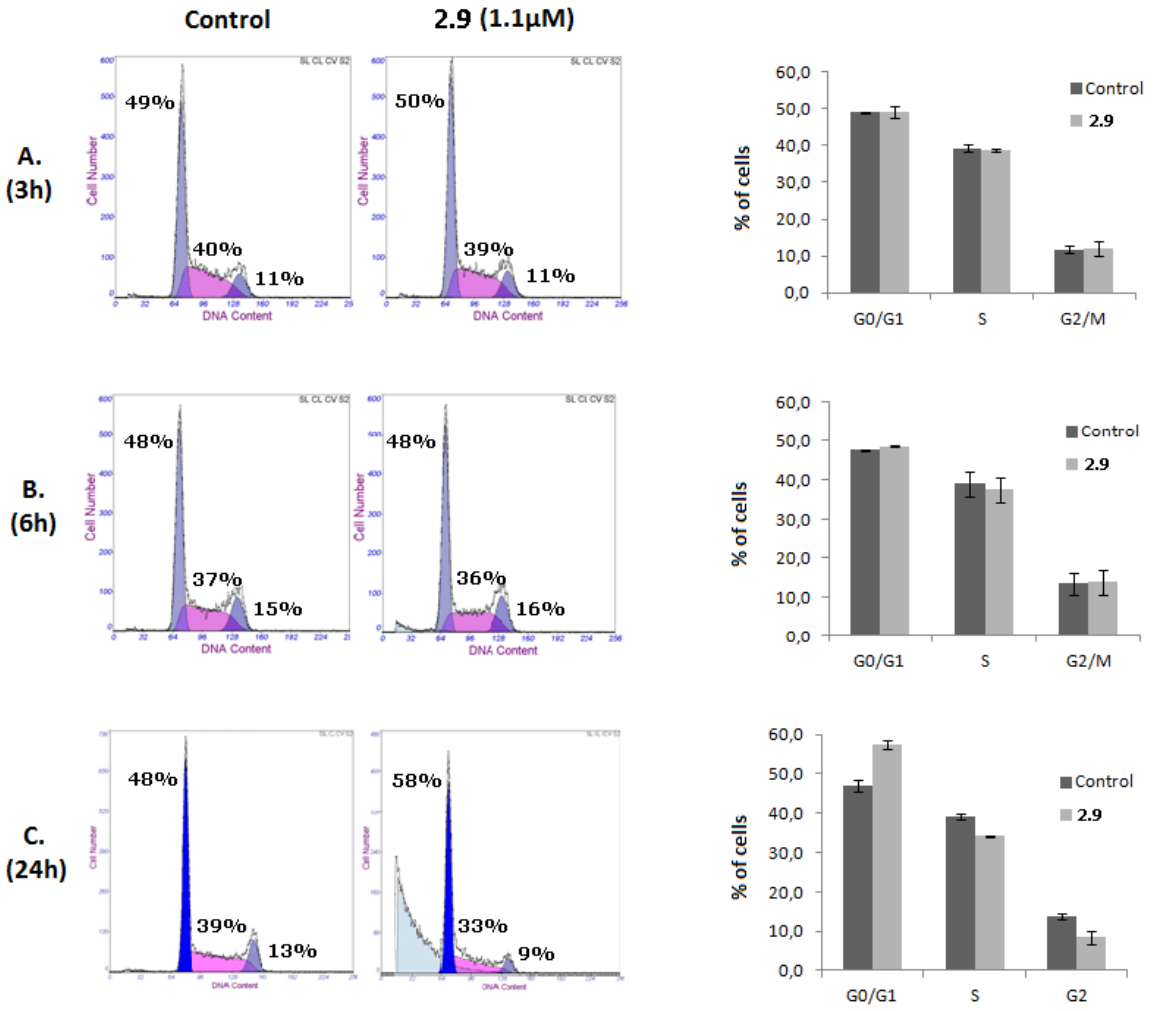

Figure 2.18 Effect of compound **2.9** on cell cycle distribution. Cell cycle analysis of Jurkat cells untreated (Control) or treated with 1.1 µM compound **2.9** for 3 (**A**), 6 (**B**) and 24 h (**C**). After treatment, cells were stained with PI and DNA content analysed by flow cytometry. A representative histogram is shown for each time of incubation and condition. Results are presented as means ± SD of three independent experiments.

Hypodiploid sub-G0 peaks that correspond to cells with DNA fragmentation were observed after 6 and 24 h of incubation. These results suggest that compound **2.9** has the ability to induce cell death in Jurkat cells.

Apoptosis assays were then conducted to elucidate the mechanism underlying the cytotoxic effect of this heterocyclic derivative. The Annexin V-FITC/PI flow cytometry assay employs the ability of Annexin V to bind to phosphatidylserine (PS) and the ability of propidium iodide (PI) to enter cells with damaged cell membranes and to bind to DNA. Early apoptosis is characterized by the loss of membrane asymmetry, with translocation of PS from the inner to the outer membrane, prior to the loss of membrane integrity. Therefore, this assay allows the discrimination of live cells (Annexin-V^-/PI^-) from early apoptotic (Annexin-V^+/PI^-), late apoptotic (Annexin-V^+/PI^+) or necrotic (Annexin-V^-/PI^+). Considering the results obtained in the cell viability and cell cycle experiments, we performed this assay on Jurkat cells after 6 and 24 h of treatment with compound **2.9** at a concentration corresponding to its IC_{50} value at 72 h of treatment. Flow cytometry dot plots representing Annexin V and PI staining are shown in Figure 2.19. Compound **2.9** induced 32% of cells to enter the early stage of apoptosis after 6 h of treatment. No significant changes were observed in the late apoptotic and necrotic populations. Exposure to the compound for 24 h increased the early apoptotic population by 25% and the late apoptotic population by 20%. The percentage of necrotic cells did not change significantly. We also performed this assay after 48 and 72 h of treatment; the Annexin V/PI profiles observed for these incubation times were similar to those obtained at 24 h (data not shown). The results of the Annexin V-FITC/PI assays are in good agreement with the hypodiploid sub-G0 peaks and their respective magnitudes, observed in the cell cycle experiments. Moreover, the fact that the appearance of G0/G1 arrest occured after the beginning of the apoptotic events indicates that cell death was caused by a primary effect of compound **2.9** and not by the activation of apoptosis as a consequence of the inability of cells to overcome cell growth arrest and proceed through the cell cycle.

We further confirmed the induction of apoptosis by examining its characteristic morphological changes in Jurkat cells treated with the same concentration of compound **2.9** for 6 h. As shown in Figure 2.20, apoptotic bodies were observed in the treated cells using a phase-contrast microscope, and Hoechst 33342 staining showed that some of those cells exhibited a highly condensed nuclear morphology. In contrast, untreated cells presented intact plasma membranes and normal nuclear morphology.

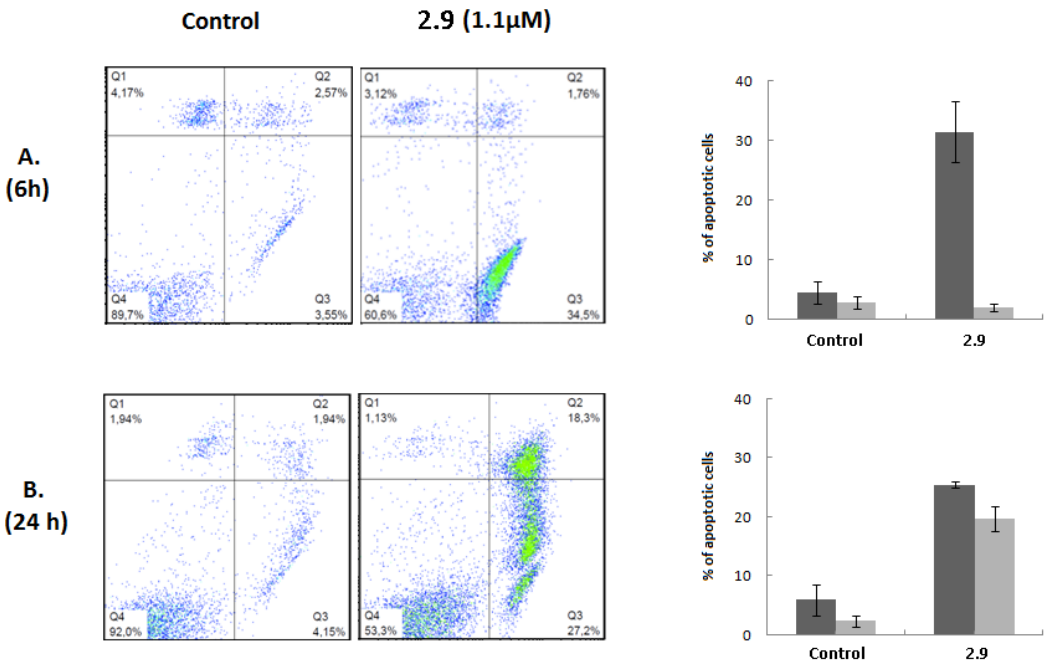

Figure 2.19 Induction of apoptosis by compound **2.9**. Flow cytometric quantification of apoptosis in Jurkat cells untreated (Control) or treated with 1.1 µM compound **2.9** for 6 (**A**) and 24 h (**B**). After treatment, cells were stained with annexin V-FICT/PI and analysed by flow cytometry. A representative dot plot is shown for each time of incubation and condition; the right quadrants of each diagram (annenix+/PI- and annexin+/PI+) represent apoptotic cells. The percentage of early (dark grey bar) and late (light grey bar) apoptotic cells in each condition is represented as a bars diagram, calculated from dot plots. Results are presented as means ± SD of three independent experiments.

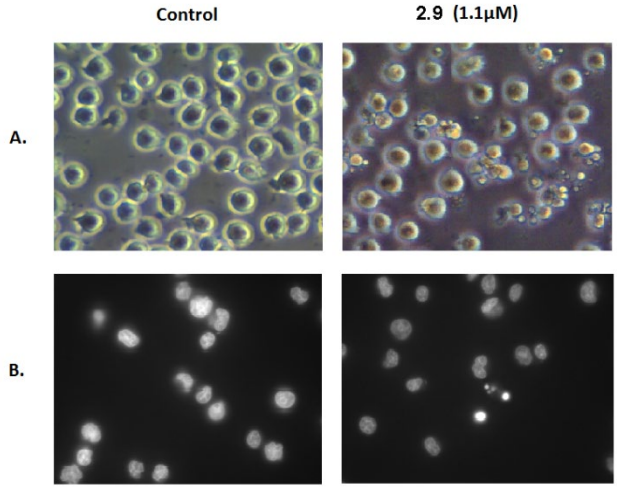

Figure 2.20 Morphological changes in Jurkat cells. Morphology of Jurkat cells untreated (Control) or treated with 1.1 µM compound **2.9** for 6 h was examined using a phase-contrast microscope (**A**) and fluorescence microscopy after Hoechst 33342 staining (**B**).

Taken together, the results described above reveal that compound **2.9** is a potent inducer of apoptosis.

Apoptosis is a process that involves the activation of caspases, as described in the first chapter. Caspase 8 is the upstream caspase for the extrinsic or death receptor pathway, whereas caspase 9 is that of the intrinsic or mitochondrial pathway. These pathways converge to caspase 3, the action of which is required for the morphological changes that are associated with apoptosis. Several reports in the literature have shown that **GA** induces apoptosis involving both the extrinsic and intrinsic pathways. To explore the mechanism via which the **GA** heterocyclic derivative **2.9** triggers this programmed cell death, we investigated its effects on the activation of caspases 3, 8 and 9 via western blotting. The proteolytic cleavage of all mentioned caspases was observed after 6 h of treatment at a dose corresponding to the IC_{50} recorded at 72 h (Fig. 2.21). These results indicate that the induced apoptosis is mediated by the activation of the both extrinsic and intrinsic pathways.

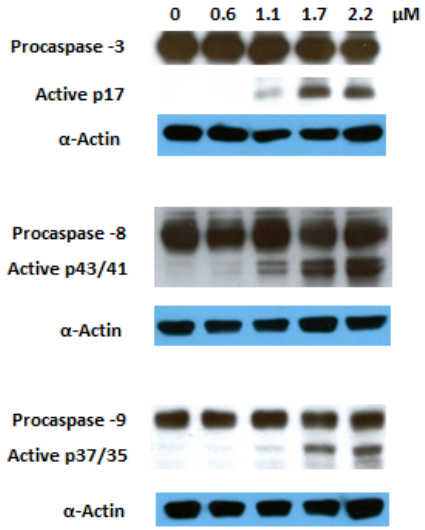

Figure 2.21 Effect of compound **2.9** on caspases 3, 8 and 9 activation in Jurkat cells after 6 h of treatment; α-actin was used as a loading control.

Cancer cells suppress apoptosis through several mechanisms, including impairing the function of the p53 tumor suppressor protein. The fact that Jurkat cells are a cancer p53-deficient cell line [213] indicates that compound **2.9** can activate the apoptotic machinery in a p53-independent manner.

Taken together, our results suggest that the induction of apoptosis involving both the intrinsic and extrinsic pathways is the main mechanism responsible for the antiproliferative activity of the **GA** heterocyclic derivative **2.9**.

2.3. Conclusion

In this study, we prepared a series of novel **GA** derivatives via the introduction of different heterocyclic rings conjugated with an α,β-unsaturated ketone in its ring A.

Screening for antiproliferative activity in a panel of nine human cancer cell lines showed that the most active compound **2.9** was 31- to 96-fold more potent than **GA**. This derivative was also 4-fold more selective towards tumor cells. Further biological studies performed in Jurkat cells suggest that potent apoptosis induction involving both the intrinsic and extrinsic pathways is the main mechanism underlying the antiproliferative activity of compound **2.9**.

The enhanced potency and selectivity, and the biological activity of this new **GA** heterocyclic derivative warrant further preclinical evaluation.

2.4. Experimental section

2.4.1. Chemistry

GA and all reagents were purchased from Sigma-Aldrich Co. (St. Louis, MO, USA). The solvents used in the reactions were obtained from Merck Co. (Kenilworth, NJ, USA) and were purified and dried according to the literature procedures. The solvents used in workups were purchased from VWR Portugal.

Thin-layer chromatography (TLC) analysis was performed in Kieselgel 60HF254/Kieselgel 60G. Purification of compounds by flash column chromatography (FCC) was carried out using Kiesegel 60 (230–400 mesh, Merck) (Kenilworth, NJ, USA).

Melting points were determined using a BUCHI melting point B-540 apparatus and were uncorrected. IR spectra were obtained on a Fourier transform spectrometer. ^{1}H and ^{13}C NMR spectra were recorded on a Bruker Avance-400 Digital NMR spectrometer, in $CDCl_3$, with Me_4Si as the internal standard. Chemical shifts values (δ) are given in parts per million (ppm) and coupling constants (*J*) are presented in hertz (Hz). Massa spectra were obtained using a Quadrupole/Ion Trap Mass Spectrometer (QIT-MS) (LCQ Advantage MAX, THERMO FINNINGAN). Elemental analysis was performed in an Analyzer Elemental Carlo Erba 1108 by chromatographic combustion.

3β-hydroxy-olean-12-en-30-oic acid (2.1): Compound **2.1** was prepared according to the literature [166], from **GA** to give a white solid (90%).m.p.: 315-317ºC.

Methyl 3β-hydroxy-11-oxo-olean-12-en-30-oate (2.2): Compound **2.2** was prepared according to the literature [143], from **GA** to give a colorless solid (90%). m.p.: 254-256ºC.

Methyl 3β-hydroxy-olean-12-en-30-oate (2.3): Compound **2.3** was prepared from **2.1**, using the same method as for the preparation of **2.2**, with the obtention of a white solid (88%). m.p.: 239-242ºC.

Methyl 3,11-dioxo-olean-12-en-30-oate (2.4): Compound **2.4** was prepared according to the literature [206], from **2.2** to give a white solid (94%). m.p.: 248-250ºC.

Methyl 3-oxo-olean-12-en-30-oate (2.5): Compound **2.5** was prepared from **2.3**, using the same method as for the preparation of **2.4**, with the obtention of a white solid (92%). m.p.: 185-188ºC.

Methyl 2-hydroxymethylene-3,11-dioxo-olean-12-en-30-oate (2.6): Compound **2.6** was prepared according to the literature [206], from **2.4** to give a colorless solid (82%). m.p.: 231-234ºC.

Methyl 2-hydroxymethylene-3-oxo-olean-12-en-30-oate (2.7): Compound **2.7** was prepared from **2.5**, using the same method as for the preparation of **2.6**, with the obtention of a white solid (80%). m.p.: 136-139ºC.

Methyl 2-(1*H*-imidazol-1-yl)-methylene-3,11-dioxo-olean-12-en-30-oate (2.8): To a solution of compound **2.6** (300 mg, 0.59 mmol) in anhydrous THF (5 ml), CDI (191 mg,

1.18 mmol) was added. After 4 h under magnetic stirring at reflux temperature and N_2 atmosphere, the reaction was completed. Water (50 ml) and ethyl acetate (50 ml) were added to the reaction mixture. The aqueous phase was further extracted with ethyl acetate (2 x 50 ml). The combined organic extract was then washed with water (2 x 50 ml) and brine (50 ml), dried over Na_2SO_4, filtered and evaporated to dryness. The resulting solid was subjected to FCC [petroleum ether/ ethyl acetate from (1:1) to (1:2)] to afford **2.8** as white solid (67%). m.p.: 249-251°C. IR ν_{max}/cm^{-1} (KBr): 3113, 2953, 1728, 1685, 1649, 1601, 1518, 1485, 1458, 1385, 1306, 1028. ^{1}H NMR (400MHz, $CDCl_3$): δ 7.76 (1H,s), 7.66 (1H, s), 7.33 (1H,s), 7.10 (1H, s), 5.75 (1H, s), 4.19 (1H, d, *J* = 16.5), 3.67 (3H, s), 2.52 (1H, s), 1.39 (3H, s), 1.18 (3H, s), 1.16 (3H, s), 1.13 (6H, s), 1.12 (3H, s), 0.81 (3H, s). ^{13}C NMR (100MHz, $CDCl_3$): δ 206.2, 199.2, 176.8, 170.6, 139.1, 130.7, 130.3, 128.4, 122.1, 119.0, 59.2, 52.8, 51.7, 48.4, 45.3, 44.8, 44.0, 43.3, 43.2, 41.2, 37.6, 35.9, 31.8, 31.3, 31.0, 29.7, 28.5, 28.2, 26.5, 26.3, 23.1, 22.3, 19.5, 17.9, 15.5. ESI-MS *m/z*: 561.71 ($[M+H]^+$, 100%). Found C 74.45, H 8.80, N 5.05, calcd for $C_{35}H_{48}N_2O_4$: C 74.96, H 8.63, N 5.00%.

Methyl 2-(1*H*-imidazol-1-yl)-methylene-3-oxo-olean-12-en-30-oate (2.9): The method followed that described for compound **2.8** but using compound **2.7** (300 mg, 0.60 mmol) and CDI (195 mg, 1.20 mmol) in anhydrous THF (5 ml) at reflux for 5 h. The resulting solid was purified by FCC with petroleum ether/ ethyl acetate (1:1) and afforded compound **2.9** as a white solid (60%). m.p.: 151-154°C. IR ν_{max}/cm^{-1} (KBr): 3118, 2951, 1730, 1687, 1610, 1518, 1487, 1458, 1383, 1306, 1028. ^{1}H NMR (400MHz, $CDCl_3$): δ 7.78 (1H,s), 7.70 (1H,s), 7.22 (1H,s), 7.15 (1H,s), 5.34 (1H, t, *J* = 3.4), 3.68 (3H, s), 2.90 (1H, d, *J* = 16.0), 1.18 (6H, s), 1.13 (6H, s), 1.02 (3H, s), 0.91 (3H, s), 0.78 (3H, s). ^{13}C NMR (100MHz, $CDCl_3$): δ 206.7, 177.6, 144.6, 138.7, 130.7, 130.5, 122.9, 122.0, 119.2, 52.6, 51.6, 48.4, 45.4, 45.2, 44.3, 43.2, 42.8, 41.9, 39.7, 38.3, 36.0, 32.0, 31.7, 31.3, 29.8, 28.5, 28.2, 27.0, 26.1, 25.7, 23.8, 22.5, 20.3, 16.4, 15.6. ESI-MS *m/z*: 547.73 ($[M+H]^+$, 100%). Found C 76.72, H 9.43, N 4.98, calcd for $C_{35}H_{50}N_2O_3$: C 76.88, H 9.22, N 5.12%.

Methyl 2-(2'-methyl-1*H*-imidazol-1-yl)-methylene-3,11-dioxo-olean-12-en-30-oate (2.10): To a solution of compound **2.6** (300 mg, 0.59 mmol) in anhydrous THF (5 ml), CBMI (231 mg, 1.18 mmol) was added. After 2 h under magnetic stirring at reflux

temperature and N_2 atmosphere, the reaction was completed. The workup was performed according to the same method as for **2.8**. The resulting solid was submitted to FCC [petroleum ether/ ethyl acetate from (1:1) to (1:4)] to afford **2.10** as a white solid (70%). m.p.: 146-149°C.IR ν_{max}/cm^{-1} (KBr): 3116, 2953, 1730, 1686, 1657, 1608, 1541, 1502, 1458, 1412, 1385. ^{1}H NMR (400MHz, $CDCl_3$): δ 7.64 (1H,s), 7.29 (1H,s), 6.94 (1H,s), 5.75 (1H,s), 4.17 (1H, d, *J* = 16.3), 3.67 (3H, s), 2.52 (1H, s), 2.47 (3H, s), 1.39 (3H, s), 1.19 (3H, s), 1.17 (3H, s), 1.14 (9H, s), 0.82 (3H, s). ^{13}C NMR (100MHz, $CDCl_3$): δ 206.4, 199.3, 176.8, 170.5, 147.3, 129.9, 128.7, 128.5, 122.3, 118.1, 59.2, 53.0, 51.8, 48.5, 45.4, 44.9, 44.0, 43.4, 42.6, 41.2, 37.7, 36.0, 31.8, 31.3, 31.1, 29.7, 28.6, 28.3, 26.5, 26.3, 23.2, 22.4, 19.5, 18.0, 15.4, 13.7. ESI-MS *m/z*: 575.86 ($[M+H]^+$, 100%). Found C 74.91, H 9.01, N 4.78, calcd for $C_{36}H_{50}N_2O_4$: C 75.22, H 8.77, N 4.87%.

Methyl 2-(2'-methyl-1*H*-imidazol-1-yl)-methylene-3-oxo-olean-12-en-30-oate (2.11): The method followed that described for compound **2.10** but using compound **2.7** (300 mg, 0.60 mmol) and CBMI (235 mg, 1.20 mmol) in anhydrous THF (5 ml) at reflux for 4 h. The resulting solid was subjected to FCC [petroleum ether/ ethyl acetate from (1:1) to (1:4)] to afford **2.11** (63%). m.p.: 134-137°C. IR ν_{max}/cm^{-1} (KBr): 3118, 2951, 1730, 1687, 1606, 1541, 1502, 1456, 1412, 1383. ^{1}H NMR (400MHz, $CDCl_3$): δ 7.66 (1H,s), 7.14 (1H,s), 7.00 (1H,s), 5.33 (1H, t, *J* = 3.4), 3.67 (3H, s), 2.87 (1H, d, *J* = 15.9), 2.48 (3H, s), 1.18 (6H, s), 1.15 (3H, s), 1.12 (3H, s), 1.01 (3H, s), 0.90 (3H, s), 0.78 (3H, s). ^{13}C NMR (100MHz, $CDCl_3$): δ 206.7, 177.6, 147.3, 144.6, 130.2, 128.3, 123.8, 122.0, 118.2, 52.7, 51.6, 48.4, 45.4, 45.3, 44.3, 42.8, 42.5, 41.9, 39.7, 38.3, 36.1, 32.0, 31.7, 31.3, 29.7, 28.5, 28.2, 26.9, 26.1, 25.7, 23.7, 22.6, 20.3, 16.4, 15.5, 13.6. ESI-MS *m/z*: 561.77 ($[M+H]^+$, 100%). Found C 76.85, H 9.67, N 4.64, calcd for $C_{36}H_{52}N_2O_3$: C 77.10, H 9.35, N 5.00%.

Methyl 2-(1*H*-triazol-1-yl)-methylene-3,11-dioxo-olean-12-en-30-oate (2.12): To a solution of compound **2.6** (300 mg, 0.59 mmol) in anhydrous THF (6 ml), CDT (581 mg, 3.54 mmol) was added. The workup was performed after 24 h of reaction, under magnetic stirring at reflux temperature and N2 atmosphere, using the same procedure as for compound **2.8**. The resulting solid was purified by FCC with petroleum ether/ ethyl acetate (1:2) and afforded **2.12** as a white solid (41%). m.p.: 148-151°C. IR ν_{max}/cm^{-1}

(KBr): 3122, 2953, 1730, 1691, 1657, 1618, 1508, 1460, 1385. ^{1}H NMR (400MHz, $CDCl_3$): δ 8.40 (1H,s), 8.06 (1H,s), 7.80 (1H,s), 5.76 (1H,s), 4.42 (1H, d, *J* = 18.6), 3.69 (3H, s), 2.57, 1.40 (3H, s), 1.22 (3H, s), 1.17 (3H, s), 1.15 (3H, s), 1.14 (6H, s), 0.82 (3H, s). ^{13}C NMR (100MHz, $CDCl_3$): δ 206.4, 199.1, 176.9, 170.1, 152.7, 145.3, 128.7, 128.6, 125.1, 59.1, 53.0, 51.8, 48.5, 45.4, 44.9, 44.0, 43.7, 43.4, 41.2, 37.7, 35.7, 31.9, 31.4, 31.1, 29.8, 28.6, 28.3, 26.6, 26.4, 23.1, 22.4, 19.6, 18.0, 15.5. ESI-MS *m/z*: 274.48 (87%), 302.51 (15), 318.49 (100), 346.54 (22), 362.37 (37), 374.60 (11), 562.68 ($[M+H]^+$, 93), 563.71 ($[M+2H]^{2+}$, 26), 575.80 (24), 622.48 (15), 624.80 (21).

Methyl 2-(1*H*-triazol-1-yl)-methylene-3-oxo-olean-12-en-30-oate (2.13): The method followed that described for compound **2.12** but using compound **2.7** (300 mg, 0.60 mmol) and CDT (591 mg, 3.60 mmol) in anhydrous THF (6 ml) at reflux for 26 h. The resulting solid was purified by FCC with petroleum ether/ ethyl acetate (3:1) and afforded **2.13** as a white solid (44%). m.p.: 137-140°C. IR ν_{max}/cm^{-1} (KBr): 3122, 2951, 1732, 1689, 1622, 1512, 1456, 1383. ^{1}H NMR (400MHz, $CDCl_3$): δ 8.34 (1H,s), 8.07 (1H,s), 7.78 (1H,s), 5.36 (1H, t, *J* = 3.2), 3.69 (3H, s), 3.41 (1H, d, *J* = 17.6), 1.20 (3H, s), 1.19 (3H, s), 1.14 (3H, s), 1.13 (3H, s), 1.03 (3H, s), 0.92 (3H, s), 0.79 (3H, s). ^{13}C NMR (100MHz, $CDCl_3$): δ 207.4, 177.8, 153.1, 146.0, 144.5, 128.4, 125.6, 122.5, 52.9, 51.7, 48.6, 45.5, 45.3, 44.4, 43.5, 43.0, 42.0, 39.8, 38.5, 35.9, 32.2, 31.8, 31.4, 29.9, 28.7, 28.4, 27.1, 26.2, 25.8, 23.9, 22.6, 20.5, 16.5, 15.9. ESI-MS *m/z*: 274.53 (89%), 302.57 (23), 318.52 (100), 330.56 (14), 346.56 (27), 362.53 (25), 374.60 (16), 548.68 ($[M+H]^+$, 93), 549.70 ($[M+2H]^{2+}$, 28), 561.81 (23), 578.36 (20).

3-Oxo-olean-12-en-30-oic acid (2.14): Compound **2.14** was prepared from **2.1**, using the same method as for the preparation of **2.4**, with the obtention of a white solid (93%). m.p.: 245-248°C. IR ν_{max}/cm^{-1} (KBr): 3396, 2949, 1732, 1703, 1460, 1385. ^{1}H NMR (400MHz, $CDCl_3$): δ 5.31 (1H, t, *J* = 3.2), 2.33-2.59 (2H, m), 1.20 (3H, s), 1.14 (3H, s), 1.09 (3H, s), 1.06 (3H, s), 1.05 (3H, s), 1.01 (3H, s), 0.82 (3H, s). ^{13}C NMR (100MHz, $CDCl_3$): δ 217.9, 183.4, 144.2, 122.5, 55.3, 48.0, 47.4, 46.8, 44.0, 42.4, 41.6, 39.7, 38.2, 36.6, 34.1, 32.1, 31.9, 31.0, 28.6, 28.1, 26.9, 26.4, 26.0, 25.8, 23.5, 21.4, 19.6, 16.6, 15.1. ESI-MS^2 (25%) *m/z*: 274.98 ($[M+H-C_{12}H_{20}O]^+$, 16%), 408.61 ($[M+H-H_2O-C_2H_4]^+$ or $[M+H-HCOOH]^+$, 39); 437 ($[M+H-H_2O]^+$, 7), 455.42 ($[M+H]^+$, 100).

2-Hydroxymethylene-3-oxo-olean-12-en-30-oic acid (2.15): The method followed that described for compound **2.6** but using compound **2.14** (850 mg, 1.87 mmol), ethyl formate (1.1 ml, 13.09 mmol) and sodium methoxide (1010 mg, 18.70 mmol), with the obtention of a white solid (77%). m.p.: 154-158 °C. IR ν_{max}/cm^{-1} (KBr): 3442, 2953, 1731, 1699, 1643, 1587, 1456, 1383. ^{1}H NMR (400MHz, $CDCl_3$): δ 14.91 (1H, d, *J* = 3.0), 8.59 (1H, d, *J* = 2.7), 5.35 (1H, t, *J* = 3.4), 2.30 (1H, d, *J* = 14.4), 1.21 (3H, s), 1.20 (3H, s), 1.16 (3H, s), 1.13 (3H, s), 1.02 (3H, s), 0.93 (3H, s), 0.83 (3H, s). ^{13}C NMR (100MHz, $CDCl_3$): δ 190.8, 188.4, 183.4, 144.3, 122.6, 105.8, 52.1, 48.1, 45.6, 44.1, 42.6, 41.7, 40.2, 39.6, 39.4, 38.3, 36.2, 32.0, 31.9, 31.1, 28.7, 28.5, 28.2, 27.0, 26.1, 25.8, 23.5, 20.9, 19.6, 16.6, 14.7. ESI-MS^2 (25%) *m/z*: 437.35 ($[M+H-H_2O-C_2H_4]^+$ or $[M+H-HCOOH]^+$, 44%), 465.36 ($[M+H-H_2O]^+$, 100), 483.32 ($[M+H]^+$, 56).

30-(1*H*-Imidazol-1-yl)-3,30-dioxo-olean-12-en-2-(1*H*-imidazol-1-yl)-methylene (2.16): Compound **2.16** was prepared using the same method as for the preparation of **2.8**, but using compound **2.15** (300 mg, 0.62 mmol) and CDI (302 mg, 1.86 mmol) in anhydrous THF (6 ml) at reflux for 6 h. The resulting solid was submitted to FCC [petroleum ether/ ethyl acetate from (1:2) to (1:8)] to afford **2.16** as a white solid (56%). m.p.: 162-165°C. IR ν_{max}/cm^{-1} (KBr): 3124, 2937, 1713, 1687, 1610, 1522, 1489, 1456, 1383, 1308, 1227, 1173, 1030. ^{1}H NMR (400MHz, $CDCl_3$): δ 8.30 (1H, s), 7.78 (1H, s), 7.70 (1H, s), 7.58 (1H, s), 7.24 (1H, s), 7.17 (1H, s), 7.08 (1H, s), 5.19 (1H, t, *J* = 3.4), 2.90 (1H, d, *J* = 16.0), 1.44 (3H, s), 1.19 (3H, s), 1.18 (3H, s), 1.13 (3H, s), 0.99 (3H, s), 0.90 (3H, s), 0.79 (3H, s). ^{13}C NMR (100MHz, $CDCl_3$): δ 206.6, 174.0, 143.8, 138.7, 137.2, 130.7, 130.6, 129.8, 122.8, 122.7, 119.2, 117.4, 52.5, 48.1, 46.6, 45.4, 45.2, 44.4, 43.2, 41.9, 39.6, 37.5, 35.9, 32.9, 32.2, 31.7, 29.8, 27.9, 27.9, 27.2, 25.9, 25.5, 23.7, 22.4, 20.3, 16.4, 15.6. ESI-MS^2 (25%) *m/z*: 487.54 ($[M+H-C_3H_3N_2-C_2H_4]^+$ or $[M+H-C_4H_3N_2O]^+$, 100%), 555.31 ($[M+H-C_2H_4]^+$, 2), 583.44 ($[M+H]^+$, 16).

30-(1*H*-Triazol-1-yl)-3,30-dioxo-olean-12-en-2-(1*H*-triazol-1-yl)-methylene (2.17): The method followed that described for compound **2.16** but using compound **2.15** (300 mg, 0.62 mmol) and CDT (1018 mg, 6.20 mmol) in anhydrous THF (6 ml) at reflux for 38 h. The resulting solid was submitted to FCC [petroleum ether/ ethyl acetate from (2:1)

to (1:1)] to afford **2.17** as a white solid (38%). m.p.: 142-145°C. IR ν_{max}/cm^{-1} (KBr): 3126, 2954, 1713, 1695, 1618, 1512, 1456, 1383, 1279, 1161, 1132. ^{1}H NMR (400MHz, $CDCl_3$): δ 8.39 (1H, s), 8.25 (2H, s), 8.09 (1H, s), 7.80 (1H, s), 5.39 (1H, t, *J* = 3.4), 3.39 (1H, d, *J* = 17.5), 1.21 (3H, s), 1.20 (6H, s), 1.14 (3H, s), 1.03 (3H, s), 0.92 (3H, s), 0.82 (3H, s). ^{13}C NMR (100MHz, $CDCl_3$): δ 207.6, 182.0, 152.8, 146.9 (2), 146.0, 144.5, 128.4, 125.8, 122.6, 52.9, 48.4, 45.5, 45.3, 44.2, 43.5, 42.8, 42.0, 39.8, 38.4, 35.9, 32.2, 31.8, 31.3, 29.9, 28.9, 28.4, 27.1, 26.2, 25.8, 23.9, 22.6, 20.5, 16.5, 15.9. ESI-MS^2 (35%) *m/z*: 488.42 ($[M+H-C_2H_3N_3-C_2H_4]^+$ ou $[M+H-C_3H_3N_3O]^+$, 100%), 514.64 ($[M+H-C_4H_6O]^+$, 5), 584.67 (M^+, 4), 585.77 ($[M+H]^+$, 3).

Methyl 2-azidomethylene-3,11-dioxo-olean-12-en-30-oate (2.18): To a solution of compound **2.6** (700 mg, 1.37 mmol) in dichloromethane (14 ml), triethylamine (Et_3N) (573 µl, 4.11 mmol) and tosyl chloride (TsCl) (654 mg, 3.43 mmol) were added. After 3.5 h under magnetic stirring at room temperature, the reaction was completed. The solvent of the reaction mixture was removed under reduced pressure and the residue was suspended in acetone (14 ml); sodium azide (NaN_3) (134 mg, 2.06 mmol) was added. After 5 h under magnetic stirring at room temperature, the reaction was completed. The acetone was removed under reduced pressure and water (60 ml) and ethyl acetate (60 ml) were added to the residue. The aqueous phase was further extracted with ethyl acetate (2 x 60 ml). The combined organic extract was then washed with water (3 x 50 ml), dried over Na_2SO_4, filtered and evaporated to the dryness, to afford a solid. The solid was subjected to flash FCC with petroleum ether/ ethyl acetate (15:1) to afford **2.18** as a white solid (62%). m.p.: 167-170°C. IR ν_{max}/cm^{-1} (KBr): 2951, 2127, 1730, 1659, 1460, 1387. ^{1}H NMR (400MHz, $CDCl_3$): δ 7.37 (1H, d, *J* = 1.5), 5.72 (1H, s), 3.76 (1H, d, *J* = 16.5), 3.69 (3H,s), 2.46 (1H,s), 1.37 (3H,s), 1.15 (3H,s), 1.14 (3H,s), 1.11 (3H,s), 1.09 (6H,s), 0.81 (3H,s). ^{13}C NMR (100MHz, $CDCl_3$): δ 205.0, 199.1, 176.9, 169.7, 137.2, 128.6, 123.0, 59.1, 53.4, 51.8, 48.3, 45.2, 44.9, 44.0, 43.3, 41.2, 40.6, 37.7, 35.7, 31.8, 31.6, 31.1, 29.3, 28.6, 28.3, 26.5, 26.4, 23.2, 22.5, 19.5, 18.0, 15.2. ESI-MS^2 (35%) *m/z*: 462.38 ($[M+H-C_3H_6O_2]^+$, 100%), 508.46 ($[M+H-CO]^+$ ou$[M+H-C_2H_4]^+$, 12), 518.37 ($[M+H-H_2O]^+$, 43), 536.61 ($[M+H]^+$, 7).

Methyl 2-azidomethylene-3-oxo-olean-12-en-30-oate (2.19): Compound **2.19** was prepared using the same method as for the preparation of **2.18**, but using compound **2.7** (700 mg, 1.41 mmol) in dichloromethane (14 ml), Et_3N (492 µl, 3.53 mmol), TsCl (538 mg, 2.82 mmol), and then NaN_3 (138 mg, 2.12 mmol) in acetone (14 ml). The resulting solid was subjected to flash FCC with petroleum ether/ ethyl acetate (20:1) to afford **2.19** as a white solid (57%). m.p.: 186-189°C. IR ν_{max}/cm^{-1} (KBr): 2943, 2116, 1730, 1672, 1589, 1452, 1383. ^1H NMR (400MHz, $CDCl_3$): δ 7.36 (1H, d, *J* = 1.6), 5.33 (1H, t, *J* = 3.4), 3.68 (3H,s), 2.66 (1H, d, *J* = 16.6), 1.15 (3H,s), 1.13 (3H,s), 1.09 (6H,s), 1.01 (3H,s), 0.88 (3H,s), 0.79 (3H,s). ^{13}C NMR (100MHz, $CDCl_3$): δ 205.7, 177.6, 144.3, 137.1, 123.2, 122.4, 53.1, 51.6, 48.3, 45.2, 45.1, 44.3, 42.8, 41.8, 40.2, 39.6, 38.3, 35.7, 32.0, 31.8, 31.3, 29.2, 28.5, 28.2, 27.0, 26.0, 25.7, 23.6, 22.6, 20.3, 16.4, 15.4. ESI-MS^2 (35%) *m/z*: 462.48 $([M+H-H_3COH-C_2H_4]^+$ ou $[M+H-H_3CCOOH]^+$, 32%), 504.31 $([M+H-H_2O]^+$, 100), 522.38 $([M+H]^+$, 7).

Compound 2.20: To a solution of compound **2.18** (350 mg, 0.65 mmol) in THF (7 ml), methyl propiolate (64.4 µl, 0.72 mmol) and CuI (12.4 mg, 0.065 mmol) were added. After 4 h under magnetic stirring at 65°C, the reaction was completed. The reaction mixture was filtered and evaporated to dryness. The resulting solid was purified by FCC [petroleum ether/ ethyl acetate from (8:1) to (2:1)] to afford **2.20** as a white solid (42%). m.p.: 184-186°C. IR ν_{max}/cm^{-1} (KBr): 3136, 2951, 1747, 1726, 1691, 1651, 1620, 1554, 1458, 1385, 1209, 1034. ^1H NMR (400MHz, $CDCl_3$): δ 8.42 (1H, s), 7.99 (1H, s), 5.74 (1H,s), 4.17 (1H, d, *J* = 17.5), 3.96 (3H, s), 3.69 (3H,s), 2.53 (1H,s), 1.41 (3H, s), 1.22 (3H, s), 1.16 (3H,s), 1.14 (9H,s), 0.81 (3H,s). ^{13}C NMR (100MHz, $CDCl_3$): δ 205.8, 198.8, 176.9, 170.3, 160.7, 140.1, 128.8, 128.5, 128.2, 127.7, 59.0, 53.0, 52.4, 51.8, 48.5, 45.6, 44.9, 44.0, 43.6, 43.4, 41.2, 37.7, 35.9, 31.9, 31.3, 31.1, 29.7, 28.6, 28.3, 26.5, 26.4, 23.1, 22.3, 19.5, 17.9, 15.6. ESI-MS *m/z*: 620.59 $([M+H]^+$, 100%). Found C 69.39, H 8.21, N 6.66, calcd for $C_{36}H_{49}N_3O_6$: C 69.76, H 7.97, N 6.78%.

Compound 2.21: Compound **2.21** was prepared using the same method as for the preparation of **2.20**, but using compound **2.19** (350 mg, 0.67 mmol), methyl propiolate (66.0 µl, 0.74 mmol) and CuI (12.8 mg, 0.067 mmol). The resulting solid was purified by FCC [petroleum ether/ ethyl acetate from (8:1) to (2:1)] to afford **2.21** as a white solid

(44%). m.p.: 125-127°C. IR ν_{max}/cm^{-1} (KBr): 3143, 2953, 1730, 1699, 1620, 1556, 1456, 1385, 1221, 1034. ^{1}H NMR (400MHz, $CDCl_3$): δ 8.30 (1H, s), 7.90 (1H, s), 5.32 (1H, t, *J* = 3.4), 3.98 (3H, s), 3.68 (3H,s), 3.18 (1H, d, *J* = 18.5), 1.21 (3H, s), 1.18 (3H,s), 1.15 (3H, s), 1.13 (3H, s), 1.01 (3H,s), 0.92 (3H,s), 0.78 (3H, s). ^{13}C NMR (100MHz, $CDCl_3$): δ 206.6, 177.6, 160.7, 144.3, 139.8, 129.2, 128.5, 128.3, 122.2, 52.7, 52.5, 51.6, 48.4, 45.5, 45.2, 44.2, 43.6, 42.7, 41.8, 39.6, 38.3, 35.9, 32.0, 31.6, 31.3, 29.6, 28.5, 28.2, 26.9, 26.0, 25.6, 23.7, 22.4, 20.3, 16.3, 15.8. ESI-MS *m/z*: 606.33 ($[M+H]^+$, 100%) Found C 71.58, H 8.58, N 6.88, calcd for $C_{36}H_{51}N_3O_5$: C 71.37, H 8.49, N 6.94%.

2.4.2. Biology

HT-29, A549, MIA PaCa 2, HeLa, A375, MCF7, HepG2, SH-SY5Y, Jurkat and BJ cells were purchased from the American Type Culture Collection (ATCC, Rockville, MD). Dulbecco´s Modified Eagle's Medium (DMEM), Roswell Park Memorial Institute (RPMI)-1640 medium, Phosphate Buffered Saline (PBS), glucose 45%, insulin human 10 mg/ml, dimethyl sulfoxide (DMSO), MTT powder, Trypan Blue (TB) 0.4%, PI, Hoescht 33342 and Protease Inhibitor Cocktail were obtained from Sigma Aldrich Co. (St. Luis, MO, USA). Minimum Essential Medium (MEM), penicillin/streptomycin (P/S) and L-glutamine were purchased from Gibco-BRL (Eggenstein, Germany). Sodium pyruvate, trypsin/EDTA (0.05%/0.02%), MEM-Eagle Non Essential Aminoacids 100x and ECL Western Blotting Detection Kit Reagent were obtained from Biological Industries (Kibbutz Beit Haemek, Israel). Fetal Bovine Serum (FBS) was obtained from PAA Laboratories (Pasching, Austria), the Cell Proliferation Kit II (XTT kit) was purchased from Roche (Roche Molecular Biochemicals, Indianapolis, IN) and annexin V-FITC was obtained from Bender MedSystems (Vienna, Austria). Primary antibodies against caspases 3 (#9662), 8 (#9746) and 9 (#9502) were purchased from Cell Signaling Technology (Beverly, MA, USA) and primary antibody against α-actin (#69100) was obtained from MP Biomedicals (Santa Ana, CA, USA). Secondary antibodies HRP-conjugated goat anti-rabbit (NA934) and HRP-conjugated rabbit anti-mouse (P02060) were purchased from Amersham Biosciences (Uppsala, Sweden) and DAKO (Copenhagen, Denmark), respectively.

Stock solutions of 20 mM in DMSO of the synthesized compounds were prepared and stored at -20°C. Working solutions were prepared in culture medium and appropriate amounts of DMSO were included in controls; all solutions had a final concentration of 0.5% DMSO.

2.4.2.1. Cell culture

HT-29, A549, MIA PaCa 2, HeLa, A375 and SH-SY5Y cells were cultured in DMEM supplemented with 10% heat-inactivated FBS and 1% P/S. HepG2 and BJ cells were grown in DMEM supplemented with 10% heat-inactivated FBS, 1% P/S and 1 mM sodium pyruvate. Jurkat cells were cultured in RPMI-1640 medium supplemented with 10% heat-inactivated FBS, 1% P/S and 2 mM L-glutamine. MCF7 cells were maintained in MEM supplemented with 10% heat-inactivated FBS, 0.1% P/S, 1 mM sodium pyruvate, 2 mM L-glutamine, 1x MEM-Eagle Non Essential Aminoacids, 0.01mg/ml insulin human and 10 mM glucose.

All cell cultures were incubated in a 5% CO_2 humidified atmosphere at 37°C.

2.4.2.2. Antiproliferative assays

The antiproliferative activity of the synthesized compounds on HT-29, A549, MIA PaCa 2, HeLa, A375, MCF7, HepG2 and BJ cells was determined by the MTT assay. Exponentially growing cells were plated in 96-well plates at a density of 1-8 x 10^3 cells/ well. After 24 h of incubation, the growth medium was replaced with fresh medium containing either the compounds dissolved in DMSO at different concentrations or only with DMSO, in triplicate, and the cells were continued to culture for 72h. After incubation with the compounds, the medium was removed and 100 µl of MTT solution (0.5 mg/ml) were added to each well and the plates were incubated for 1 h. MTT was removed and 100 µl of DMSO was added to dissolve the formazan crystals. The absorbance was immediately read at 550 nm on an ELISA plate reader (Tecan Sunrise MR20-301, TECAN, Austria). For SH-SY5Y and Jurkat cells, the antiproliferative activity was determined by XTT assay. SH-SY5Y cells were plated with 1.6 x 10^4 cells/ well in 96-well plates in 100 µl medium. The compounds at different concentrations or only the vehicle (medium with 0.5% DMSO), in 100 µl, were added 24 h after seeding, in triplicate, and incubated for 72 h. For Jurkat cells, 5.5 x 10^3 cells/ well were plated

simultaneously with the addition of the different concentrations of compounds or vehicle, in triplicate, and were allowed to incubate for 72 h. In both cases, after that incubation period, 100 µl of the XTT labelling mixture were added to each well and the plates were incubated again for 4 h. Then, the absorbance was read at 450 nm on the ELISA plate reader.

Concentrations that inhibit cell proliferation by 50% (IC_{50}) represent an average of a minimum of three independent experiments and were expressed as means ± standard deviation (SD).

2.4.2.3. Cell Viability over Time assays

The viability over time of Jurkat cells, treated with compound **2.9**, was assessed by TB cell counting experiments. For these assays, 1.6 x 10^5 cells were plated per well in 6-well plates simultaneously with the addition of compound **2.9**, in the concentration of its IC_{50} value at 72 h, or only vehicle, in a total volume of 2 ml of medium. After each incubation time (3, 6, 12, 24, 48 and 72 h), the suspension of cells of each well was collected. Equal amounts of TB solution and suspension were mixed and the mixture was placed in a Neubauer chamber in order to perform the counting.

The number of cells determined for each condition, in each incubation time, represents an average of three independent experiments, with two replicates per experiment.

2.4.2.4. Cell Cycle Analysis

Cell cycle was assessed by flow cytometry using a fluorescence-activated cell sorter (FACS). Jurkat cells were plated in 6-well plates at a density of 1.6 x 10^5 cells, simultaneously with the addition of compound **2.9**, at a concentration corresponding to its IC_{50} value at 72 h of treatment, or with only the vehicle, in a total volume of 2 ml of medium. The cells were allowed to incubate for 3, 6 and 24 h. After incubation, cells were collected and centrifuged. The supernatant was removed and the pellet was resuspended in 1 ml of TBS containing 1mg/ml PI, 10 mg/ml RNase free of DNase and 0.1% Igepal CA-630, for 1 h, at 4°C. FACS analysis was performed at 488 nm in an Epics XL flow cytometer (Coulter Corporation, Hialeah, FL, USA). Data were collected

and analyzed using the Multicycle software (Phoenix Flow Systems, San Diego, CA, USA).

Three independent experiments were performed, with two replicates per experiment.

2.4.2.5. Annexin V-FITC/ PI Flow Citometry Assay

Apoptosis was assessed by flow cytometry using a FACS. The same number of Jurkat cells taken for the cell cycle assay was treated as described above. The cells were allowed to incubate for 6 and 24 h. After incubation, cells were collected and centrifuged. The supernatant was removed and the pellet was resuspended in 95 µl of binding buffer (10 mM HEPES/NaOH, pH 7.4, 140 mM NaCl, 2.5 mM $CaCl_2$). Annexin V-FITC conjugate (3 µl) was added and cells were incubated for 30 min, at room temperature, in darkness. After incubation, 0.8 ml of binding buffer were added. Just before the FACS analysis, cells were stained with 20 µl of 1mg/ml PI solution.

Three independent experiments were performed, with two replicates per experiment.

2.4.2.6. Hoechst 33342 Staining

The morphological changes were observed by fluorescence microscopy using Hoechst staining. Jurkat cells were plated in 6-well plates at a density of 1.6 x 10^5 cells, simultaneously with the addition of compound **2.9**, at a concentration corresponding to its IC_{50} value at 72 h of treatment, or with only the vehicle, in a total volume of 2 ml of medium (six wells per condition). The cells were incubated for 6 h. Before collecting, morphological changes were observed under a phase-contrast microscope. Cells were collected by centrifugation, washed twice with PBS and stained with 500 µl of Hoechst 33342 solution (2 µg/ ml in PBS) for 15 min, at room temperature, in darkness. Finally, cells were washed and resuspended in 10 µl PBS. The samples were mounted on a slide and observed with a fluorescence microscope (DMRB, Leica Microssystems, Wetzlar, Germany) with a 4',6-diamidino-2'-phenylindole dihydrochloride (DAPI) filter. Three independent experiments were conducted.

2.4.2.7. Western Blot Analysis

Jurkat cells (1.6 x 10^6 cells) were cultured in 25 cm^2 flasks and treated for 6 h with compound **2.9** at different concentrations. After incubation, the cells were washed twice with ice-cold PBS and resuspended in lysis buffer containing 20 mM Tris/ acetate, pH 7.5, 270 mM sucrose, 1 mM EDTA, 1 mM EGTA, 1% Triton X-100 and 1% protease inhibitor cocktail. The samples were sonicated, incubated on ice for 20 min and centrifuged at 13200 rpm for 12 min at 4°C, and the pellets were discarded. The supernatants were assayed for protein concentration using a BCA kit (Thermo fisher Scientific, Waltham, MA, USA). Protein extracts (50 μg) were separated on 15% sodium dodecyl sulfate (SDS)-polyacrilamide gels and transferred to a polyvinilnitrocellulose transfer membrane (Bio-Rad Laboratories, Hercules, CA, USA). The membranes were blocked by incubation in TBS buffer (20 mM Tris, pH=7.5 and 132 mM NaCl) containing 0.1% of Tween and 5% of BSA or nonfat milk, for 1 h, at room temperature. Then, membranes were blotted with the primary antibodies anti-caspase 3, 8 and 9 (1:1000) overnight at 4 °C. The blots were washed three times with TBS-0.1% Tween and incubated with the appropriate secondary antibodies, for 1 h, at room temperature. Before protein detection, membranes were washed again five times with TBS-0.1% Tween. Immunocomplexes were visualized using the Immobilon ECL Western Blotting Detection Kit Reagent.

Three independent experiments were performed.

3. A-Ring Cleaved Glycyrrhetinic Acid Derivatives

3.1. Introduction

Semisynthesis is an essential strategy that is able to provide structural analogues with higher potency and selectively.

Many derivatizations have been performed on the **GA** scaffold, however the cleavage of its ring A is still poorly explored [131]. On the other hand, is well known that the conjugation of an amino acid moiety to PTs improves their cytotoxicity and their selectively towards tumor cells [143,214,215].

The establishment of an amide bond, one of the most common reactions used in the pursuit of new drug agents [216], is typically formed via an activated carboxylic acid, which OH group is converted into a good leaving group prior to the treatment with the amine. In this work, the coupling agent used to that activation was the bis(2-methoxyethyl)aminosulfur trifluoride (Deoxo-Fluor®) reagent [217,218]. The reaction of carboxylic acids with Deoxo-Fluor leads to the formation of acyl fluorides, which possess better stability than the corresponding acyl chlorides towards neutral oxygen nucleophiles, such as the water, yet have high reactivity toward anionic nucleophiles and amines [219]. These reactions are simple, efficient, proceed under mild conditions and even allow one pot direct synthesis of amides, oxazolines, benzoxazoles, oxadiazoles, acyl azides or nitriles [220-222].

In this study, we synthesized new **GA** derivatives via the opening of its ring A along with the coupling with an amino acid.

The novel semisynthetic derivatives were tested for their antiproliferative activity against a panel of nine human cancer lines. Further biological assays were conducted for the most active compound **3.16** (Scheme 3.2) in the leukemia Jurkat cancer cell line, which yielded the best results, to investigate its preliminary mechanism of action.

The study of selectivity was performed on human fibroblasts (BJ).

3.2. Results and discussion

3.2.1. Chemistry

The synthesis of the **GA** derivatives is outlined in Schemes 3.1-3.3. Full structural elucidation of the newly synthesized compounds was achieved using NMR, MS and elemental analysis. The analytical data obtained for the known compounds **3.1**-**3.4** and **3.7**-**3.9**, were in agreement with those reported in the literature [143,161,206,223].

The synthesis of compounds **3.1**-**3.6** is summarized in Scheme 3.1. Methyl ester **3.1** was obtained from the reaction of **GA**, the starting material, with methyl iodide in the presence of potassium carbonate [143]. The 3β-hydroxyl group of compound **3.1** was then oxidized using the Jones reagent [206] to give the 3-keto derivative **3.2**. The reaction of this derivative with *m*-chloroperbenzoic acid (*m*-CPBA) provided lactone **3.3**. The lactone ring of **3.3** was opened by treatment with *p*-toluenesulfonic acid (*p*-TSA) in dichloromethane [161]. Reaction of compound **3.4** with Deoxo-Fluor® provided the acyl fluoride intermediate which was reacted either with glycine methyl ester hydrochloride or with L-alanine methyl ester hydrochloride to afford compounds **3.5** and **3.6**, in yields of 69% and 61%, respectively.

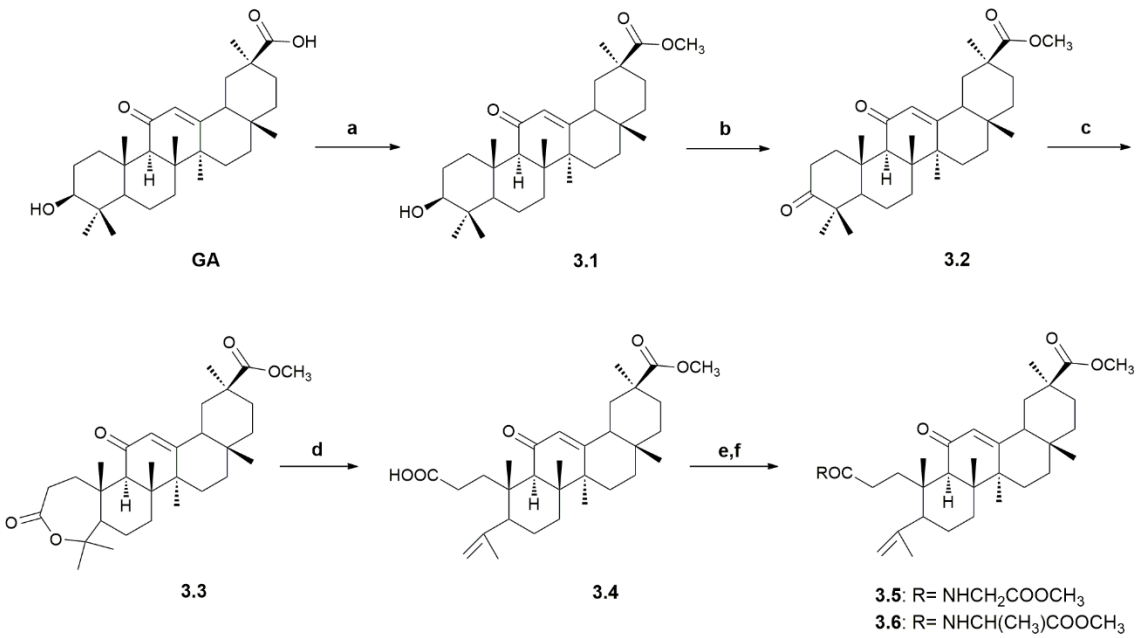

Scheme 3.1 Synthesis of derivatives **3.1**-**3.6**. Reagents and conditions: (a) CH_3I, K_2CO_3, DMF, r.t.; (b) Jones reagent, acetone, 0°C; (c) *m*-CPBA,CH_2Cl_2, r.t.; (d) *p*-TSA, CH_2Cl_2, r.t.; (e) Deoxo-Fluor®, CH_2Cl_2, r.t.; (f) glycine methyl ester hydrochloride or L-alanine methyl ester hydrochloride, Et_3N, CH_2Cl_2, r.t.

We found that the acyl fluoride, in this position of the structure, decomposes on standing. For that reason the crude compound was employed without further purification, and immediately, in the subsequent reactions.

The preparation of compounds **3.5** and **3.6** was confirmed by the presence of the proton signals of the amino acid side chains. On the ^{1}H NMR spectrum of compound **3.5** (Fig. 3.1) , the δ signals of the glycine methyl ester side chain were observed around 6.1 ppm (NH), 4.0 ppm (NCH_2) and 3.7 ppm (CH_3). Compound **3.6**, with an alanine methyl ester side chain, had δ signals around 6.1 ppm (NH), 4.6 ppm (NCH) and 3.7 ppm (CH_3) (Fig.3.2).

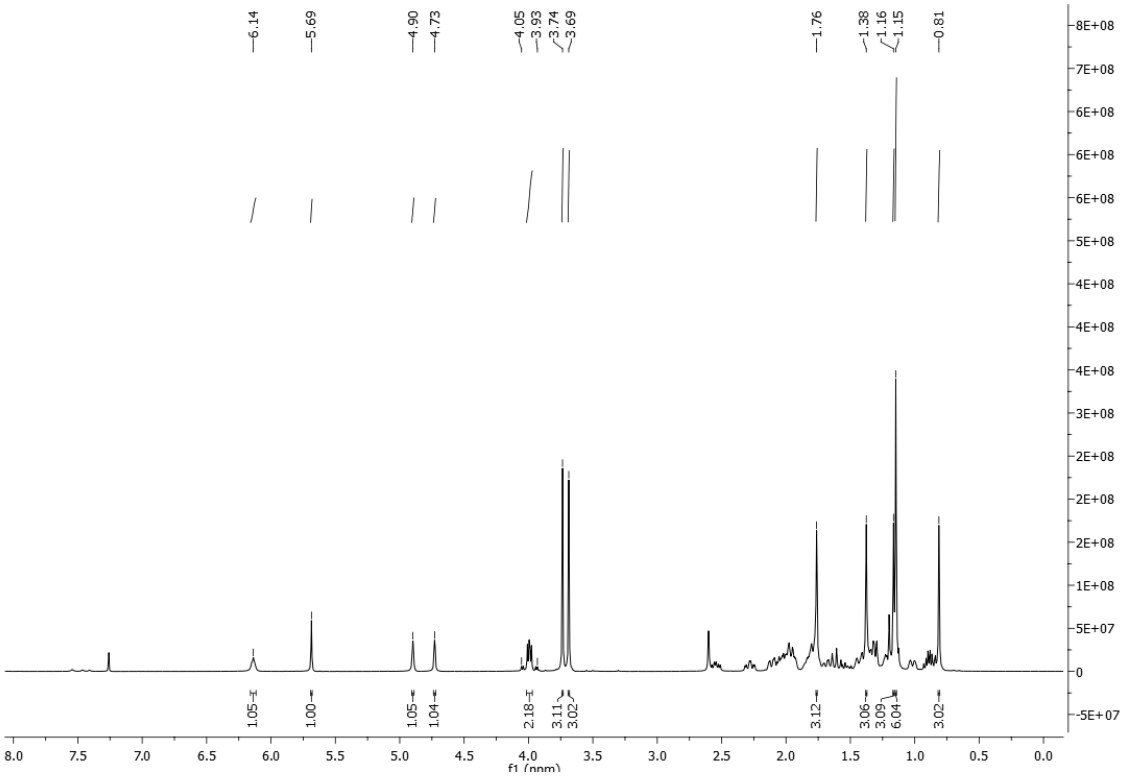

Figure 3.1 ^{1}H NMR spectrum of compound **3.5**.

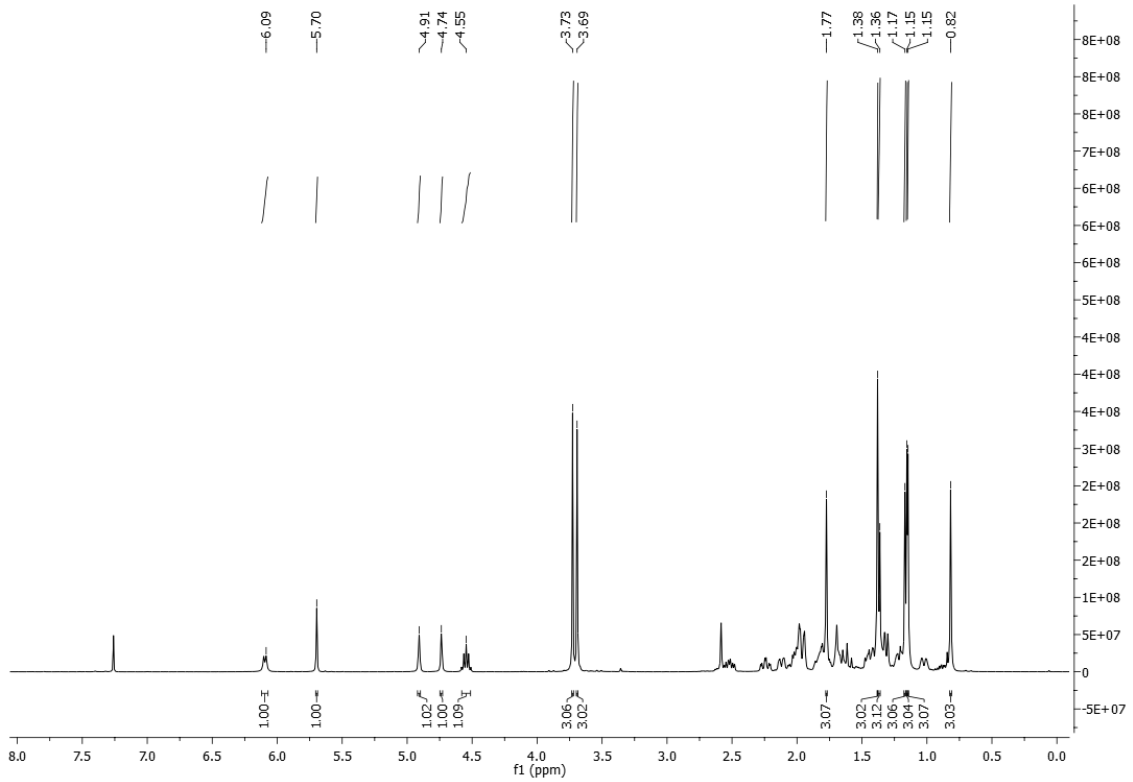

Figure 3.2 [1]H NMR spectrum of compound **3.6**.

Compounds **3.7**-**3.16** were synthesized as depicted in Scheme 3.2. **GA** was oxidized using the Jones reagent [206] to afford compound **3.7**, which was reacted with *m*-CPBA to give the derivative **3.8**. The lactone ring of **3.8** was cleaved by treatment with *p*-TSA in methanol and dichloromethane [161] to provide compound **3.9**. The derivative **3.10** and the three pairs of compounds synthesized in the following steps were prepared to explore the influence of the keto group in position C-11 on the antiproliferative activity. The removal of the keto group was performed by a Clemmensen reduction [224] with zinc dust and concentrated HCl in dioxane at room temperature to afford **3.10** (75%). The reduction was confirmed on the ^{13}C NMR spectrum, by the absence of the δ signal around 200 ppm, which corresponds to the carbonyl group in ring C (Fig. 3.3). Acyl fluorides **3.11** and **3.12** were obtained from the reaction of compounds **3.9** and **3.10** with Deoxo-Fluor, in yields of 75% and 61%, respectively. The synthesis of acyl fluorides was detected on the ^{13}C NMR spectra. The carbon C30 appeared as a doublet with a δ signal around 166 ppm and a coupling constant of 375 Hz, in both compounds **3.11** (Fig.s 3.4 and 3.5) and **3.12**.

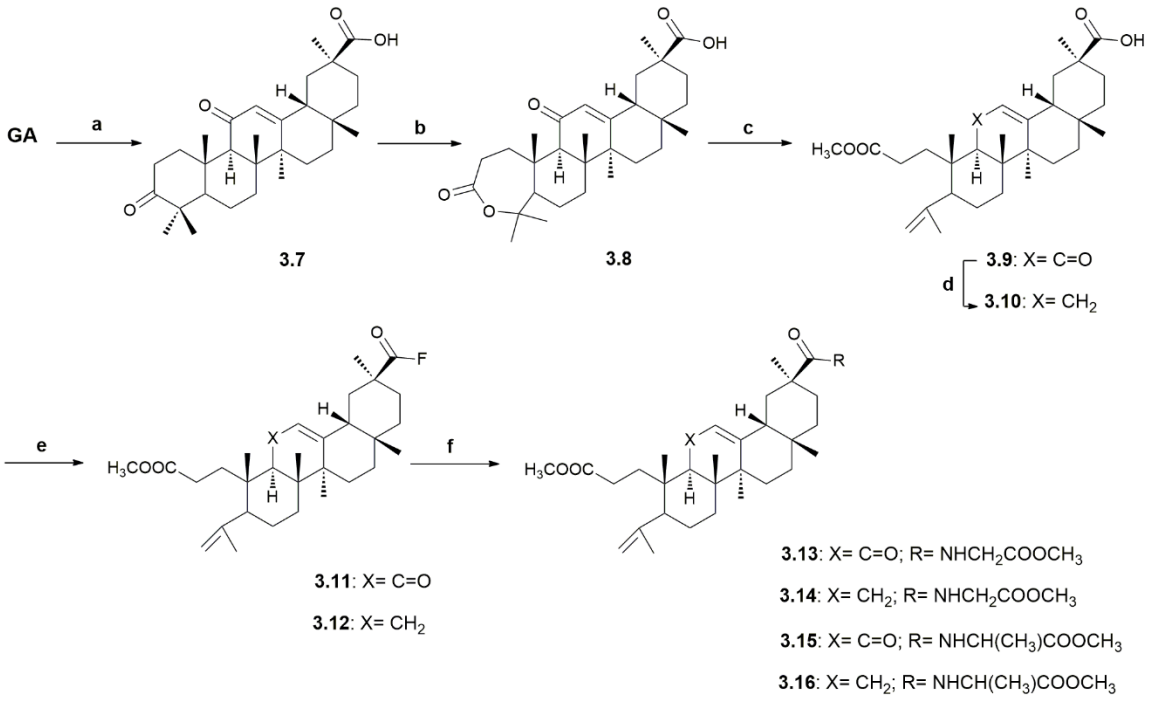

Scheme 3.2 Synthesis of derivatives **3.7**-**3.16**. Reagents and conditions: (a) Jones reagent, acetone, 0°C; (b) *m*-CPBA,CH_2Cl_2, r.t.; (c) MeOH, *p*-TSA, CH_2Cl_2, r.t.; (d) zinc dust, conc. HCl, dioxane, r.t.; (e) Deoxo-Fluor®, CH_2Cl_2, r.t.; (f) glycine methyl ester hydrochloride or L-alanine methyl ester hydrochloride, Et_3N, CH_2Cl_2, r.t.

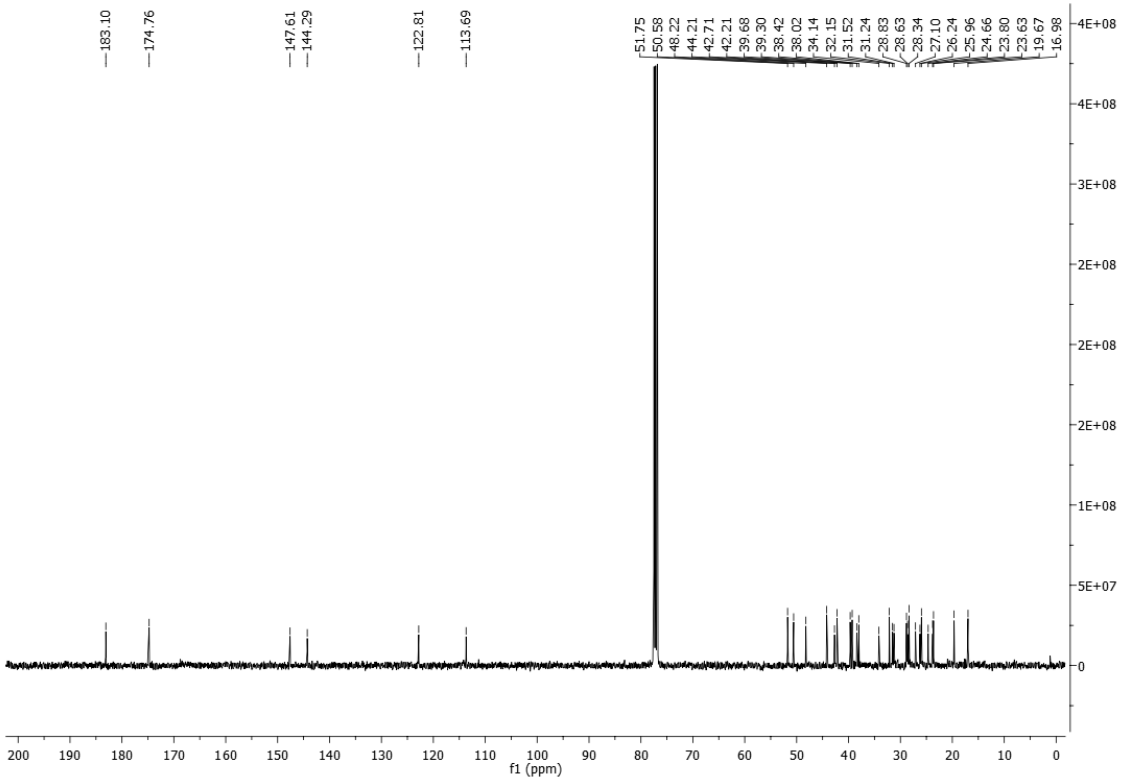

Figure 3.3 ^{13}C NMR spectrum of compound **3.10.**

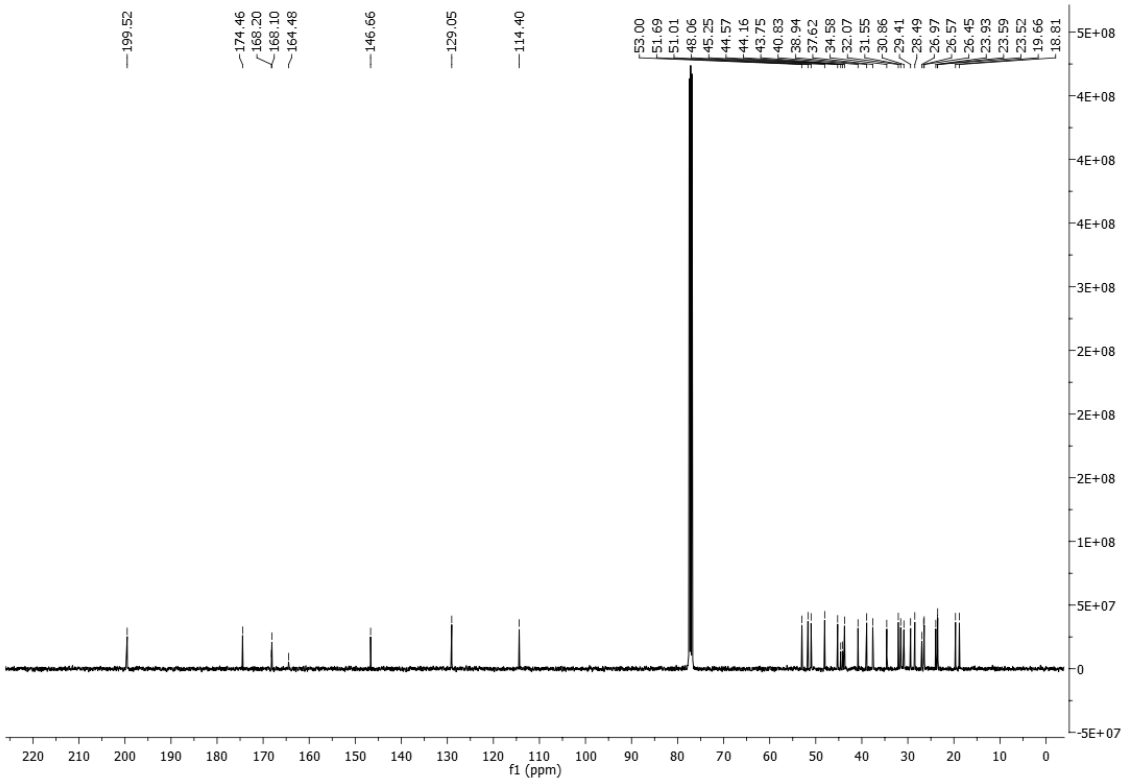

Figure 3.4 ^{13}C NMR spectrum of compound **3.11.**

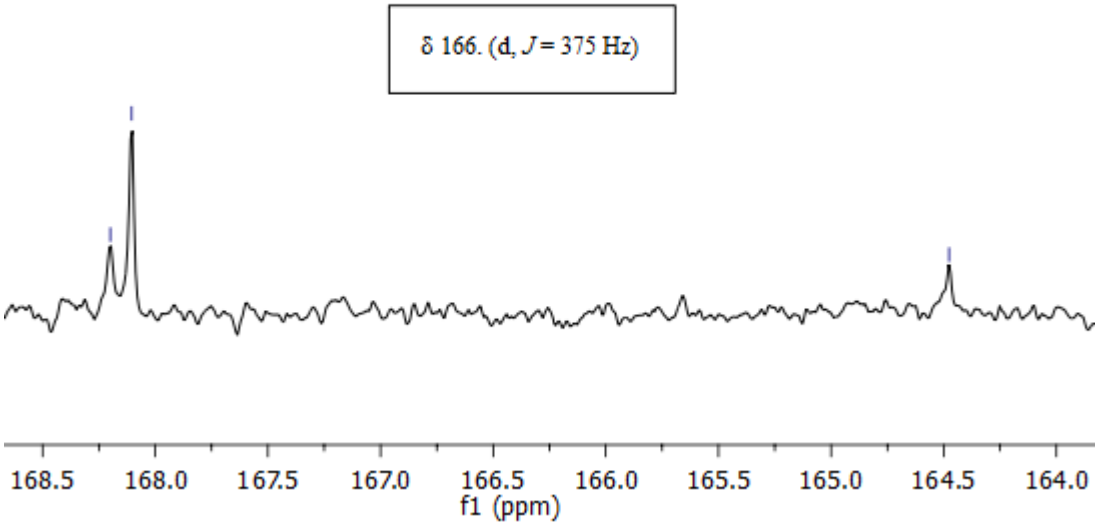

Figure 3.5 Detail of the ^{13}C NMR spectrum of compound **3.11.**

These derivatives were reacted either with glycine methyl ester hydrochloride or with L-alanine methyl ester hydrochloride to afford compounds **3.13**-**3.16**, in yields ranging from 43% to 83%.The glycine methyl ester side chain of compounds **3.13** (Fig. 3.6) and **3.14** was detected on the ^{1}H NMR spectra. Its proton signals were observed around 6.2 ppm (NH), 4.0 ppm (NCH_2) and 3.8 ppm (CH_3). Compounds **3.15** and **3.16** (Fig. 3.7), with an alanine methyl ester side chain, had δ signals around 6.2 ppm (NH), 4.6 ppm (NCH) and 3.8 ppm (CH_3).

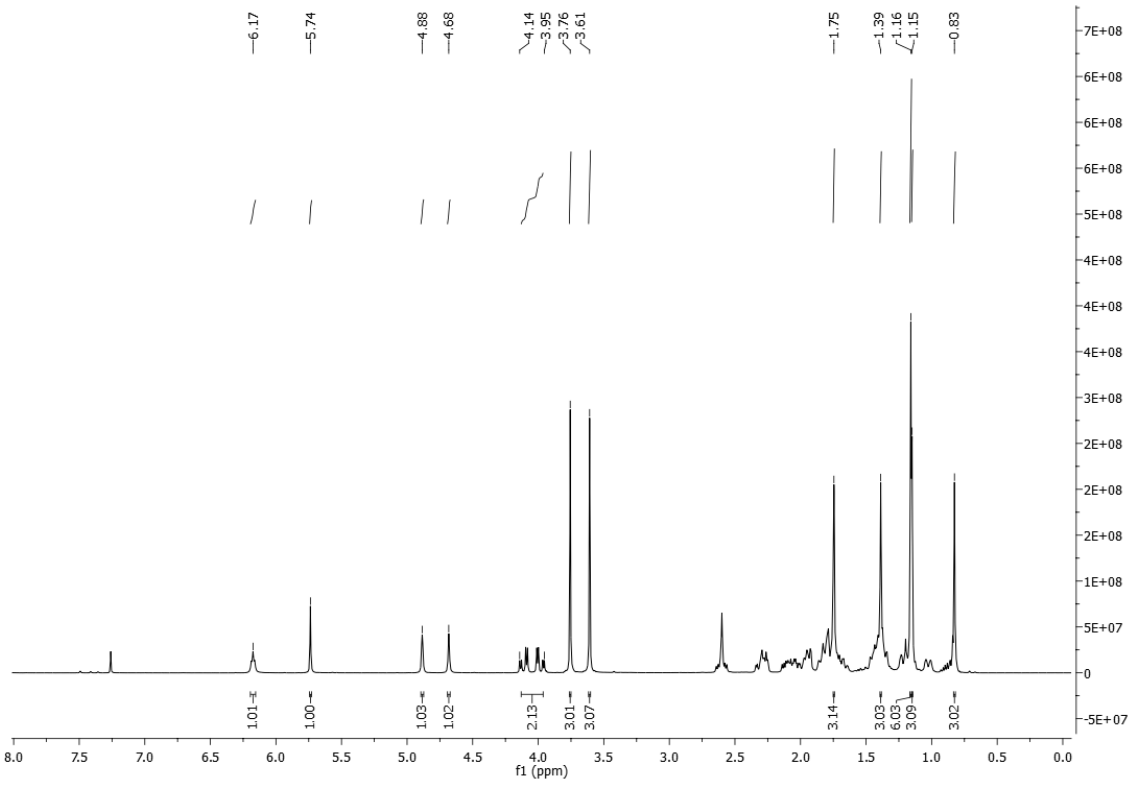

Figure 3.6 ^{1}H NMR spectrum of compound **3.13.**

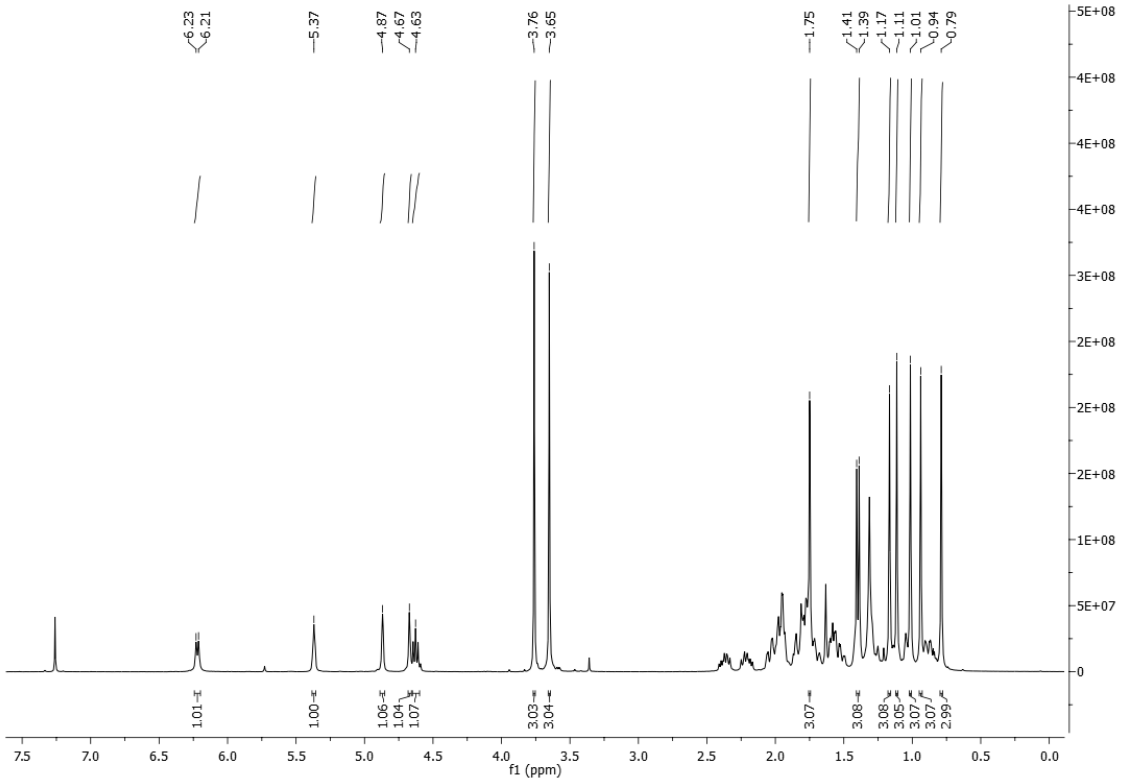

Figure 3.7 ^{1}H NMR spectrum of compound **3.16.**

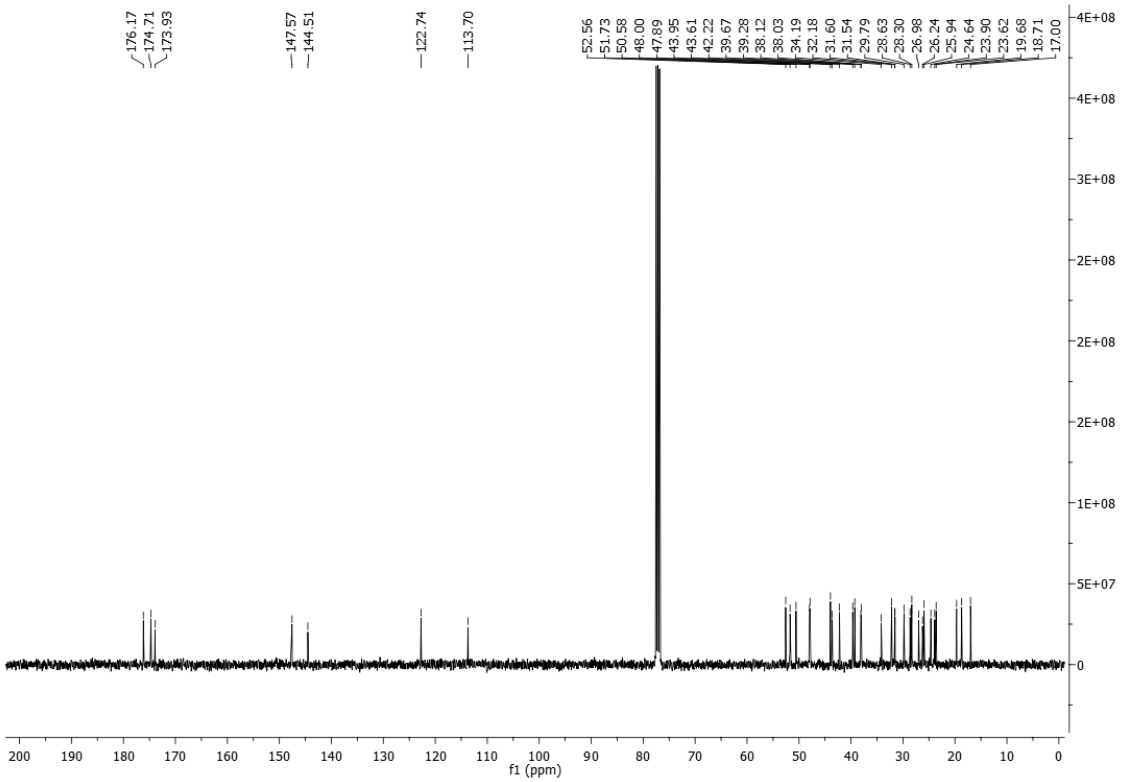

Figure 3.8 ^{13}C NMR spectrum of compound **3.16**.

Deprotection of the carboxyl group of the amino acid chain was performed in compounds **3.5**, **3.6**, **3.13** and **3.15**, by alkaline hydrolysis (Scheme 3.3). This reaction also caused deprotection of the other carboxyl group on compounds **3.13** and **3.15**. Compounds **3.17**-**3.20** were obtained in yields ranging from 94% to 98%.

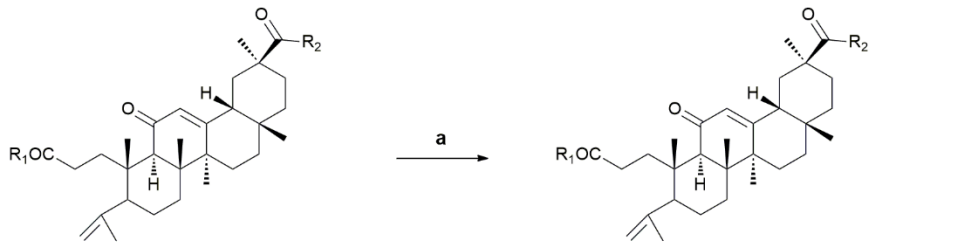

	R_1	R_2
3.5:	$NHCH_2COOCH_3$	OCH_3
3.6:	$NHCH(CH_3)COOCH_3$	OCH_3
3.13:	OCH_3	$NHCH_2COOCH_3$
3.15:	OCH_3	$NHCH(CH_3)COOCH_3$

	R_1	R_2
3.17:	$NHCH_2COOH$	OCH_3
3.18:	$NHCH(CH_3)COOH$	OCH_3
3.19:	OH	$NHCH_2COOH$
3.20:	OH	$NHCH(CH_3)COOH$

Scheme 3.3 Synthesis of derivatives **3.17**-**3.20**. Reagents and conditions: (a) KOH 4N, THF/MeOH, r.t.

Deprotection of the carboxyl group of the amino acid chains was confirmed by the absence of δ signals around 3.7-3.8 ppm, on the ^{1}H NMR spectra of compounds **3.17**-**3.20** (Fig.s. 3.9-3.11). The loss the other methyl group of compounds **3.13** and **3.15** was detected by the absence of the δ signal around 3.6 ppm, on the ^{1}H NMR spectra of compounds **3.19** (Fig. 3.11) and **3.20**.

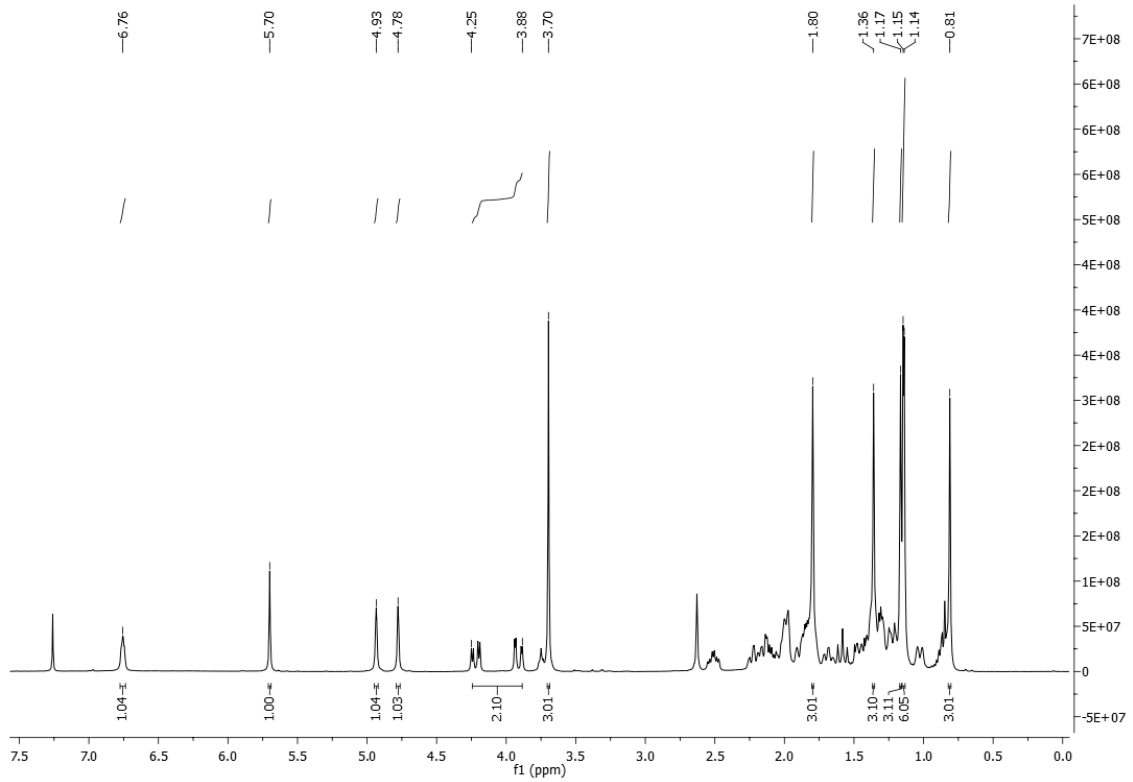

Figure 3.9 [1]H NMR spectrum of compound **3.17**.

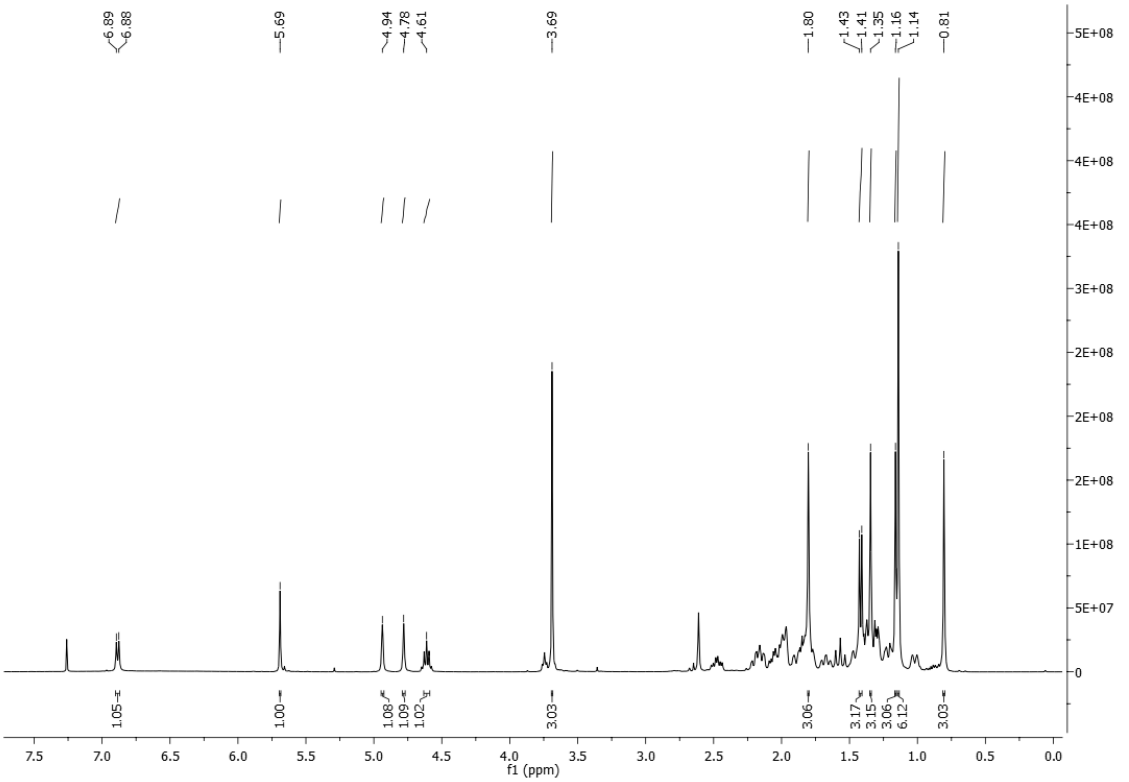

Figure 3.10 [1]H NMR spectrum of compound **3.18**.

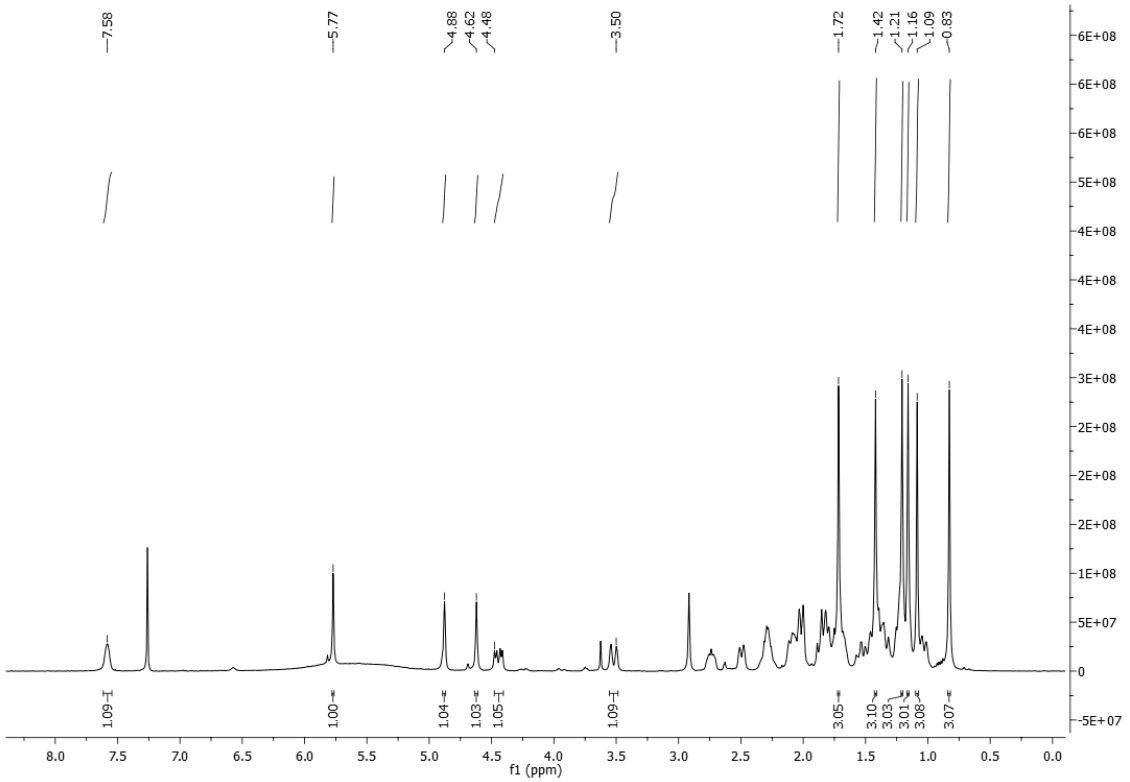

Figure 3.11 ^{1}H NMR spectrum of compound **3.19**.

3.2.2. Biology

3.2.2.1. Antiproliferative Activity

Several cancer cell lines were used to evaluate the potential cytotoxicity of the synthesized compounds against human cancers. This evaluation was based on the determination of the concentration that inhibits cell proliferation at 50% (IC_{50}), using MTT or XTT assays, after 72 h of treatment with the compounds.

GA and compounds **3.4**-**3.6** and **3.9**-**3.20** were screened for their antiproliferative activity on A549 (lung adenocarcinoma) and HT-29 (colon adenocarcinoma) cell lines (Table 3.1). Compounds **3.1**-**3.3**, **3.7** and **3.8** were not evaluated because they have already been tested with no improvements in potency and/or selectivity [131,133,141,143].

Table 3.1 Antiproliferative activities of **GA**, its derivatives **3.4**-**3.6** and **3.9**-**3.20**, and cisplatin against A549 and HT-29 cell lines.

Compound	Cell line (IC_{50}, μM) [1]	
	A549	HT-29
GA	110.5 ± 3.9	115.7 ± 1.6
3.4	59.4 ± 2.1	66.6 ± 3.2
3.5	31.6 ± 1.5	37.4 ± 1.0
3.6	26.2 ± 2.4	24.4 ± 1.7
3.9	52.2 ± 3.0	61.7 ± 1.4
3.10	33.7 ± 2.0	43.0 ± 1.5
3.11	> 100	> 100
3.12	> 100	> 100
3.13	33.7 ± 1.8	35.0 ± 1.7
3.14	26.4 ± 2.2	24.7 ± 0.9
3.15	24.4 ± 1.4	23.8 ± 0.3
3.16	14.8 ± 0.9	13.0 ± 0.5
3.17	> 100	> 100
3.18	> 100	> 100
3.19	> 100	> 100
3.20	> 100	> 100
Cisplatin	12.6 ± 0.8 [208]	6.1 [207]

[1] The cell lines were treated with different concentrations of each compound for 72 h. IC_{50} values were determined by by MTT assay. Results are expressed as means ± SD (standard deviation) of three independent experiments.

Intermediates **3.4** and **3.9**, afforded by the cleavage of the ring A, were more potent than the parent compound **GA**. Removal of the keto group from ring C, that provided compound **3.10**, resulted in an increment of cytotoxicity. Acyl fluorides **3.11** and **3.12** were less potent compared to their substrates. Analysis of the IC_{50} values of the derivatives **3.5**, **3.6** and **3.13**-**3.16** showed that the conjugation of an amino acid methyl ester provided more potent compounds. Deprotection of the carboxyl groups resulted in a loss of cytotoxicity. Compounds **3.17**-**3.20**, afforded by the alkaline hydrolysis, were further tested in Jurkat (acute T cell leukemia) and MOLT-4 (acute lymphoblastic leukemia) cell lines (Table 3.2). The results of these assays confirmed that the deprotection provided less active compounds. Derivatives **3.5**, **3.6** and **3.13**-**3.16** and the parent compound **GA** were also screened for their antiproliferative activity in seven additional human cancer cell lines: Jurkat, MOLT-4, MIAPaCa 2 (pancreas adenocarcinoma), MCF7 (breast adenocarcinoma), HeLa (cervix adenocarcinoma), A375 (melanoma) and HepG2 (hepatocellular carcinoma) (Tables 3.2 and 3.3). Comparing IC_{50} values of compounds **3.5** and **3.6** with those obtained for compounds **3.13** and **3.15**, no significant differences were found regarding the position in which the amino acid methyl ester was introduced. Derivatives **3.14** and **3.16** were respectively more potent than compounds **3.13** and **3.15** in all tested cell lines, which confirmed that the removal of the

keto group from ring C enhanced the cytotoxicity. Compounds **3.6**, **3.15** and **3.16**, which have an alanin methyl ester chain, were more active than compounds **3.5**, **3.13** and **3.14**, with a glicine methyl ester chain, respectively. These results suggest that the type of amino acid moiety introduced influences the antiproliferative activity. Within the newly synthesized derivatives, compound **3.16**, with a reduced ring C and with an alanin methyl ester chain, was the most potent derivative. This compound was 5 to 17-fold more active than **GA**, depending on the cancer cell line.

Table 3.2 Antiproliferative activities of **GA**, its derivatives **3.5**-**3.6** and **3.13**-**3.20**, and cisplatin against Jurkat, MOLT-4, Mia PaCa2 and MCF7 cell lines.

Compound	Cell line (IC50, μM) [1]			
	Jurkat	MOLT-4	Mia PaCa2	MCF7
GA	105.6 ± 5.0	95.5 ± 3.9	101.6 ± 1.6	97.8 ± 3.9
3.5	11.9 ± 0.2	18.9 ± 1.6	28.2 ± 0.5	32.9 ± 1.6
3.6	11.7 ± 0.6	18.5 ± 0.9	24.9 ± 1.2	24.9 ± 0.9
3.13	13.3 ± 1.1	23.5 ± 0.8	32.5 ± 3.2	28.8 ± 0.7
3.14	12.5 ± 0.5	18.9 ± 1.6	20.2 ± 1.2	24.8 ± 1.3
3.15	9.6 ± 0.4	19.1 ± 1.3	22.6 ± 0.6	23.8 ± 1.6
3.16	6.1 ± 0.2	15.3 ± 0.7	11.8 ± 1.1	21.6 ± 0.6
3.17	46.4 ± 3.7	51.9 ± 2.5	N.D.	N.D.
3.18	40.8 ± 2.7	49.0 ± 1.6	N.D.	N.D.
3.19	> 100	> 100	N.D.	N.D.
3.20	> 100	> 100	N.D.	N.D.
Cisplatin	5.0 ± 1.0 [211]	2.3 ± 0.3 [211]	3.1 ± 1.0 [212]	19.1 ± 4.5 [209]

[1] The cell lines were treated with different concentrations of each compound for 72 h. IC_{50} values were determined by XTT assay in Jurkat and MOLT-4 cells and by MTT assay in Mia PaCa2 and MCF7 cells. Results are expressed as means ± SD of three independent experiments. N.D.: not determined.

Table 3.3 Antiproliferative activities of **GA**, its derivatives **3.5**-**3.6** and **3.13**-**3.20**, and cisplatin against HeLa, A375 and HepG2 cancer cell lines, and the nontumoral BJ cell line.

Compound	Cell line (IC50, μM) [1]			
	HeLa	A375	HepG2	BJ
GA	107.2 ± 2.5	112.2 ± 2.6	125.1 ± 9.1	165.0 ± 7.1
3.5	34.5 ± 2.5	30.0 ± 1.5	30.6 ± 0.5	N.D.
3.6	25.7 ± 0.6	24.5 ± 1.0	24.8 ± 0.4	N.D.
3.13	34.2 ± 2.4	30.0 ± 2.2	34.7 ± 1.1	N.D.
3.14	22.2 ± 0.3	18.8 ± 1.1	25.4 ± 1.3	N.D.
3.15	19.1 ± 0.5	17.0 ± 1.1	25.7 ± 0.8	N.D.
3.16	13.0 ± 0.5	11.3 ± 0.4	16.0 ± 0.3	> 100
3.17	N.D.	N.D.	N.D.	N.D.
3.18	N.D.	N.D.	N.D.	N.D.
3.19	N.D.	N.D.	N.D.	N.D.
3.20	N.D.	N.D.	N.D.	N.D.
Cisplatin	2.3 ± 0.3 [209]	3.1 ± 1.0 [208]	2.9 [207]	10.1 ± 2.0[209]

[1] The cell lines were treated with different concentrations of each compound for 72 h. IC_{50} values were determined by MTT assay. Results are expressed as means ± SD of three independent experiments. N.D.: not determined.

The selectivity towards cancer cells was studied for **GA** and compound **3.16** by incubating them with a human nontumoral cell line (BJ) (Table 3.3). **GA** and compound **3.16** showed IC_{50} values that were 1.6 and more than 16.4 times lower on Jurkat cells than on the nontumoral BJ cells, respectively. Therefore, the novel derivative **3.16** was up to 10 times more selective towards malignant cells than its parent compound. This compound also showed a significant improvement in selectivity compared to the chemotherapy agent cisplatin. Considering also the Jurkat cell line, cisplatin presented an IC_{50} value that was 5.3 times lower than on BJ cells (Table 3.3); therefore, compound **3.16** was up to 3 times more selective than cisplatin towards Jurkat cells.

3.2.2.2. Analysis of Cell Cycle Distribution and Apoptosis

The Jurkat cell line which was the most susceptible to these derivatives was selected to investigate the mechanism of action of compound **3.16**. To evaluate the effects on the cell cycle distribution, Jurkat cells were treated with compound **3.16**, at a concentration corresponding to its IC_{50} value at 72 h of treatment, for 24, 48 and 72 h and then analysed by flow cytometry. The calculation of the fraction of cells in G0/G1, S and G2/M phases was performed using the fraction of live cells. Treatment for 24 h induced significant increase in the population at S phase with respect to untreated cells (Fig. 3.12); after 48 h this effect has decreased and after 72 h it was no longer observed. DNA fragmentation was detected after 72 h of incubation based on the appearance of a sub-G0 peak. This sequence of events suggests that the cell cycle arrest at S phase may have led cells to undergo apoptosis.

Apoptosis assays were then performed to better elucidate the mechanism of cell death involved in the cytotoxic effect of compound **3.16**. The experiments were conducted on Jurkat cells treated with compound **3.16** at a concentration corresponding to its IC_{50} value at 72 h of treatment (6.1 μM) for 24 and 48 h, and at concentrations of 6.1 μM and 12.2 μM for 72 h. Exposure to this compound for 24 and 48 h did not change significantly the apoptotic (Fig 3.13.A) and necrotic (data not shown) populations. Treatment for 72 h with compound **3.16** at concentrations of 6.1 μM and 12.2 μM increased the early apoptotic population by 19% and 30%, respectively. No significant changes were observed in the late apoptotic population. These results were in good agreement with those obtained in the cell cycle experiments.

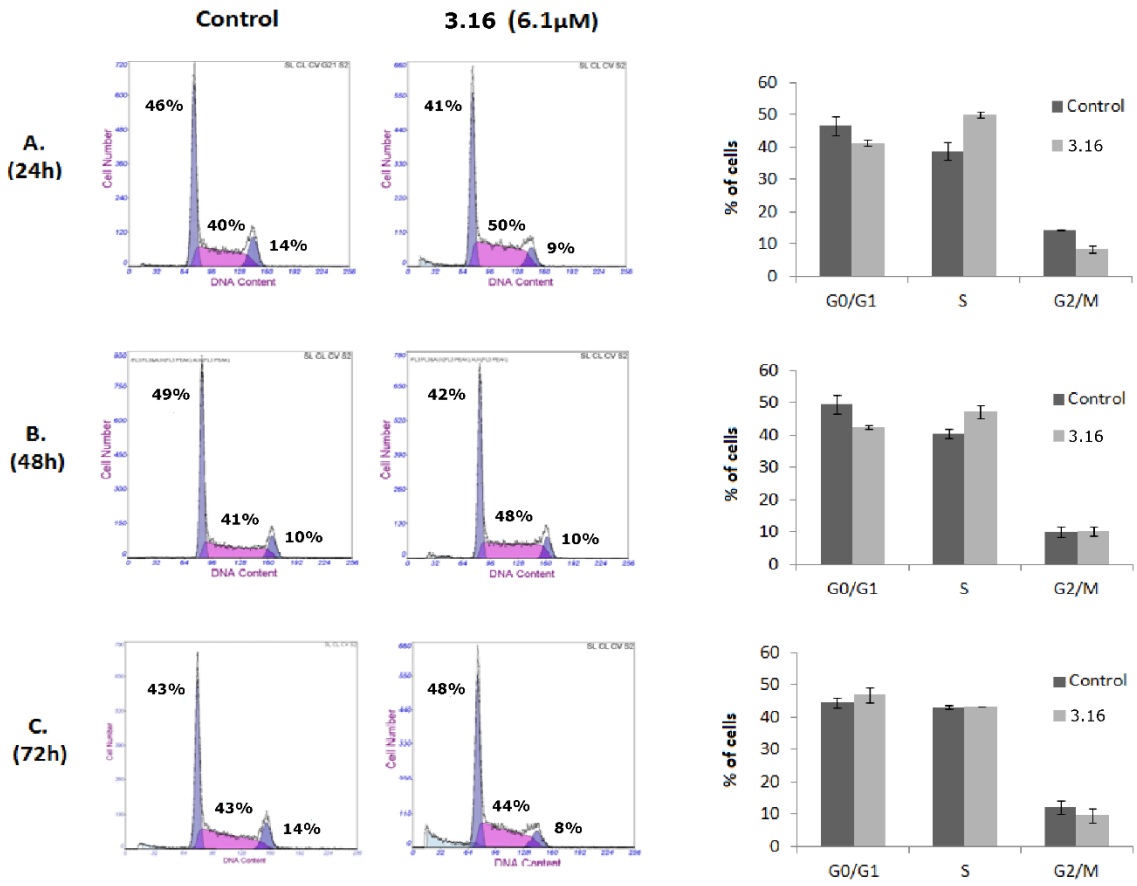

Figure 3.12 Effect of compound **3.16** on cell cycle distribution. Cell cycle analysis of Jurkat cells untreated (Control) or treated with 6.1 µM compound **3.16** for 24 (**A**), 48 (**B**), and 72 h (**C**). After treatment, cells were stained with PI and DNA content analysed by flow cytometry. A representative histogram is shown for each incubation time and condition. Results are presented as means ± SD of three independent experiments.

The induction of apoptosis was further confirmed by the observation of its characteristic morphological changes. Hoechst 33342 staining showed volume reduction, chromatin condensation and apoptotic bodies in Jurkat cells treated in the same conditions for 72 h (Fig.3.13.B). In contrast, untreated cells presented a normal morphological profile.

Taken together, the results described above suggest that compound **3.16** inhibits cell growth through cell cycle arrest at the S phase and induction of apoptosis. Its mechanism of action needs to be studied further.

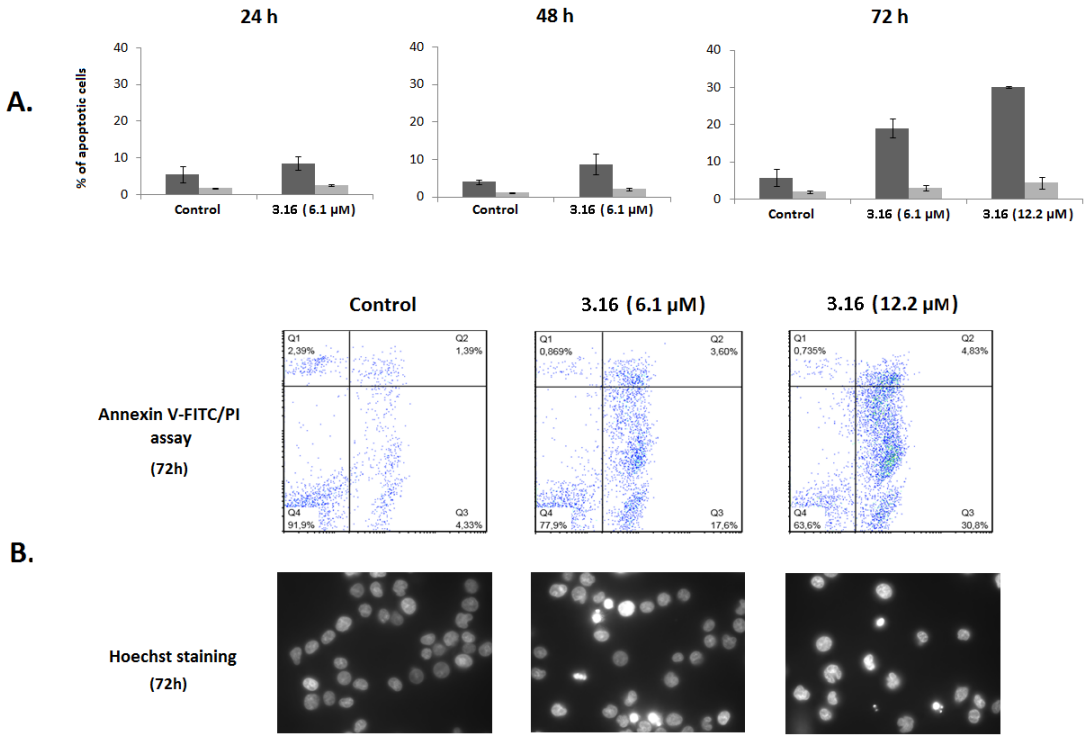

Figure 3.13 Induction of apoptosis by compound **3.16**. (**A**) Flow cytometry quantification of apoptosis in Jurkat cells untreated (Control) or treated with compound **3.16** at specified concentrations for 24, 48 and 72 h. After treatment, cells were stained with annexin V-FITC/PI and analysed by flow cytometry. The percentage of early (dark grey bar) and late (light grey bar) apoptotic cells in each condition is represented as a bar diagram, calculated from dot plots. Results are presented as means ± SD of three independent experiments. (**B**) *Upper panel*: Representative dot plots of annexin V-FITC/PI assays of Jurkat cells untreated (Control) or treated with compound **3.16** at specified concentrations for 72 h; the right quadrants of each diagram (annexin$^+$/PI$^-$ and annexin$^+$/PI$^+$) represent apoptotic cells. *Lower panel*: Representative fluorescence microscopic images of Jurkat cells untreated (Control) or treated with compound **3.16** at specified concentrations for 72 h; Jurkat cells were stained with Hoechst 33342 before analysis by fluorescence microscopy.

3.3. Conclusion

In summary, we synthesized a series of new **GA** derivatives via the opening of its ring A along with the coupling of an amino acid.

Antiproliferative activity assays in a panel of nine human cancer cell lines showed that the most potent compound **3.16** was 5 to 17-fold more active than **GA**. The study of selectivity revealed that this new derivative was up to 10 times more selective towards malignant cells than its parent compound. Preliminary mechanism investigation indicated that compound **3.16** may act through arresting cell cycle progression at the S phase and inducing apoptosis.

The enhanced potency and the high selectivity of this new **GA** derivative warrant further biological evaluation.

3.4. Experimental section

3.4.1. Chemistry

GA and all reagents were purchased from Sigma-Aldrich Co. (Saint Louis, MO, USA). The solvents used in the reactions were obtained from Merck Co. (Kenilworth, NJ, USA) and were purified and dried according to the literature procedures. The solvents used in workups were purchased from VWR Portugal.

TLC analysis was performed in Kieselgel 60HF254/Kieselgel 60G. Purification of compounds by FCC was carried out using Kiesegel 60 (230–400 mesh, Merck).

Melting points were determined using a BUCHI melting point B-540 apparatus and were uncorrected. ^{1}H and ^{13}C NMR spectra were recorded on a Bruker Avance-400 Digital NMR spectrometer, in $CDCl_3$, with Me_4Si as the internal standard. Chemical shifts values (δ) are given in parts per million (ppm) and coupling constants (*J*) are presented in hertz (Hz). Mass spectra were obtained using a Quadrupole/Ion Trap Mass Spectrometer (QIT-MS) (LCQ Advantage MAX, THERMO FINNINGAN). Elemental

analysis was performed in an Analyzer Elemental Carlo Erba 1108 by chromatographic combustion.

Methyl 3β-hydroxy-11-oxo-olean-12-en-30-oate (3.1): Compound **3.1** was prepared according to the literature [143], from **GA** to give a colorless solid (90%). m.p.: 254-256°C.

Methyl 3,11-dioxo-olean-12-en-30-oate (3.2): Preparation of **3.2** was performed according to a previously described method [206], from **3.1** providing a white solid (94%). m.p.: 248-250°C.

Methyl 3,11-dioxo-4-oxa-A-homo-olean-12-en-30-oate (3.3): Compound **3.3** was prepared according to the literature [161], from **3.2** to give a white solid (77%). m.p.: 168-170°C.

3,4-*seco*-30-methyloxicarbonyl-11-oxo-olean-4(23),12-dien-3-oic acid (3.4): Preparation of **3.4** was performed according to a previously described method [161], from **3.3** providing a white solid (72%). m.p.: 90-92°C.

Methyl 3,4-*seco*-3-*N*-methylglycinamido-11-oxo-olean-4(23),12-dien-30-oate (3.5): To a solution of compound **3.4** (300 mg, 0.60 mmol) in dichloromethane (8 ml), Deoxo-Fluor (50% in THF, 0.52 ml, 1.20 mmol) was added and the reaction mixture was stirred, at room temperature, for 2.5 h, after which additional Deoxo-Fluor (50% in THF, 0.26 ml, 0.60 mmol) was added. After 2 h, the reaction was completed. The reaction mixture was quenched by addition of water (2 ml). The organic layer was diluted with chloroform (40 ml), washed with water (2 × 30 ml), dried over Na_2SO_4, filtered and evaporated to the dryness (280 mg, 93%). The residue was dissolved in dichloromethane (6 ml) and glycine methyl ester hydrochloride (105 mg, 0.84 mmol) and triethylamine (0.15 ml, 1.12 mmol) were added. After 1 h under magnetic stirring at room temperature, the reaction was completed. The reaction mixture was evaporated to dryness and ethyl acetate (40 ml) and water (30 ml) were added to the residue. The aqueous phase was further extracted with

ethyl acetate (2 × 40 ml). The combined organic phase was washed with 5% aqueous HCl (2 × 30 ml), 10% aqueous $NaHCO_3$ (2 × 30 ml), water (30 ml) and brine (30 ml), dried over Na_2SO_4, filtered and the solvent was removed under reduced pressure to afford a white solid. The solid was purified by flash column chromatography (FCC) with petroleum ether/ethyl acetate (2:1) to afford compound **3.5** as a white solid (69%). m.p.: 199-201°C. ^{1}H NMR (400MHz, $CDCl_3$): δ 6.14 (1H, m), 5.69 (1H, s), 4.90 (1H, br s), 4.73 (1H, br s), 3.93-4.05 (2H, m), 3.74 (3H, s), 3.69 (3H, s), 1.76 (3H, s), 1.38 (3H, s), 1.16 (3H, s), 1.15 (6H, s), 0.81 (3H, s). ^{13}C NMR (100MHz, $CDCl_3$): δ 200.3, 177.1, 173.7, 170.6, 170.3, 146.7, 128.6, 114.5, 53.3, 52.4, 51.9, 51.3, 48.5, 45.2, 44.2, 43.8, 41.4, 41.3, 39.1, 37.9, 35.7, 32.0, 31.8, 31.5, 31.3, 28.7, 28.4, 26.7, 26.6, 24.0, 23.6, 23.5, 19.7, 18.8. ESI-MS *m/z*: 570.34 ($[M + H]^+$, 100%). Found C 70.78, H 9.39, N 2.41, calcd for $C_{34}H_{51}NO_6 \cdot 0.25H_2O$: C 71.11, H 9.04, N 2.44%.

Methyl 3,4-*seco*-3-*N*-methyalaninamido-11-oxo-olean-4(23),12-dien-30-oate (3.6): The method followed that described for compound **3.5**. The resulting solid (274 mg, 0.55 ml; 91%) from the first step was dissolved in dichloromethane (6 ml) and L-alanine methyl ester hydrochloride (116 mg, 0.83 mmol) and triethylamine (0.15 ml, 1.10 mmol) were added. After 1 h, the reaction was completed. The workup was performed as described for compound **3.5**. The resulting solid was subjected to FCC with petroleum ether/ethyl acetate (2:1) to afford compound **3.6** as a white solid (61%). m.p.: 193-195°C. ^{1}H NMR (400MHz, $CDCl_3$): δ 6.09 (1H, m), 5.70 (1H, s), 4.91 (1H, br s), 4.74 (1H, br s), 4.55 (1H, m), 3.73 (3H, s), 3.69 (3H, s), 1.77 (3H, s), 1.38 (3H, s), 1.37 (3H, m), 1.17 (3H, s), 1.15 (3H, s), 1.15 (3H,s), 0.82 (3H, s). ^{13}C NMR (100MHz, $CDCl_3$): δ 200.3, 177.1, 173.8, 173.0, 170.2, 146.7, 128.6, 114.5, 53.3, 52.5, 51.9, 51.1, 48.5, 48.1, 45.2, 44.2, 43.9, 41.4, 39.1, 37.9, 35.8, 32.0, 31.9, 31.5, 31.3, 28.8, 28.4, 26.7, 26.6, 24.0, 23.7, 23.5, 19.7, 18.8, 18.5. ESI-MS *m/z*: 584.29 ($[M + H]^+$, 100%). Found C 71.40, H 9.31, N 2.32, calcd for $C_{35}H_{53}NO_6 \cdot 0.25H_2O$: C 71.46, H 9.17, N 2.38%.

3,11-Dioxo-olean-12-en-30-oic acid (3.7): Compound **3.7** was prepared according to the literature [206], from **GA** to give a colorless solid (92%). m.p.: 308-310°C.

3,11-Dioxo-4-oxa-A-homo-olean-12-en-30-oic acid (3.8): Compound **3.8** was prepared from **3.7**, using the same method as for the preparation of **3.9**, with the obtention of a white solid. (75%). m.p.: 268-270°C.

3,4-*seco*-3-methyloxicarbonyl-11-oxo-olean-4(23),12-dien-30-oic acid (3.9): Preparation of **3.9** was performed according to a previously described method [161], from **3.8** providing a colorless solid (62%). m.p.: 130-132°C.

3,4-*seco*-3-methyloxicarbonyl-olean-4(23),12-dien-30-oic acid (3.10): Preparation of **3.10** was done according to a previously described method [224]. Compound **3.9** (900 mg, 1.80 mmol) was dissolved in dioxane (25 ml) and Zn powder (941 mg, 14.40 mmol) was added. Concentrated HCl (37%, 3.6 ml, 43.20 mmol) was added dropwise for 30 min with stirring. After 4.5 h under magnetic stirring at room temperature, the reaction was completed. The reaction mixture was filtered and the solvent was removed under pressure. Diethyl ether (75 ml) and water (60 ml) were added to the residue. The aqueous phase was further extracted with diethyl ether (2 × 70 ml). The combined organic extract was then washed with 5% aqueous HCl (2 × 50 ml), 10% aqueous $NaHCO_3$ (2 × 50 ml), water (50 ml) and brine (50 ml), dried over Na_2SO_4, filtered and evaporated to the dryness. The resulting solid was purified by FCC with petroleum ether/ ethyl acetate (1:1) to afford compound **3.10** as a white solid (75%). m.p.: 138-140°C. ^{1}H NMR (400MHz, $CDCl_3$): δ 5.32 (1H, m), 4.87 (1H, br, s), 4.67 (1H, br), 3.65 (3H, s), 1.75 (3H, s), 1.21 (3H, s), 1.16 (3H, s), 1.02 (3H, s), 0.94 (3H, s), 0.82 (3H, s). ^{13}C NMR (100MHz, $CDCl_3$): δ 183.1, 174.8, 147.6, 144.3, 122.8, 113.7, 51.8, 50.6, 48.2, 44.2, 42.7, 42.2, 39.7, 39.3, 38.4, 38.0, 34.1, 32.2, 31.5, 31.2, 28.8, 28.6, 28.3, 27.1, 26.2, 26.0, 24.7, 23.8, 23.6, 19.7, 17.0. ESI-MS *m/z*: 118.11 (19%), 274.50 (32), 318.46 (75), 346.48 (11), 362.45 (15), 485.38 ($[M + H]^+$, 100%).

Methyl 3,4-*seco*-30-fluorcarbonyl-11-oxo-olean-4(23),12-dien-3-oate (3.11): To a solution of compound **3.9** (500 mg, 1.00 mmol) in dichloromethane (10 ml), Deoxo-Fluor (50% in THF, 0.87 ml, 2.00 mmol) was added. After 1.5 h under magnetic stirring at room temperature, the reaction was completed. The reaction mixture was quenched by

addition of water (3 ml). The organic layer was diluted with chloroform (50 ml), washed with water (2 × 40 ml), dried over Na_2SO_4, filtered and evaporated to the dryness. The resulting solid was subjected to FCC [petroleum ether/ethyl acetate from (6:1) to (4:1)] to afford compound **3.11** as a white solid (75%). m.p.: 183-185°C. ^{1}H NMR (400MHz, $CDCl_3$): δ 5.71 (1H, s), 4.90 (1H, br s), 4.69 (1H, br s), 3.62 (3H, s), 1.75 (3H, s), 1.38 (3H, s), 1.30 (3H, s), 1.17 (3H, s), 1.16 (3H, s), 0.86 (3H, s). ^{13}C NMR (100MHz, $CDCl_3$): δ 199.5, 174.5, 168.1, 166.3 (*J* = 374.6 Hz), 146.7, 129.1, 114.4, 53.0, 51.7, 51.0, 48.1, 45.3, 44.4 (*J* = 42.0 Hz), 43.8, 40.8, 38.9, 37.6, 34.6, 32.1, 31.6, 30.9, 29.4, 28.5, 27.0, 26.6, 26.5, 23.9, 23.6, 23.5, 19.7, 18.8. ESI-MS *m/z*: 501.16 ($[M + H]^+$, 100%).

Methyl 3,4-*seco*-30-fluorcarbonyl-olean-4(23),12-dien-3-oate (3.12): The method followed that described for compound **3.11** but using compound **3.10** (600 mg, 1.24 mmol) and Deoxo-Fluor (50% in THF, 1.08 ml, 2.48 mmol) in dichloromethane (12 ml) for 2 h. The resulting solid was purified by FCC [petroleum ether /ethyl acetate from (10:1) to (4:1)] to afford compound **3.12** as a white solid (61%). m.p.: 174-176°C. ^{1}H NMR (400MHz, $CDCl_3$): δ 5.32 (1H, m), 4.87 (1H, br s), 4.67 (1H, br s), 3.65 (3H, s), 1.75 (3H, s), 1.27 (3H, s), 1.15 (3H, s), 1.02 (3H, s), 0.94 (3H, s), 0.83 (3H, s). ^{13}C NMR (100MHz, $CDCl_3$): δ 174.7, 167.0 (*J* = 375.0 Hz), 147.5, 143.6, 123.4, 113.7, 51.7, 50.6, 48.3, 44.6 (*J* = 41.2 Hz), 42.4, 42.2, 39.7, 39.3, 38.1, 38.0, 34.1, 32.2, 31.5, 31.1, 28.6, 28.1, 27.2, 27.0, 26.1, 26.0, 24.6, 23.8, 23.6, 19.7, 17.0. ESI-MS *m/z*: 439.51 (38%), 440.52 (14), 485.44 (27), 487.36 ($[M + H]^+$, 100%).

Methyl 3,4-*seco*-30-*N*-methylglycinamido-11-oxo-olean-4(23),12-dien-3-oate (3.13): To a solution of compound **3.11** (300 mg, 0.60 mmol) and glycine methyl ester hydrochloride (226 mg, 1.80 mmol) in dichloromethane (8 ml), triethylamine (0.33 ml, 2.40 mmol) was added. After 13 h under magnetic stirring at room temperature, the reaction was completed. The reaction mixture was evaporated to dryness and ethyl acetate (50 ml) and water (40ml) were added to the residue. The aqueous phase was further extracted with ethyl acetate (2 × 50 ml). The resulting organic phase was washed with 5% aqueous HCl (2 × 30 ml), 10% aqueous $NaHCO_3$ (2 × 30 ml), water (30 ml) and brine (30 ml), dried over Na_2SO_4, filtered and the solvent was removed under reduced pressure to afford a solid. The solid was subjected to (FCC) [petroleum ether /ethyl acetate from (2:1)

to (1:1)] to afford compound **3.13** as a white solid (77%). m.p.:126-128°C. ^{1}H NMR (400MHz, $CDCl_3$): δ 6.17 (1H, m), 5.74 (1H, s), 4.88 (1H, br s), 4.68 (1H, br s), 3.95-4.14 (2H, m), 3.76 (3H, s), 3.61 (3H, s), 1.75 (3H, s), 1.39 (3H, s), 1.16 (6H, s), 1.15 (3H, s), 0.83 (3H, s). ^{13}C NMR (100MHz, $CDCl_3$): δ 199.7, 176.3, 174.5, 170.7, 169.5, 146.7, 128.6, 114.3, 52.9, 52.5, 51.7, 51.0, 47.9, 45.2, 43.8 (2), 42.1, 41.3, 38.9, 37.4, 34.6, 32.0, 31.6 (2), 29.5, 29.4, 28.6, 26.7, 26.5, 23.9, 23.6, 23.4, 19.6, 18.8. ESI-MS *m/z*: 570.32 ($[M + H]^+$, 100%). Found C 70.83, H 9.27, N 2.49, calcd for $C_{34}H_{51}NO_6 \cdot 0.25H_2O$: C 71.11, H 9.04, N 2.44%.

Methyl 3,4-*seco*-30-*N*-methylglycinamido-olean-4(23),12-dien-3-oate (3.14): The method followed that described for compound **3.13** but using compound **3.12** (290 mg, 0.60 mmol), glycine methyl ester hydrochloride (226 mg, 1.80 mmol) and triethylamine (0.33 ml, 2.40 mmol) in dichloromethane (8 ml). The workup was performed after 16 h. The resulting solid was purified by FCC with petroleum ether/ ethyl acetate (3:2) to afford compound **3.14** as a white solid (43%). m.p.: 190-192°C. ^{1}H NMR (400MHz, $CDCl_3$): δ 6.18 (1H, m), 5.34 (1H, m), 4.87 (1H, br s), 4.67 (1H, br s), 3.97-4.17 (2H, m), 3.77 (3H, s), 3.65 (3H, s), 1.75 (3H, s), 1.17 (3H, s), 1.13 (3H, s), 1.01 (3H, s), 0.93 (3H, s), 0.79 (3H, s). ^{13}C NMR (100MHz, $CDCl_3$): δ 177.0, 174.7, 171.0, 147.6, 144.4, 122.8, 113.7, 52.5, 51.7, 50.6, 48.1, 44.1, 43.6, 42.2, 41.4, 39.7, 39.3, 38.0 (2),34.2, 32.2, 31.7, 31.5, 29.8, 28.6, 28.3, 27.0, 26.2, 25.9, 24.6, 23.9, 23.6, 19.7, 17.0. ESI-MS *m/z*: 274.37 (25%), 318.32 (27), 556.24 ($[M + H]^+$, 100%). Found C 73.18, H 9.83, N 2.55, calcd for $C_{34}H_{53}NO_5$: C 73.47, H 9.61, N 2.52 %.

Methyl 3,4-*seco*-30-*N*-methylalaninamido-11-oxo-olean-4(23),12-dien-3-oate (3.15): To a solution of compound **3.11** (300 mg, 0.60 mmol) and L-alanine methyl ester hydrochloride (251 mg, 1.80 mmol) in dichloromethane (8 ml), triethylamine (0.33 ml, 2.40 mmol) was added and the reaction mixture was stirred, at room temperature, for 8h, after which additional dichloromethane (1 ml) and triethylamine (0.17 ml, 1.20 mmol) were added. After 16 h, the reaction was completed. The workup was performed as described for compound **3.13**. The solid was subjected to FCC with petroleum ether/ethyl acetate (1:2) to afford compound **3.15** as a white solid (83%). m.p.: 130-132°C. ^{1}H NMR (400MHz, $CDCl_3$): δ 6.15 (1H, m), 5.77 (1H, s), 4.89 (1H, br s), 4.69 (1H, br s), 4.62 (1H,

m), 3.76 (3H, s), 3.61(3H, s), 1.75 (3H, s), 1.39 (6H, m), 1.17 (3H, s), 1.16 (3H, s), 1.14 (3H, s), 0.82 (3H, s). ^{13}C NMR (100MHz, $CDCl_3$): δ 199.7, 175.4, 174.5, 173.7, 169.5, 146.7, 128.6, 114.3, 53.0, 52.7, 51.7, 51.0, 47.9 (2), 45.2, 43.8, 43.7, 42.1, 38.9, 37.5, 34.6, 32.0, 31.6, 31.5, 29.5, 29.4, 28.6, 26.7, 26.5, 24.0, 23.6, 23.4, 19.7, 18.8, 18.6. ESI-MS *m/z*: 570.36 (17%), 584.36 ([M + H]$^+$, 100%). Found C 71.09, H 9.51, N 2.35, calcd for $C_{35}H_{53}NO_6 \cdot 0.25H_2O$: C 71.46, H 9.17, N 2.38%.

Methyl 3,4-*seco*-30-*N*-methylalaninamido-olean-4(23),12-dien-3-oate (3.16): To a solution of compound **3.12** (290 mg, 0.60 mmol) and L-alanine methyl ester hydrochloride (251 mg, 1.80 mmol) in dichloromethane (8 ml), triethylamine (0.33 ml, 2.40 mmol) was added and the reaction mixture was stirred, at room temperature, for 10h, after which additional dichloromethane (2 ml) and triethylamine (0.17 ml, 1.20 mmol) and L-alanine methyl ester hydrochloride (84 mg, 0.60 mmol) were added. After 24 h, the reaction was completed. The work-up was performed as described for compound **3.14**. The solid was purified by FCC with petroleum ether/ ethyl acetate (3:2) to afford compound **3.16** as a white solid (48%). m.p.: 100-102°C. ^{1}H NMR (400MHz, $CDCl_3$): δ 6.22 (1H, m), 5.37 (1H, m), 4.87 (1H, br s), 4.67 (1H, br s), 4.63 (1H, m), 3.76 (3H, s), 3.65 (3H, s), 1.75 (3H, s), 1.40 (3H, m), 1.17 (3H, s), 1.11 (3H, s), 1.01 (3H, s), 0.94 (3H, s), 0.79 (3H, s). ^{13}C NMR (100MHz, $CDCl_3$): δ 176.2, 174.7, 173.9, 147.6, 144.5, 122.7, 113.7, 52.6, 51.7, 50.6, 48.0, 47.9, 44.0, 43.6, 42.2, 39.7, 39.3, 38.1, 38.0, 34.2, 32.2, 31.6, 31.5, 29.8, 28.6, 28.3, 27.0, 26.2, 25.9, 24.6, 23.9, 23.6, 19.7, 18.7, 17.0. ESI-MS *m/z*: 570.33 ([M + H]$^+$, 100%). Found C 73.04, H 9.94, N 2.45, calcd for $C_{35}H_{55}NO_5 \cdot 0.25H_2O$: C 73.20, H 9.74, N 2.44%.

Methyl 3,4-*seco*-3-*N*-glycinamido-11-oxo-olean-4(23),12-dien-30-oate (3.17): To a solution of compound **3.5** (120 mg, 0.21 mmol) in methanol (1 ml) and tetrahydrofuran (THF) (1.5 ml), KOH 4N (0.53 ml, 2.10 mmol) was added. After 10 min under magnetic stirring at room temperature, the reaction was completed. The pH of the reaction mixture was neutralized with 10% aqueous HCl. Dichloromethane (30 ml) and water (20 ml) were added to the mixture. The aqueous phase was further extracted with dichloromethane (2 × 30 ml). The combined organic phase was washed with water (2 × 30 ml) and brine (30 ml), dried over Na_2SO_4, filtered and the solvent was removed under reduced pressure to

afford compound **3.17** as a white solid (98%). m.p.: 223-225°C. ^{1}H NMR (400MHz, $CDCl_3$): δ 6.76 (1H, m), 5.70 (1H, s), 4.93 (1H, br s), 4.78 (1H, br s), 3.88-4.25 (2H, m), 3.70 (3H, s), 1.80 (3H, s), 1.36 (3H, s), 1.17 (3H, s), 1.15 (3H, s), 1.14 (3H, s), 0.81 (3H, s). ^{13}C NMR (100MHz, $CDCl_3$): δ 202.2, 177.0, 174.5, 173.3, 172.3, 146.5, 127.7, 114.8, 53.3, 52.0, 50.8, 48.6, 45.4, 44.2, 44.1, 41.8, 41.4, 39.2, 37.8, 36.1, 32.0, 31.9, 31.5, 31.3, 28.8, 28.3, 26.7, 26.5, 23.9, 23.8, 23.4, 19.7, 18.7. ESI-MS *m/z*: 556.26 ($[M + H]^+$, 100%).

Methyl 3,4-*seco*-3-*N*-alaninamido-11-oxo-olean-4(23),12-dien-30-oate (3.18): Compound **3.18** was prepared using the same method as for the preparation of **3.17**, but using compound **3.6** (116 mg, 0.20 mmol), methanol (1 ml), THF (1.5 ml) and KOH 4N (0.50 ml, 2.00 mmol), at room temperature for 10 min, to afford a white solid (94%). m.p.: 216-218°C. ^{1}H NMR (400MHz, $CDCl_3$): δ 6.89 (1H, m), 5.69 (1H, s), 4.94 (1H, br s), 4.78 (1H, br s), 4.61 (1H, m), 3.69 (3H, s), 1.80 (3H, s), 1.42 (3H, m), 1.35 (3H, s), 1.16 (3H, s), 1.14 (6H, s), 0.81 (3H, s). ^{13}C NMR (100MHz, $CDCl_3$): δ 202.0, 176.8, 175.3, 174.0, 173.1, 146.3, 127.6, 114.6, 53.2, 51.9, 50.6, 48.5, 48.0, 45.3, 44.0 (2), 41.2, 39.0, 37.7, 36.1, 31.9, 31.8, 31.3, 31.1, 28.6, 28.1, 26.5, 26.4, 23.8 (2), 23.2, 19.5, 18.7, 18.6. ESI-MS *m/z*: 570.26 ($[M + H]^+$, 100%).

3,4-*seco*-30-*N*-glycinamido-11-oxo-olean-4(23),12-dien-3-oic acid (3.19): The method followed that of compound **3.17**, using compound **3.13** (145 mg, 0.26 mmol), methanol (1 ml), THF (1.5 ml) and KOH 4N (0.65 ml, 2.60 mmol), at room temperature for 10 min, to afford compound **3.19** as a white solid (97%). m.p.: 213-215°C. ^{1}H NMR (400MHz, $CDCl_3$): δ 7.58 (1H, m), 5.77 (1H, s), 4.88 (1H, br s), 4.62 (1H, br s), 3.50-4.48 (2H, m), 1.72 (3H, s), 1.42 (3H, s), 1.21 (3H, s), 1.16 (3H, s), 1.09 (3H, s), 0.83 (3H, s). ^{13}C NMR (100MHz, $CDCl_3$): δ 202.1, 181.0, 177.3, 173.1, 172.7, 146.5, 128.0, 114.5, 52.5, 50.6, 47.5, 45.7, 44.2, 44.0, 42.1, 41.1, 39.5, 37.5, 34.5, 31.8, 31.6 (2), 30.2, 29.1, 28.7, 26.8 (2), 23.7, 23.4, 22.9, 19.8, 18.8. ESI-MS *m/z*: 542.26 ($[M + H]^+$, 100%).

3,4-*seco*-30-*N*-alaninamido-11-oxo-olean-4(23),12-dien-3-oic acid (3.20): Compound **3.20** was prepared using the same method as for the preparation of **3.17**, but using

compound **3.15** (170 mg, 0.29 mmol), methanol (1 ml), THF (1.5 ml) and KOH 4N (0.73 ml, 2.90 mmol), at room temperature for 10 min, to afford a white solid (98%). m.p.: 224-226°C. ^{1}H NMR (400MHz, $CDCl_3$): δ 7.37 (1H, m), 5.74 (1H, s), 4.88 (1H, br s), 4.78 (1H, m), 4.68 (1H, br s), 1.74 (3H, s), 1.15-1.35 (15H, m), 0.82 (3H, s). ^{13}C NMR (100MHz, $CDCl_3$): δ 201.1, 179.8, 176.9, 176.3, 171.8, 146.6, 128.1, 114.5, 52.7, 50.7, 47.8, 47.7, 45.7, 44.0, 43.8, 41.9, 39.2, 37.6, 34.1, 31.9, 31.6 (2), 29.6, 29.1, 28.7, 26.8, 26.7, 23.8, 23.5, 23.2, 19.8, 18.8, 17.6. ESI-MS *m/z*: 272.01 (10%), 527.35 (12), 556.25 ($[M + H]^+$, 100%).

3.4.2. Biology

A549, HT-29, Jurkat, MOLT-4, MIA PaCa 2, MCF7, HeLa, A375, HepG2, and BJ cells were obtained from the American Type Culture Collection (ATCC, Rockville, MD, USA). DMEM, RPMI-1640 medium, PBS, glucose 45%, human insulin 10 mg/ml, DMSO, MTT powder, TB 0.4%, PI and Hoescht 33342 were purchased from Sigma Aldrich Co. (St Louis, MO, USA). MEM, P/S and L-glutamine were purchased from Gibco-BRL (Eggenstein, Germany). Sodium pyruvate, trypsin/EDTA (0.05%/0.02%) and MEM-Eagle Non Essential Aminoacids 100× were obtained from Biological Industries (Kibbutz Beit Haemek, Israel). FBS was obtained from PAA Laboratories (Pasching, Austria), the Cell Proliferation Kit II (XTT kit) was purchased from Roche (Roche Molecular Biochemicals, Indianapolis, IN, USA) and annexin V-FITC was obtained from Bender MedSystems (Vienna, Austria).

Stock solutions of 20 mM in DMSO of the synthesized compounds were prepared and stored at -20°C. Working solutions were prepared in culture medium and appropriate amounts of DMSO were included in controls; all solutions had a final concentration of 0.5% DMSO.

3.4.2.1. Cell culture

A549, HT-29, MIA PaCa 2, HeLa and A375 cells were cultured in DMEM supplemented with 10% heat-inactivated FBS and 1% P/S. HepG2 and BJ cells were grown in DMEM supplemented with 10% heat-inactivated FBS, 1% P/S and 1mM

sodium pyruvate. Jurkat and MOLT-4 cells were cultured in RPMI-1640 medium supplemented with 10% heat-inactivated FBS, 1% P/S and 2 mM L-glutamine. MCF7 cells were maintained in MEM supplemented with 10% heat-inactivated FBS, 0.1% P/S, 1mM sodium pyruvate, 2 mM L-glutamine, 1× MEM-Eagle Non Essential Aminoacids, 0.01 mg/ml insulin human and 10mM glucose.

All cell cultures were performed at 37ºC in an atmosphere of 5% CO_2.

3.4.2.2. Antiproliferative Activity Assays

The antiproliferative activity of the synthesized compounds on A549, HT-29, MIA PaCa 2, MCF7, HeLa, A375, HepG2 and BJ adherent cells was determined by the MTT assay. Exponentially growing cells were plated in 96-well plates at a density of 1-8 × 10^3 cells/ well. After 24 h cells were attached to the plate, and the growth medium was replaced with fresh medium containing either the compounds dissolved in DMSO at different concentrations or only DMSO, in triplicate, and the cells were continued to culture for 72 h. After incubation with the compounds, the medium was removed and 100 µl of MTT solution (0.5 mg/ml) were added to each well and the plates were incubated for 1h. MTT was removed and 100 µl of DMSO was added to dissolve the formazan crystals. The absorbance was immediately read at 550 nm on an ELISA read plater (Tecan Sunrise MR20-301, TECAN, Austria). For Jurkat and MOLT-4 non-adherent cells, the antiproliferative activity was determined by XTT assay. These cell lines were plated with 5.5 × 10^3 and 1 × 10^4 cells/ well, respectively, in 96-well plates in 100 µl medium. The seeding was executed simultaneously with the addition of the different concentrations of compounds or vehicle, in triplicate, and cells were allowed to incubate for 72 h. After that incubation period, 100 µl of the XTT labelling mixture were added to each well and the plates were incubated again for 4 h. Then, the absorbance was read at 450 nm on the ELISA plate reader.

Concentrations that inhibit cell proliferation by 50% (IC_{50}) represent an average of a minimum of three independent experiments and were expressed as means ± standard deviation (SD).

3.4.2.3. Cell Cycle Analysis

Cell cycle was assessed by flow cytometry using a FACS. Jurkat cells were plated in 6-well plates at a density of 1.6×10^5 cells/well, simultaneously with the addition of compound **3.16**, at a concentration corresponding to its IC_{50} value at 72 h of treatment, or with only the vehicle, in a total volume of 2 ml of medium. The cells were allowed to incubate for 24, 48 and 72 h. After incubation, cells were collected and centrifuged. The supernatant was removed and the pellet was resuspended in 1 ml of TBS containing 1 mg/ml PI, 10 mg/ml RNase free of DNase and 0.1% Igepal CA-630, for 1 h, at 4ºC. FACS analysis was performed at 488 nm in an Epics XL flow cytometer (Coulter Corporation, Hialeah, FL, USA). Data were collected and analysed using the Multicycle software (Phoenix Flow Systems, San Diego, CA, USA).

Three independent experiments were performed, with two replicates per experiment.

3.4.2.4. Annexin V-FITC/ PI Flow Cytometry Assay

Apoptosis was assessed by flow cytometry using a FACS. Jurkat cells were plated in six-well plates at a density of 1.6×10^5 cells/well, simultaneously with the addition of compound **3.16**, at specified concentrations, or with only the vehicle, in a total volume of 2 ml of medium. The cells were allowed to incubate for 24, 48 and 72 h. After incubation, cells were collected and centrifuged. The supernatant was removed and the pellet was resuspended in 95 µl of binding buffer (10 mM HEPES/NaOH, pH 7.4, 140 mM NaCl, 2.5 mM $CaCl_2$). Annexin V-FITC conjugate (3 µl) was added and cells were incubated for 30 min, at room temperature, in darkness. After incubation, 0.8 ml of binding buffer were added. Just before the FACS analysis, cells were stained with 20 µl of 1mg/ml PI solution.

Three independent experiments were performed, with two replicates per experiment.

3.4.2.5. Hoechst 33342 Staining

The morphological changes were observed by fluorescence microscopy using Hoechst staining. Jurkat cells were plated in six-well plates at a density of 1.6×10^5 cells/well, simultaneously with the addition of compound **3.16**, at specified

concentrations, or with only the vehicle, in a total volume of 2 ml of medium. The cells were incubated for 72 h. After incubation, cells were collected by centrifugation, washed twice with PBS and stained with 500 µl of Hoechst 33342 solution (2 µg/ml in PBS), for 15 min, at room temperature, in darkness. Finally, cells were washed and resuspended in 10 µl PBS. The samples were mounted on a slide and observed with a fluorescence microscope (DMRB, Leica Microssystems, Wetzlar, Germany) with a DAPI filter.

Three independent experiments were conducted.

4. Concluding remarks

Cancer is still a disease with poor prognosis that requires more effective and safer chemotherapeutic options.

Natural products have been and will remain the most reliable source of new scaffolds for anticancer drug development. The ability of natural compounds to impact multiple signaling pathways is a remarkable feature that could face the intricate networks of the different cancers that render them resistant to the available current treatments.

Glycyrrhetinic acid is a pentacyclic triterpenoid that can be considered as a potential lead because of its promising multi-target anticancer activity and its commercial availability. However, this natural compound lacks potency and selectivity as an antitumor agent. The chemical modification of its skeleton can generate compounds with improved anticancer activity.

In this work, two series of new glycyrrhetinic acid derivatives were designed and prepared, adopting different semisynthetic strategies. As described in Chapter 2, we prepared a series of derivatives via the introduction of different heterocyclic rings conjugated with an α,β-unsaturated ketone in its ring A. This conjugation was achieved through distinct chemical reactions, including the Cu (I)-catalysed azide-alkyne cycloaddition. In Chapter 3, the synthesis of the new compounds was performed via the opening of the ring A along with the coupling of an amino acid. The conjugation of the amino acid moiety was carried out using the coupling reagent Deoxo-Fluor®. The structures of the new derivatives were elucidated using different techniques, including, ^{1}H NMR, ^{13}C NMR, IR and MS.

The glycyrrhetinic acid derivatives were tested for their antiproliferative activity against several cancer lines, and many compounds were found to be more active than the parent compound. The most potent derivative of each series was also tested in the nontumoral BJ cell line, to evaluate their selectivity. The leukemia Jurkat cell line, in which the antiproliferative assays had the best results for both series, was selected to the execution of further biological assays.

The most potent derivative of the first series was compound **2.9**, which bears an imidazole ring conjugated to the α,β-unsaturated ketone in the ring A , has a reduced ring C and a methyl ester at C-30 position. This compound had an IC_{50} value of 1.1μM on Jurkat cells, which was 96-fold more potent than glycyrrhetinic acid and was also 4-fold more selective toward that cells. Further biological studies showed that compound **2.9** is a

potent inducer of apoptosis that activates both the intrinsic and extrinsic pathways, as early as at 6 h of treatment.

In the second group of derivatives, compound **3.16**, with a cleaved ring A, a reduced ring C and an alanine methyl esther chain at C-30 position, was the more active compound. It had an IC50 value of 6.1 μM on Jurkat cells, which was 17-fold more potent than that of glycyrrhetinic acid, and was up to 10 times more selective toward that cells. Preliminary mechanism investigation indicated that the antiproliferative activity of compound **3.16** was due to cell cycle arrest at the S phase and induction of apoptosis.

Additional studies are needed to further precise the molecular pathways that drive the anticancer activity of these derivatives.

The obtained results demonstrated that the semisynthetic strategies used in this work were able to enhance the potency and selectivity of the promising lead glycyrrhetinic acid.

5. References

1. Sung, H.; Ferlay, J.; Siegel, R.L.; Laversanne, M.; Soerjomataram, I.; Jemal, A.; Bray, F. Global cancer statistics 2020: GLOBOCAN estimates of incidence and mortality worldwide for 36 cancers in 185 countries. *CA-Cancer J. Clin.* **2021**, *71*, 209-249, doi:10.3322/caac.21660.
2. Weinberg, R.A. *Biology of Cancer, Second Edition*; Garland Science, Taylor & Francis: New York, 2014.
3. Cooper, G.M. *The cell : a molecular approach*, 8th ed.; Sinauer Associates: 2018.
4. Hanahan, D.; Weinberg, R.A. The hallmarks of cancer. *Cell* **2000**, *100*, 57-70, doi:10.1016/s0092-8674(00)81683-9.
5. Hanahan, D.; Weinberg, R.A. Hallmarks of Cancer: The Next Generation. *Cell* **2011**, *144*, 646-674, doi:10.1016/j.cell.2011.02.013.
6. Su, Z.Y.; Yang, Z.Z.; Xu, Y.Q.; Chen, Y.B.; Yu, Q. Apoptosis, autophagy, necroptosis, and cancer metastasis. *Mol. Cancer* **2015**, *14*, 14, doi:10.1186/s12943-015-0321-5.
7. Nishida, N.; Yano, H.; Nishida, T.; Kamura, T.; Kojiro, M. Angiogenesis in cancer. *Vasc. Health Risk Manag.* **2006**, *2*, 213-219, doi:10.2147/vhrm.2006.2.3.213.
8. Ma, W. Cell Cycle Checkpoint. In *Encyclopedia of Cancer*, Schwab, M., Ed. Springer Berlin Heidelberg: Berlin, Heidelberg, 2017; 10.1007/978-3-662-46875-3_996pp. 897-901.
9. Schafer, K.A. The cell cycle: A review. *Vet. Pathol.* **1998**, *35*, 461-478, doi:10.1177/030098589803500601.
10. Vermeulen, K.; Van Bockstaele, D.R.; Berneman, Z.N. The cell cycle: a review of regulation, deregulation and therapeutic targets in cancer. *Cell Prolif.* **2003**, *36*, 131-149, doi:10.1046/j.1365-2184.2003.00266.x.
11. Otto, T.; Sicinski, P. Cell cycle proteins as promising targets in cancer therapy. *Nat. Rev. Cancer* **2017**, *17*, 93-115, doi:10.1038/nrc.2016.138.
12. Pucci, B.; Kasten, M.; Giordano, A. Cell cycle and apoptosis. *Neoplasia* **2000**, *2*, 291-299, doi:10.1038/sj.neo.7900101.
13. Williams, G.H.; Stoeber, K. The cell cycle and cancer. *J. Pathol.* **2012**, *226*, 352-364, doi:10.1002/path.3022.
14. Golias, C.H.; Charalabopoulos, A.; Charalabopoulos, K. Cell proliferation and cell cycle control: a mini review. *Int. J. Clin. Pract.* **2004**, *58*, 1134-1141, doi:10.1111/j.1742-1241.2004.00284.x.
15. Park, M.T.; Lee, S.J. Cell cycle and cancer. *J. Biochem. Mol. Biol.* **2003**, *36*, 60-65.
16. Malumbres, M.; Barbacid, M. Cell cycle, CDKs and cancer: a changing paradigm. *Nat. Rev. Cancer* **2009**, *9*, 153-166, doi:10.1038/nrc2602.
17. Diaz-Moralli, S.; Tarrado-Castellarnau, M.; Miranda, A.; Cascante, M. Targeting cell cycle regulation in cancer therapy. *Pharmacol. Ther.* **2013**, *138*, 255-271, doi:10.1016/j.pharmthera.2013.01.011.
18. Schwartz, G.K.; Shah, M.A. Targeting the cell cycle: A new approach to cancer therapy. *J. Clin. Oncol.* **2005**, *23*, 9408-9421, doi:10.1200/jco.2005.01.5594.

19. Sun, Y.; Peng, Z.L. Programmed cell death and cancer. *Postgraduate Medical Journal* **2009**, *85*, 134-140, doi:10.1136/pgmj.2008.072629.

20. Ouyang, L.; Shi, Z.; Zhao, S.; Wang, F.T.; Zhou, T.T.; Liu, B.; Bao, J.K. Programmed cell death pathways in cancer: a review of apoptosis, autophagy and programmed necrosis. *Cell Prolif.* **2012**, *45*, 487-498, doi:10.1111/j.1365-2184.2012.00845.x.

21. Mishra, A.P.; Salehi, B.; Sharifi-Rad, M.; Pezzani, R.; Kobarfard, F.; Sharifi-Rad, J.; Nigam, M. Programmed Cell Death, from a Cancer Perspective: An Overview. *Molecular Diagnosis & Therapy* **2018**, *22*, 281-295, doi:10.1007/s40291-018-0329-9.

22. Kasibhatla, S.; Tseng, B. Why target apoptosis in cancer treatment? *Molecular Cancer Therapeutics* **2003**, *2*, 573-580.

23. Elmore, S. Apoptosis: A review of programmed cell death. *Toxicologic Pathology* **2007**, *35*, 495-516, doi:10.1080/01926230701320337.

24. Cotter, T.G. Apoptosis and cancer: the genesis of a research field. *Nat. Rev. Cancer* **2009**, *9*, 501-507, doi:10.1038/nrc2663.

25. Wong, R.S.Y. Apoptosis in cancer: from pathogenesis to treatment. *J. Exp. Clin. Cancer Res.* **2011**, *30*, 14, doi:10.1186/1756-9966-30-87.

26. Pistritto, G.; Trisciuoglio, D.; Ceci, C.; Garufi, A.; D'Orazi, G. Apoptosis as anticancer mechanism: function and dysfunction of its modulators and targeted therapeutic strategies. *Aging-Us* **2016**, *8*, 603-619, doi:10.18632/aging.100934.

27. D'Arcy, M.S. Cell death: a review of the major forms of apoptosis, necrosis and autophagy. *Cell Biology International* **2019**, *43*, 582-592, doi:10.1002/cbin.11137.

28. Fernald, K.; Kurokawa, M. Evading apoptosis in cancer. *Trends in Cell Biology* **2013**, *23*, 620-633, doi:10.1016/j.tcb.2013.07.006.

29. Galluzzi, L.; Vitale, I.; Aaronson, S.A.; Abrams, J.M.; Adam, D.; Agostinis, P.; Alnemri, E.S.; Altucci, L.; Amelio, I.; Andrews, D.W., et al. Molecular mechanisms of cell death: recommendations of the Nomenclature Committee on Cell Death 2018. *Cell Death Differ.* **2018**, *25*, 486-541, doi:10.1038/s41418-017-0012-4.

30. Pfeffer, C.M.; Singh, A.T.K. Apoptosis: A Target for Anticancer Therapy. *International Journal of Molecular Sciences* **2018**, *19*, doi:10.3390/ijms19020448.

31. Letai, A. Apoptosis and Cancer. In *Annual Review of Cancer Biology, Vol 1*, Jacks, T., Sawyers, C.L., Eds. 2017; Vol. 1, pp. 275-294.

32. Carneiro, B.A.; El-Deiry, W.S. Targeting apoptosis in cancer therapy. *Nature Reviews Clinical Oncology* **2020**, *17*, 395-417, doi:10.1038/s41571-020-0341-y.

33. Tan, M.L.; Ooi, J.P.; Ismail, N.; Moad, A.I.H.; Muhammad, T.S.T. Programmed Cell Death Pathways and Current Antitumor Targets. *Pharmaceutical Research* **2009**, *26*, 1547-1560, doi:10.1007/s11095-009-9895-1.

34. Vogelstein, B.; Lane, D.; Levine, A.J. Surfing the p53 network. *Nature* **2000**, *408*, 307-310, doi:10.1038/35042675.

35. Brady, C.A.; Attardi, L.D. p53 at a glance. *J. Cell Sci.* **2010**, *123*, 2527-2532, doi:10.1242/jcs.064501.

36. Dias, D.A.; Urban, S.; Roessner, U. A Historical Overview of Natural Products in Drug Discovery. *Metabolites* **2012**, *2*, 34, doi:10.3390/metabo2020303.

37. Chopra, B.; Dhingra, A.K. Natural products: A lead for drug discovery and development. *Phytother. Res.* 10.1002/ptr.7099, 43, doi:10.1002/ptr.7099.

38. Atanasov, A.G.; Zotchev, S.B.; Dirsch, V.M.; Supuran, C.T.; Int Nat Prod Sci, T. Natural products in drug discovery: advances and opportunities. *Nat. Rev. Drug Discov.* **2021**, *20*, 200-216, doi:10.1038/s41573-020-00114-z.

39. Newman, D.J.; Cragg, G.M. Natural Products as Sources of New Drugs over the Nearly Four Decades from 01/1981 to 09/2019. *J. Nat. Prod.* **2020**, *83*, 770-803, doi:10.1021/acs.jnatprod.9b01285.

40. Cragg, G.M.; Newman, D.J. Plants as a source of anti-cancer agents. *J. Ethnopharmacol.* **2005**, *100*, 72-79, doi:10.1016/j.jep.2005.05.011.

41. Khazir, J.; Mir, B.A.; Pilcher, L.; Riley, D.L. Role of plants in anticancer drug discovery. *Phytochem. Lett.* **2014**, *7*, 173-181, doi:10.1016/j.phytol.2013.11.010.

42. Seca, A.M.L.; Pinto, D. Plant Secondary Metabolites as Anticancer Agents: Successes in Clinical Trials and Therapeutic Application. *International Journal of Molecular Sciences* **2018**, *19*, 22, doi:10.3390/ijms19010263.

43. Choudhari, A.S.; Mandave, P.C.; Deshpande, M.; Ranjekar, P.; Prakash, O. Phytochemicals in Cancer Treatment: From Preclinical Studies to Clinical Practice. *Front. Pharmacol.* **2020**, *10*, 17, doi:10.3389/fphar.2019.01614.

44. Dehelean, C.A.; Marcovici, I.; Soica, C.; Mioc, M.; Coricovac, D.; Iurciuc, S.; Cretu, O.M.; Pinzaru, I. Plant-Derived Anticancer Compounds as New Perspectives in Drug Discovery and Alternative Therapy. *Molecules* **2021**, *26*, 29, doi:10.3390/molecules26041109.

45. Salehi, B.; Zucca, P.; Sharifi-Rad, M.; Pezzani, R.; Rajabi, S.; Setzer, W.N.; Varoni, E.M.; Iriti, M.; Kobarfard, F.; Sharifi-Rad, J. Phytotherapeutics in cancer invasion and metastasis. *Phytother. Res.* **2018**, *32*, 1425-1449, doi:10.1002/ptr.6087.

46. Bernardini, S.; Tiezzi, A.; Masci, V.L.; Ovidi, E. Natural products for human health: an historical overview of the drug discovery approaches. *Nat. Prod. Res.* **2018**, *32*, 1926-1950, doi:10.1080/14786419.2017.1356838.

47. Huang, M.; Lu, J.J.; Ding, J. Natural Products in Cancer Therapy: Past, Present and Future. *Nat. Product. Bioprospecting* **2021**, *11*, 5-13, doi:10.1007/s13659-020-00293-7.

48. Atanasov, A.G.; Waltenberger, B.; Pferschy-Wenzig, E.M.; Linder, T.; Wawrosch, C.; Uhrin, P.; Temml, V.; Wang, L.M.; Schwaiger, S.; Heiss, E.H., et al. Discovery and resupply of pharmacologically active plant-derived natural products: A review. *Biotechnol. Adv.* **2015**, *33*, 1582-1614, doi:10.1016/j.biotechadv.2015.08.001.

49. Cragg, G.M.; Grothaus, P.G.; Newman, D.J. Impact of Natural Products on Developing New Anti-Cancer Agents. *Chem. Rev.* **2009**, *109*, 3012-3043, doi:10.1021/cr900019j.

50. Li, G.; Lou, H.X. Strategies to diversify natural products for drug discovery. *Med. Res. Rev.* **2018**, *38*, 1255-1294, doi:10.1002/med.21474.

51. Lachance, H.; Wetzel, S.; Kumar, K.; Waldmann, H. Charting, Navigating, and Populating Natural Product Chemical Space for Drug Discovery. *J. Med. Chem.* **2012**, *55*, 5989-6001, doi:10.1021/jm300288g.

52. Harvey, A.L.; Edrada-Ebel, R.; Quinn, R.J. The re-emergence of natural products for drug discovery in the genomics era. *Nat. Rev. Drug Discov.* **2015**, *14*, 111-129, doi:10.1038/nrd4510.

53. Basmadjian, C.; Zhao, Q.; Bentouhami, E.; Djehal, A.; Nebigil, C.G.; Johnson, R.A.; Serova, M.; de Gramont, A.; Faivre, S.; Raymond, E., et al. Cancer wars: natural products strike back. *Front. Chem.* **2014**, *2*, 18, doi:10.3389/fchem.2014.00020.

54. Thomford, N.E.; Senthebane, D.A.; Rowe, A.; Munro, D.; Seele, P.; Maroyi, A.; Dzobo, K. Natural Products for Drug Discovery in the 21st Century: Innovations for Novel Drug Discovery. *International Journal of Molecular Sciences* **2018**, *19*, 29, doi:10.3390/ijms19061578.

55. Harvey, A.L. Natural products in drug discovery. *Drug Discov. Today* **2008**, *13*, 894-901, doi:10.1016/j.drudis.2008.07.004.

56. Li, J.W.H.; Vederas, J.C. Drug Discovery and Natural Products: End of an Era or an Endless Frontier? *Science* **2009**, *325*, 161-165, doi:10.1126/science.1168243.

57. Gordaliza, M. Natural products as leads to anticancer drugs. *Clin. Transl. Oncol.* **2007**, *9*, 767-776, doi:10.1007/s12094-007-0138-9.

58. Majhi, S.; Das, D. Chemical derivatization of natural products: Semisynthesis and pharmacological aspects- A decade update. *Tetrahedron* **2021**, *78*, 22, doi:10.1016/j.tet.2020.131801.

59. Yao, H.; Liu, J.K.; Xu, S.T.; Zhu, Z.Y.; Xu, J.Y. The structural modification of natural products for novel drug discovery. *Expert. Opin. Drug Discov.* **2017**, *12*, 121-140, doi:10.1080/17460441.2016.1272757.

60. Yuan, H.D.; Ma, Q.Q.; Ye, L.; Piao, G.C. The Traditional Medicine and Modern Medicine from Natural Products. *Molecules* **2016**, *21*, 18, doi:10.3390/molecules21050559.

61. Cragg, G.M.; Newman, D.J. Natural products: A continuing source of novel drug leads. *Biochim. Biophys. Acta-Gen. Subj.* **2013**, *1830*, 3670-3695, doi:10.1016/j.bbagen.2013.02.008.

62. Gershenzon, J.; Dudareva, N. The function of terpene natural products in the natural world. *Nat. Chem. Biol.* **2007**, *3*, 408-414, doi:10.1038/nchembio.2007.5.

63. Hanson, J.R. *THE PENTACYCLIC TRITERPENES*; Nova Science Publishers, Inc: Hauppauge, 2010; pp. 1-11.

64. Cox-Georgian, D.; Ramadoss, N.; Dona, C.; Basu, C. *Therapeutic and Medicinal Uses of Terpenes*; Springer International Publishing Ag: Cham, 2019; 10.1007/978-3-030-31269-5_15pp. 333-359.

65. Ghosh, S. Biosynthesis of Structurally Diverse Triterpenes in Plants: the Role of Oxidosqualene Cyclases. *Proceedings of the Indian National Science Academy* **2016**, *82*, 1189-1210, doi:10.16943/ptinsa/2016/48578.

66. Tetali, S.D. Terpenes and isoprenoids: a wealth of compounds for global use. *Planta* **2019**, *249*, 1-8, doi:10.1007/s00425-018-3056-x.

67. Yang, W.Q.; Chen, X.; Li, Y.L.; Guo, S.F.; Wang, Z.; Yu, X.L. Advances in Pharmacological Activities of Terpenoids. *Nat. Prod. Commun.* **2020**, *15*, 13, doi:10.1177/1934578x20903555.

68. Salvador, J.A.R.; Moreira, V.M.; Goncalves, B.M.F.; Leal, A.S.; Jing, Y.K. Ursane-type pentacyclic triterpenoids as useful platforms to discover anticancer drugs. *Nat. Prod. Rep.* **2012**, *29*, 1463-1479, doi:10.1039/c2np20060k.

69. Thimmappa, R.; Geisler, K.; Louveau, T.; O'Maille, P.; Osbourn, A. Triterpene Biosynthesis in Plants. In *Annual Review of Plant Biology, Vol 65*, Merchant, S.S., Ed. Annual Reviews: Palo Alto, 2014; Vol. 65, pp. 225-257.

70. Dzubak, P.; Hajduch, M.; Vydra, D.; Hustova, A.; Kvasnica, M.; Biedermann, D.; Markova, L.; Urban, M.; Sarek, J. Pharmacological activities of natural triterpenoids and their therapeutic implications. *Nat. Prod. Rep.* **2006**, *23*, 394-411, doi:10.1039/b515312n.

71. Sheng, H.M.; Sun, H.B. Synthesis, biology and clinical significance of pentacyclic triterpenes: a multi-target approach to prevention and treatment of metabolic and vascular diseases. *Nat. Prod. Rep.* **2011**, *28*, 543-593, doi:10.1039/c0np00059k.

72. Jesus, J.A.; Lago, J.H.G.; Laurenti, M.D.; Yamamoto, E.S.; Passero, L.F.D. Antimicrobial Activity of Oleanolic and Ursolic Acids: An Update. *Evid.-based Complement Altern. Med.* **2015**, *2015*, 14, doi:10.1155/2015/620472.

73. Sharma, H.; Kumar, P.; Deshmukh, R.R.; Bishayee, A.; Kumar, S. Pentacyclic triterpenes: New tools to fight metabolic syndrome. *Phytomedicine* **2018**, *50*, 166-177, doi:10.1016/j.phymed.2018.09.011.

74. Laszczyk, M.N. Pentacyclic Triterpenes of the Lupane, Oleanane and Ursane Group as Tools in Cancer Therapy. *Planta Med.* **2009**, *75*, 1549-1560, doi:10.1055/s-0029-1186102.

75. Shanmugam, M.K.; Nguyen, A.H.; Kumar, A.P.; Tan, B.K.H.; Sethi, G. Targeted inhibition of tumor proliferation, survival, and metastasis by pentacyclic triterpenoids: Potential role in prevention and therapy of cancer. *Cancer Lett.* **2012**, *320*, 158-170, doi:10.1016/j.canlet.2012.02.037.

76. Kamble, S.M.; Goyal, S.N.; Patil, C.R. Multifunctional pentacyclic triterpenoids as adjuvants in cancer chemotherapy: a review. *RSC Adv.* **2014**, *4*, 33370-33382, doi:10.1039/c4ra02784a.

77. Peron, G.; Marzaro, G.; Dall'Acqua, S. Known Triterpenes and their Derivatives as Scaffolds for the Development of New Therapeutic Agents for Cancer. *Curr. Med. Chem.* **2018**, *25*, 1259-1269, doi:10.2174/0929867324666170818111933.

78. Asl, M.N.; Hosseinzadeh, H. Review of pharmacological effects of Glycyrrhiza sp and its bioactive compounds. *Phytother. Res.* **2008**, *22*, 709-724, doi:10.1002/ptr.2362.

79. Baltina, L.A. Chemical modification of glycyrrhizic acid as a route to new bioactive compounds for medicine. *Curr. Med. Chem.* **2003**, *10*, 155-171, doi:10.2174/0929867033368538.

80. Kao, T.C.; Wu, C.H.; Yen, G.C. Bioactivity and Potential Health Benefits of Licorice. *J. Agric. Food Chem.* **2014**, *62*, 542-553, doi:10.1021/jf404939f.

81. Hosseinzadeh, H.; Nassiri-Asl, M. Pharmacological Effects of Glycyrrhiza spp. and Its Bioactive Constituents: Update and Review. *Phytother. Res.* **2015**, *29*, 1868-1886, doi:10.1002/ptr.5487.

82. Wang, C.Y.; Kao, T.C.; Lo, W.H.; Yen, G.C. Glycyrrhizic Acid and 18 beta-Glycyrrhetinic Acid Modulate Lipopolysaccharide-Induced Inflammatory Response by Suppression of NF-kappa B through PI3K p110 delta and p110 gamma Inhibitions. *J. Agric. Food Chem.* **2011**, *59*, 7726-7733, doi:10.1021/jf2013265.

83. Ku, C.M.; Lin, J.Y. Anti-inflammatory effects of 27 selected terpenoid compounds tested through modulating Th1/Th2 cytokine secretion profiles using murine primary splenocytes. *Food Chem.* **2013**, *141*, 1104-1113, doi:10.1016/j.foodchem.2013.04.044.

84. Oyama, K.; Kawada-Matsuo, M.; Oogai, Y.; Hayashi, T.; Nakamura, N.; Komatsuzawa, H. Antibacterial Effects of Glycyrrhetinic Acid and Its Derivatives on Staphylococcus aureus. *PLoS One* **2016**, *11*, 17, doi:10.1371/journal.pone.0165831.

85. Kannan, S.; Sathasivam, G.; Marudhamuthu, M. Decrease of growth, biofilm and secreted virulence in opportunistic nosocomial Pseudomonas aeruginosa ATCC 25619 by glycyrrhetinic acid. *Microb. Pathog.* **2019**, *126*, 332-342, doi:10.1016/j.micpath.2018.11.026.

86. Hardy, M.E.; Hendricks, J.M.; Paulson, J.M.; Faunce, N.R. 18 beta-glycyrrhetinic acid inhibits rotavirus replication in culture. *Virol. J.* **2012**, *9*, 7, doi:10.1186/1743-422x-9-96.

87. Paduch, R.; Kandefer-Szerszen, M. Antitumor and Antiviral Activity of Pentacyclic Triterpenes. *Mini-Rev. Org. Chem.* **2014**, *11*, 262-268, doi:10.2174/1570193x1103140915105240.

88. Farina, C.; Pinza, M.; Pifferi, G. Synthesis and anti-ulcer activity of new derivatives of glycyrrhetic, oleanolic and ursolic. *Farmaco* **1998**, *53*, 22-32, doi:10.1016/s0014-827x(97)00013-x.

89. Kalaiarasi, P.; Pugalendi, K.V. Antihyperglycemic effect of 18 beta-glycyrrhetinic acid, aglycone of glycyrrhizin, on streptozotocin-diabetic rats. *Eur. J. Pharmacol.* **2009**, *606*, 269-273, doi:10.1016/j.ejphar.2008.12.057.

90. Zhang, Y.; Yang, S.N.; Zhang, M.; Wang, Z.H.; He, X.; Hou, Y.Y.; Bai, G. Glycyrrhetinic Acid Improves Insulin-Response Pathway by Regulating the Balance between the Ras/MAPK and PI3K/Akt Pathways. *Nutrients* **2019**, *11*, 13, doi:10.3390/nu11030604.

91. Yang, M.; Zhang, M.Y.; Liu, Q.L.; Xu, T.T.; Huang, T.L.; Yao, D.S.; Wong, C.W.; Liu, J.S.; Guan, M. 18 beta-Glycyrrhetinic acid acts through hepatocyte nuclear factor 4 alpha to modulate lipid and carbohydrate metabolism. *Pharmacol. Res.* **2020**, *157*, 12, doi:10.1016/j.phrs.2020.104840.

92. Wu, S.Y.; Wang, W.J.; Dou, J.H.; Gong, L.K. Research progress on the protective effects of licorice-derived 18 beta-glycyrrhetinic acid against liver injury. *Acta Pharmacol. Sin.* **2021**, *42*, 18-26, doi:10.1038/s41401-020-0383-9.

93. Wu, S.Y.; Cui, S.C.; Wang, L.; Zhang, Y.Y.; Yan, X.X.; Lu, H.L.; Xing, G.Z.; Ren, J.; Gong, L.K. 18 beta-Glycyrrhetinic acid protects against alpha-

naphthylisothiocyanate-induced cholestasis through activation of the Sirt1/FXR signaling pathway. *Acta Pharmacol. Sin.* **2018**, *39*, 1865-1873, doi:10.1038/s41401-018-0110-y.

94. Yang, G.L.; Zhang, L.; Ma, L.; Jiang, R.; Kuang, G.; Li, K.; Tie, H.T.; Wang, B.; Cheng, X.Y.; Xie, T.J., et al. Glycyrrhetinic acid prevents acetaminophen-induced acute liver injury via the inhibition of CYP2E1 expression and HMGB1-TLR4 signal activation in mice. *Int. Immunopharmacol.* **2017**, *50*, 186-193, doi:10.1016/j.intimp.2017.06.027.

95. Mahmoud, A.M.; Hussein, O.E.; Hozayen, W.G.; Abd el-Twab, S.M. Methotrexate hepatotoxicity is associated with oxidative stress, and down-regulation of PPAR gamma and Nrf2: Protective effect of 18 beta-Glycyrrhetinic acid. *Chem.-Biol. Interact.* **2017**, *270*, 59-72, doi:10.1016/j.cbi.2017.04.009.

96. Wu, X.D.; Zhang, L.Y.; Gurley, E.; Studer, E.; Shang, J.; Wang, T.; Wang, C.F.; Yan, M.; Jiang, Z.Z.; Hylemon, P.B., et al. Prevention of free fatty acid-induced hepatic lipotoxicity by 18 beta-glycyrrhetinic acid through lysosomal and mitochondrial pathways. *Hepatology* **2008**, *47*, 1905-1915, doi:10.1002/hep.22239.

97. Jeong, H.G.; You, H.J.; Park, S.J.; Moon, A.R.; Chung, Y.C.; Kang, S.K.; Chun, H.K. Hepatoprotective effects of 18 beta-glycyrrhetinic acid on carbon tetrachloride-induced liver injury: Inhibition of cytochrome P450 2E1 expression. *Pharmacol. Res.* **2002**, *46*, 221-227, doi:10.1016/s1043-6618(02)00121-4.

98. Akasaka, Y.; Yoshida, T.; Tsukahara, M.; Hatta, A.; Inoue, H. Glycyrrhetinic acid prevents cutaneous scratching behavior in mice elicited by substance P or PAR-2 agonist. *Eur. J. Pharmacol.* **2011**, *670*, 175-179, doi:10.1016/j.ejphar.2011.08.043.

99. Kim, S.H.; Hong, J.H.; Lee, J.E.; Lee, Y.C. 18 beta-Glycyrrhetinic acid, the major bioactive component of Glycyrrhizae Radix, attenuates airway inflammation by modulating Th2 cytokines, GATA-3, STAT6, and Foxp3 transcription factors in an asthmatic mouse model. *Environ. Toxicol. Pharmacol.* **2017**, *52*, 99-113, doi:10.1016/j.etap.2017.03.011.

100. Kuang, P.H.; Zhao, W.X.; Su, W.X.; Zhang, Z.Q.; Zhang, L.; Liu, J.M.; Ren, G.L.; Yin, Z.Y.; Wang, X.M. 18 beta-glycyrrhetinic acid inhibits hepatocellular carcinoma development by reversing hepatic stellate cell-mediated immunosuppression in mice. *Int. J. Cancer* **2013**, *132*, 1831-1841, doi:10.1002/ijc.27852.

101. Kim, J.; Joo, I.; Kim, H.; Han, Y. 18 beta-Glycyrrhetinic acid induces immunological adjuvant activity of Th1 against Candida albicans surface mannan extract. *Phytomedicine* **2013**, *20*, 951-955, doi:10.1016/j.phymed.2013.04.008.

102. Jeong, H.G.; Kim, J.Y. Induction of inducible nitric oxide synthase expression by 18 beta-glycyrrhetinic acid in macrophages. *FEBS Lett.* **2002**, *513*, 208-212, doi:10.1016/s0014-5793(02)02311-6.

103. Kowalska, A.; Kalinowska-Lis, U. 18 beta-Glycyrrhetinic acid: its core biological properties and dermatological applications. *Int. J. Cosmetic Sci.* **2019**, *41*, 325-331, doi:10.1111/ics.12548.

104. Zhang, T.; Liao, J.Y.; Yu, L.; Liu, G.S. Regulating effect of glycyrrhetinic acid on bronchial asthma smooth muscle proliferation and apoptosis as well as inflammatory factor expression through ERK1/2 signaling pathway. *Asian Pac. J. Trop. Med.* **2017**, *10*, 1172-1176, doi:10.1016/j.apjtm.2017.10.025.

105. Cao, D.H.; Jiang, J.; Zhao, D.; Wu, M.H.; Zhang, H.J.; Zhou, T.Y.; Tsukamoto, T.; Oshima, M.; Wang, Q.; Cao, X.Y. The protective effects of 18 beta-glycyrrhetinic acid against inflammation microenvironment in gastric tumorigenesis targeting PGE2-EP2 receptor-mediated arachidonic acid pathway. *Eur. J. Inflamm.* **2018**, *16*, 7, doi:10.1177/2058739218762993.

106. Hasan, S.K.; Siddiqi, A.; Nafees, S.; Ali, N.; Rashid, S.; Ali, R.; Shahid, A.; Sultana, S. Chemopreventive effect of 18 beta-glycyrrhetinic acid via modulation of inflammatory markers and induction of apoptosis in human hepatoma cell line (HepG2). *Mol. Cell. Biochem.* **2016**, *416*, 169-177, doi:10.1007/s11010-016-2705-2.

107. Hasan, S.K.; Khan, R.; Ali, N.; Khan, A.Q.; Rehman, M.U.; Tahir, M.; Lateef, A.; Nafees, S.; Mehdi, S.J.; Rashid, S., et al. 18-Glycyrrhetinic acid alleviates 2-acetylaminofluorene-induced hepatotoxicity in Wistar rats: Role in hyperproliferation, inflammation and oxidative stress. *Hum. Exp. Toxicol.* **2015**, *34*, 628-641, doi:10.1177/0960327114554045.

108. Lin, D.J.; Zhong, W.; Li, J.; Zhang, B.; Song, G.; Hu, T.H. Involvement of BID Translocation in Glycyrrhetinic Acid and 11-Deoxy Glycyrrhetinic Acid-Induced Attenuation of Gastric Cancer Growth. *Nutr. Cancer* **2014**, *66*, 463-473, doi:10.1080/01635581.2013.877498.

109. Wang, S.S.; Shen, Y.; Qiu, R.F.; Chen, Z.L.; Chen, Z.H.; Chen, W.B. 18 beta-glycyrrhetinic acid exhibits potent antitumor effects against colorectal cancer via inhibition of cell proliferation and migration. *Int. J. Oncol.* **2017**, *51*, 615-624, doi:10.3892/ijo.2017.4059.

110. Cao, D.H.; Wu, Y.H.; Jia, Z.F.; Zhao, D.; Zhang, Y.Y.; Zhou, T.Y.; Wu, M.H.; Zhang, H.J.; Tsukamoto, T.; Oshima, M., et al. 18 beta-glycyrrhetinic acid inhibited mitochondrial energy metabolism and gastric carcinogenesis through methylation-regulated TLR2 signaling pathway. *Carcinogenesis* **2019**, *40*, 234-245, doi:10.1093/carcin/bgy150.

111. Hong, W.K.; Sporn, M.B. Recent advances in chemoprevention of cancer. *Science* **1997**, *278*, 1073-1077, doi:10.1126/science.278.5340.1073.

112. Tsao, A.S.; Kim, E.S.; Hong, W.K. Chemoprevention of cancer. *CA: a cancer journal for clinicians* **2004**, *54*, 150-180, doi:10.3322/canjclin.54.3.150.

113. Kowsalya, R.; Vishwanathan, P.; Manoharan, S. Chemopreventive potential of 18beta-glycyrrhetinic acid: an active constituent of liquorice, in 7,12-dimethylbenz(a)anthracene induced hamster buccal pouch carcinogenesis. *Pakistan journal of biological sciences : PJBS* **2011**, *14*, 619-626.

114. Agarwal, M.K.; Iqbal, M.; Athar, M. Inhibitory effect of 18 beta-glycyrrhetinic acid on 12-O-tetradecanoyl phorbol-13-acetate-induced cutaneous oxidative stress and tumor promotion in mice. *Redox Rep.* **2005**, *10*, 151-157, doi:10.1179/135100005x57346.

115. Li, Y.; Feng, L.; Song, Z.F.; Li, H.B.; Huai, Q.Y. Synthesis and Anticancer Activities of Glycyrrhetinic Acid Derivatives. *Molecules* **2016**, *21*, 20, doi:10.3390/molecules21020199.

116. Song, H.; Sun, Y.X.; Xu, G.L.; Hou, B.B.; Ao, G.Z. Synthesis and biological evaluation of novel hydrogen sulfide releasing glycyrrhetic acid derivatives. *J. Enzym. Inhib. Med. Chem.* **2016**, *31*, 1457-1463, doi:10.3109/14756366.2016.1144596.

117. Sharma, G.; Kar, S.; Palit, S.; Das, P.K. 18 beta-glycyrrhetinic acid (concur) induces apoptosis through modulation of Akt/FOXO3a/Bim pathway in human breast cancer MCF-7 cells. *J. Cell. Physiol.* **2012**, *227*, 1923-1931, doi:10.1002/jcp.22920.

118. Csuk, R.; Schwarz, S.; Kluge, R.; Strohl, D. Synthesis and biological activity of some antitumor active derivatives from glycyrrhetinic acid. *Eur. J. Med. Chem.* **2010**, *45*, 5718-5723, doi:10.1016/j.ejmech.2010.09.028.

119. Luo, H.; Zhang, Z.; Wu, Q.; Huang, M.; Huang, W.; Zhang, D.; Yang, F. 18β-glycyrrhetinic Acid-induced Apoptosis and Relation withIntracellular Ca2+ Release in Human Breast Carcinoma Cells. *The Chinese-German Journal of Clinical Oncology* **2004**, *3*, 137-140, doi:10.1007/s10330-003-0198-4.

120. Huang, R.Y.; Chu, Y.L.; Huang, Q.C.; Chen, X.M.; Jiang, Z.B.; Zhang, X.; Zeng, X. 18 beta-Glycyrrhetinic Acid Suppresses Cell Proliferation through Inhibiting Thromboxane Synthase in Non-Small Cell Lung Cancer. *PLoS One* **2014**, *9*, 9, doi:10.1371/journal.pone.0093690.

121. Song, J.; Ko, H.S.; Sohn, E.J.; Kim, B.; Kim, J.H.; Kim, H.J.; Kim, C.; Kim, J.E.; Kim, S.H. Inhibition of protein kinase C alpha/beta II and activation of c-Jun NH2-terminal kinase mediate glycyrrhetinic acid induced apoptosis in non-small cell lung cancer NCI-H460 cells. *Bioorg. Med. Chem. Lett.* **2014**, *24*, 1188-1191, doi:10.1016/j.bmcl.2013.12.111.

122. Hawthorne, S.; Gallagher, S. Effects of glycyrrhetinic acid and liquorice extract on cell proliferation and prostate-specific antigen secretion in LNCaP prostate cancer cells. *J. Pharm. Pharmacol.* **2008**, *60*, 661-666, doi:10.1211/jpp.60.5.0013.

123. Hibasami, H.; Iwase, H.; Yoshioka, K.; Takahashi, H. Glycyrrhetic acid (a metabolic substance and aglycon of glycyrrhizin) induces apoptosis in human hepatoma, promyelotic leukemia and stomach cancer cells. *Int. J. Mol. Med.* **2006**, *17*, 215-219.

124. Cai, H.K.; Chen, X.; Zhang, J.B.; Wang, J.J. 18 beta-glycyrrhetinic acid inhibits migration and invasion of human gastric cancer cells via the ROS/PKC-alpha/ERK pathway. *J. Nat. Med.* **2018**, *72*, 252-259, doi:10.1007/s11418-017-1145-y.

125. Satomi, Y.; Nishino, H.; Shibata, S. Glycyrrhetinic acid and related compounds induce G1 arrest and apoptosis in human hepatocellular carcinoma HepG2. *Anticancer Res.* **2005**, *25*, 4043-4047.

126. Lee, C.S.; Kim, Y.J.; Lee, M.S.; Han, E.S.; Lee, S.J. 18 beta-glycyrrhetinic acid induces apoptotic cell death in SiHa cells and exhibits a synergistic effect against antibiotic anti-cancer drug toxicity. *Life Sci.* **2008**, *83*, 481-489, doi:10.1016/j.lfs.2008.07.014.

127. Saeed, M. 18 beta-glycyrrhetinic Acid Induces Cell Cycle Arrest and Apoptosis in HPV18(+) HeLa Cervical Cancer Cells. *J. Pharm. Res. Int.* **2020**, *32*, 52-66, doi:10.9734/JPRI/2020/v32i2530823.

128. Lee, C.S.; Yang, J.C.; Kim, Y.J.; Jang, E.R.; Kim, W.; Myung, S.C. 18 beta-Glycyrrhetinic acid potentiates apoptotic effect of trichostatin A on human epithelial ovarian carcinoma cell lines. *Eur. J. Pharmacol.* **2010**, *649*, 354-361, doi:10.1016/j.ejphar.2010.09.047.

129. Haghshenas, V.; Fakhari, S.; Mirzaie, S.; Rahmani, M.; Farhadifar, F.; Pirzadeh, S.; Jalili, A. Glycyrrhetinic Acid Inhibits Cell Growth and Induces Apoptosis in Ovarian Cancer A2780 Cells. *Adv. Pharm. Bull.* **2014**, *4*, 437-441, doi:10.5681/apb.2014.064.

130. Yang, J.C.; Myung, S.C.; Kim, W.; Lee, C.S. 18 beta-Glycyrrhetinic acid potentiates Hsp90 inhibition-induced apoptosis in human epithelial ovarian carcinoma cells via activation of death receptor and mitochondrial pathway. *Mol. Cell. Biochem.* **2012**, *370*, 209-219, doi:10.1007/s11010-012-1412-x.

131. Lin, K.W.; Huang, A.M.; Hour, T.C.; Yang, S.C.; Pu, Y.S.; Lin, C.N. beta 18b-Glycyrrhetinic acid derivatives induced mitochondrial-mediated apoptosis through reactive oxygen species-mediated p53 activation in NTUB1 cells. *Bioorg. Med. Chem.* **2011**, *19*, 4274-4285, doi:10.1016/j.bmc.2011.05.054.

132. Gao, Y.A.; Guo, X.; Li, X.J.; Liu, D.; Song, D.D.; Xu, Y.; Sun, M.; Jing, Y.K.; Zhao, L.X. The Synthesis of Glycyrrhetinic Acid Derivatives Containing A Nitrogen Heterocycle and Their Antiproliferative Effects in Human Leukemia Cells. *Molecules* **2010**, *15*, 4439-4449, doi:10.3390/molecules15064439.

133. Liu, D.; Song, D.D.; Guo, G.; Wang, R.; Lv, J.L.; Jing, Y.K.; Zhao, L.X. The synthesis of 18 beta-glycyrrhetinic acid derivatives which have increased antiproliferative and apoptotic effects in leukemia cells. *Bioorg. Med. Chem.* **2007**, *15*, 5432-5439, doi:10.1016/j.bmc.2007.05.057.

134. Zhu, J.; Chen, M.J.; Chen, N.; Ma, A.Z.; Zhu, C.Y.; Zhao, R.L.; Jiang, M.; Zhou, J.; Ye, L.H.; Fu, H.A., et al. Glycyrrhetinic acid induces G1-phase cell cycle arrest in human non-small cell lung cancer cells through endoplasmic reticulum stress pathway. *Int. J. Oncol.* **2015**, *46*, 981-988, doi:10.3892/ijo.2015.2819.

135. Li, J.J.; Tang, F.; Li, R.K.; Chen, Z.J.; Lee, S.M.Y.; Fu, C.M.; Zhang, J.M.; Leung, G.P.H. Dietary compound glycyrrhetinic acid suppresses tumor angiogenesis and growth by modulating antiangiogenic and proapoptotic pathways in vitro and in vivo. *J. Nutr. Biochem.* **2020**, *77*, 13, doi:10.1016/j.jnutbio.2019.108268.

136. Jayasooriya, R.; Dilshara, M.G.; Park, S.R.; Choi, Y.H.; Hyun, J.W.; Chang, W.Y.; Kim, G.Y. 18 beta-Glycyrrhetinic acid suppresses TNF-alpha induced matrix metalloproteinase-9 and vascular endothelial growth factor by suppressing the Akt-dependent NF-kappa B pathway. *Toxicol. Vitro* **2014**, *28*, 751-758, doi:10.1016/j.tiv.2014.02.015.

137. Wang, X.F.; Zhou, Q.M.; Lu, Y.Y.; Zhang, H.; Huang, S.; Su, S.B. Glycyrrhetinic acid potently suppresses breast cancer invasion and metastasis by impairing the p38 MAPK-AP1 signaling axis. *Expert Opin. Ther. Targets* **2015**, *19*, 577-587, doi:10.1517/14728222.2015.1012156.

138. Nabekura, T.; Yamaki, T.; Ueno, K.; Kitagawa, S. Inhibition of P-glycoprotein and multidrug resistance protein 1 by dietary phytochemicals. *Cancer Chemother. Pharmacol.* **2008**, *62*, 867-873, doi:10.1007/s00280-007-0676-4.

139. Zhou, J.X.; Wink, M. Reversal of Multidrug Resistance in Human Colon Cancer and Human Leukemia Cells by Three Plant Extracts and Their Major Secondary Metabolites. *Medicines* **2018**, *5*, doi:10.3390/medicines5040123.

140. Csuk, R.; Schwarz, S.; Siewert, B.; Kluge, R.; Strohl, D. Conversions at C-30 of Glycyrrhetinic Acid and Their Impact on Antitumor Activity. *Arch. Pharm.* **2012**, *345*, 223-230, doi:10.1002/ardp.201100046.

141. Csuk, R.; Schwarz, S.; Siewert, B.; Kluge, R.; Strohl, D. Synthesis and antitumor activity of ring A modified glycyrrhetinic acid derivatives. *Eur. J. Med. Chem.* **2011**, *46*, 5356-5369, doi:10.1016/j.ejmech.2011.08.038.

142. Csuk, R.; Schwarz, S.; Kluge, R.; Strohl, D. Improvement of the Cytotoxicity and Tumor Selectivity of Glycyrrhetinic Acid by Derivatization with Bifunctional Aminoacids. *Arch. Pharm.* **2011**, *344*, 505-513, doi:10.1002/ardp.201100030.

143. Schwarz, S.; Csuk, R. Synthesis and antitumour activity of glycyrrhetinic acid derivatives. *Bioorg. Med. Chem.* **2010**, *18*, 7458-7474, doi:10.1016/j.bmc.2010.08.054.

144. Zhou, F.; Wu, G.R.; Cai, D.S.; Xu, B.; Yan, M.M.; Ma, T.; Guo, W.B.; Zhang, W.X.; Huang, X.M.; Jia, X.H., et al. Synthesis and biological activity of glycyrrhetinic acid derivatives as antitumor agents. *Eur. J. Med. Chem.* **2019**, *178*, 623-635, doi:10.1016/j.ejmech.2019.06.029.

145. Lai, Y.S.; Shen, L.H.; Zhang, Z.Z.; Liu, W.Q.; Zhang, Y.H.; Ji, H.; Tian, J. Synthesis and biological evaluation of furoxan-based nitric oxide-releasing derivatives of glycyrrhetinic acid as anti-hepatocellular carcinoma agents. *Bioorg. Med. Chem. Lett.* **2010**, *20*, 6416-6420, doi:10.1016/j.bmcl.2010.09.070.

146. Huang, L.; Yu, D.L.; Ho, P.; Qian, K.D.; Lee, K.H.; Chen, C.H. Synthesis and proteasome inhibition of glycyrrhetinic acid derivatives. *Bioorg. Med. Chem.* **2008**, *16*, 6696-6701, doi:10.1016/j.bmc.2008.05.078.

147. Liu, Y.Q.; Qian, K.D.; Wang, C.Y.; Chen, C.H.; Yang, X.M.; Lee, K.H. Synthesis and biological evaluation of novel spin labeled 18 beta-glycyrrhetinic acid derivatives. *Bioorg. Med. Chem. Lett.* **2012**, *22*, 7530-7533, doi:10.1016/j.bmcl.2012.10.041.

148. Lallemand, B.; Chaix, F.; Bury, M.; Bruyere, C.; Ghostin, J.; Becker, J.P.; Delporte, C.; Gelbcke, M.; Mathieu, V.; Dubois, J., et al. N-(2-{3- 3,5-Bis(trifluoromethyl)phenyl ureido}ethyl)-glycyrrhetinamide (6b): A Novel Anticancer Glycyrrhetinic Acid Derivative that Targets the Proteasome and Displays Anti-Kinase Activity. *J. Med. Chem.* **2011**, *54*, 6501-6513, doi:10.1021/jm200285z.

149. Tatsuzaki, J.; Taniguchi, M.; Bastow, K.F.; Nakagawa-Goto, K.; Morris-Natschke, S.L.; Itokawa, H.; Baba, K.; Lee, K.H. Anti-tumor agents 255: Novel glycyrrhetinic acid-dehydrozingerone conjugates as cytotoxic agents. *Bioorg. Med. Chem.* **2007**, *15*, 6193-6199, doi:10.1016/j.bmc.2007.06.027.

150. Nakagawa-Goto, K.; Nakamura, S.; Bastow, K.F.; Nyarko, A.; Peng, C.Y.; Lee, F.Y.; Lee, F.C.; Lee, K.H. Antitumor agents. 256. Conjugation of paclitaxel with

other antitumor agents: Evaluation of novel conjugates as cytotoxic agents. *Bioorg. Med. Chem. Lett.* **2007**, *17*, 2894-2898, doi:10.1016/j.bmcl.2007.02.051.

151. Liu, C.M.; Huang, J.Y.; Sheng, L.X.; Wen, X.A.; Cheng, K.G. Synthesis and antitumor activity of fluorouracil oleanolic acid/ursolic acid/glycyrrhetinic acid conjugates. *MedChemComm* **2019**, *10*, 1370-1378, doi:10.1039/c9md00246d.

152. Zhao, C.H.; Zhang, C.L.; Shi, J.J.; Hou, X.Y.; Feng, B.; Zhao, L.X. Design, synthesis, and biofunctional evaluation of novel pentacyclic triterpenes bearing O-4-(1-piperazinyl)-4-oxo-butyryl moiety as antiproliferative agents. *Bioorg. Med. Chem. Lett.* **2015**, *25*, 4500-4504, doi:10.1016/j.bmcl.2015.08.076.

153. Yan, T.L.; Bai, L.F.; Zhu, H.L.; Zhang, W.M.; Lv, P.C. Synthesis and Biological Evaluation of Glycyrrhetic Acid Derivatives as Potential VEGFR2 Inhibitors. *ChemMedChem* **2017**, *12*, 1087-1096, doi:10.1002/cmdc.201700271.

154. Sun, J.; Liu, H.Y.; Lv, C.Z.; Qin, J.; Wu, Y.F. Modification, Antitumor Activity, and Targeted PPAR gamma Study of 18 beta-Glycyrrhetinic Acid, an Important Active Ingredient of Licorice. *J. Agric. Food Chem.* **2019**, *67*, 9643-9651, doi:10.1021/acs.jafc.9b03442.

155. Guo, W.B.; Yan, M.M.; Xu, B.; Chu, F.H.; Wang, W.; Zhang, C.Z.; Jia, X.H.; Han, Y.T.; Xiang, H.J.; Zhang, Y.Z., et al. Design, synthesis, and biological evaluation of the novel glycyrrhetinic acid-cinnamoyl hybrids as anti-tumor agents. *Chem. Cent. J.* **2016**, *10*, 11, doi:10.1186/s13065-016-0222-8.

156. Li, X.J.; Liu, Y.H.; Wang, N.; Liu, Y.Y.; Wang, S.; Wang, H.M.; Lie, A.H.; Ren, S.D. Synthesis and discovery of 18 beta-glycyrrhetinic acid derivatives inhibiting cancer stem cell properties in ovarian cancer cells. *RSC Adv.* **2019**, *9*, 27294-27304, doi:10.1039/c9ra04961d.

157. Sommerwerk, S.; Heller, L.; Kerzig, C.; Kramell, A.E.; Csuk, R. Rhodamine B conjugates of triterpenoic acids are cytotoxic mitocans even at nanomolar concentrations. *Eur. J. Med. Chem.* **2017**, *127*, 1-9, doi:10.1016/j.ejmech.2016.12.040.

158. Wolfram, R.K.; Fischer, L.; Kluge, R.; Strohl, D.; Al-Harrasi, A.; Csuk, R. Homopiperazine-rhodamine B adducts of triterpenoic acids are strong mitocans. *Eur. J. Med. Chem.* **2018**, *155*, 869-879, doi:10.1016/j.ejmech.2018.06.051.

159. Wolfram, R.K.; Heller, L.; Csuk, R. Targeting mitochondria: Esters of rhodamine B with triterpenoids are mitocanic triggers of apoptosis. *Eur. J. Med. Chem.* **2018**, *152*, 21-30, doi:10.1016/j.ejmech.2018.04.031.

160. Jin, L.; Dai, L.M.; Ji, M.; Wang, H.S. Mitochondria-targeted triphenylphosphonium conjugated glycyrrhetinic acid derivatives as potent anticancer drugs. *Bioorganic Chem.* **2019**, *85*, 179-190, doi:10.1016/j.bioorg.2018.12.036.

161. Maitraie, D.; Hung, C.F.; Tu, H.Y.; Liou, Y.T.; Wei, B.L.; Yang, S.C.; Wang, J.P.; Lin, C.N. Synthesis, anti-inflammatory, and antioxidant activities of 18 beta-glycyrrhetinic acid derivatives as chemical mediators and xanthine oxidase inhibitors. *Bioorg. Med. Chem.* **2009**, *17*, 2785-2792, doi:10.1016/j.bmc.2009.02.025.

162. Honda, T.; Rounds, B.V.; Bore, L.; Finlay, H.J.; Favaloro, F.G.; Suh, N.; Wang, Y.P.; Sporn, M.B.; Gribble, G.W. Synthetic oleanane and ursane triterpenoids

with modified rings A and C: A series of highly active inhibitors of nitric oxide production in mouse macrophages. *J. Med. Chem.* **2000**, *43*, 4233-4246, doi:10.1021/jm0002230.

163. Couch, R.D.; Browning, R.G.; Honda, T.; Gribble, G.W.; Wright, D.L.; Sporn, M.B.; Anderson, A.C. Studies on the reactivity of CDDO, a promising new chemopreventive and chemotherapeutic agent: implications for a molecular mechanism of action. *Bioorg. Med. Chem. Lett.* **2005**, *15*, 2215-2219, doi:10.1016/j.bmcl.2005.03.031.

164. Sporn, M.B.; Liby, K.T.; Yore, M.M.; Fu, L.F.; Lopchuk, J.M.; Gribble, G.W. New Synthetic Triterpenoids: Potent Agents for Prevention and Treatment of Tissue Injury Caused by Inflammatory and Oxidative Stress. *J. Nat. Prod.* **2011**, *74*, 537-545, doi:10.1021/np100826q.

165. Chadalapaka, G.; Jutooru, I.; McAlees, A.; Stefanac, T.; Safe, S. Structure-dependent inhibition of bladder and pancreatic cancer cell growth by 2-substituted glycyrrhetinic and ursolic acid derivatives. *Bioorg. Med. Chem. Lett.* **2008**, *18*, 2633-2639, doi:10.1016/j.bmcl.2008.03.031.

166. Li, X.J.; Wang, Y.T.; Gao, Y.; Li, L.; Guo, X.; Liu, D.; Jing, Y.K.; Zhao, L.X. Synthesis of methyl 2-cyano-3,12-dioxo-18 beta-olean-1,9(11)-dien-30-oate analogues to determine the active groups for inhibiting cell growth and inducing apoptosis in leukemia cells. *Org. Biomol. Chem.* **2014**, *12*, 6706-6716, doi:10.1039/c4ob00703d.

167. Salomatina, O.V.; Markov, A.V.; Logashenko, E.B.; Korchagina, D.V.; Zenkova, M.A.; Salakhutdinov, N.F.; Vlassov, V.V.; Tolstikov, G.A. Synthesis of novel 2-cyano substituted glycyrrhetinic acid derivatives as inhibitors of cancer cells growth and NO production in LPS-activated J-774 cells. *Bioorg. Med. Chem.* **2014**, *22*, 585-593, doi:10.1016/j.bmc.2013.10.049.

168. You, R.; Long, W.Y.; Lai, Z.H.; Sha, L.; Wu, K.; Yu, X.; Lai, Y.S.; Ji, H.; Huang, Z.J.; Zhang, Y.H. Discovery of a Potential Anti-Inflammatory Agent: 3-Oxo-29-noroleana-1,9(11),12-trien-2,20-dicarbonitrile. *J. Med. Chem.* **2013**, *56*, 1984-1995, doi:10.1021/jm301652t.

169. Heller, L.; Schwarz, S.; Per, V.; Kowitsch, A.; Siewert, B.; Csuk, R. Incorporation of a Michael acceptor enhances the antitumor activity of triterpenoic acids. *Eur. J. Med. Chem.* **2015**, *101*, 391-399, doi:10.1016/j.ejmech.2015.07.004.

170. Huang, M.; Gong, P.; Wang, Y.T.; Xie, X.R.; Ma, Z.S.; Xu, Q.H.; Liu, D.; Jing, Y.K.; Zhao, L.X. Synthesis and antitumor effects of novel 18 beta-glycyrrhetinic acid derivatives featuring an exocyclic alpha,beta-unsaturated carbonyl moiety in ring A. *Bioorganic Chem.* **2020**, *103*, 13, doi:10.1016/j.bioorg.2020.104187.

171. Takeuchi, H.; Taoka, R.; Mmeje, C.O.; Jinesh, G.G.; Safe, S.; Kamat, A.M. CDODA-Me decreases specificity protein transcription factors and induces apoptosis in bladder cancer cells through induction of reactive oxygen species. *Urol. Oncol.-Semin. Orig. Investig.* **2016**, *34*, 8, doi:10.1016/j.urolonc.2016.02.025.

172. Chintharlapalli, S.; Papineni, S.; Jutooru, I.; McAlees, A.; Safe, S. Structure-dependent activity of glycyrrhetinic acid derivatives as peroxisorne proliferator-activated receptor gamma agonists in colon cancer cells. *Molecular Cancer Therapeutics* **2007**, *6*, 1588-1598, doi:10.1158/1535-7163.mct-07-0022.

173. Chintharlapalli, S.; Papineni, S.; Abdelrahim, M.; Abudayyeh, A.; Jutooru, I.; Chadalapaka, G.; Wu, F.; Mertens-Talcott, S.; Vanderlaag, K.; Cho, S.D., et al. Oncogenic microRNA-27a is a target for anticancer agent methyl 2-cyano-3,11-dioxo-18 beta-olean-1,12-dien-30-oate in colon cancer cells. *Int. J. Cancer* **2009**, *125*, 1965-1974, doi:10.1002/ijc.24530.

174. Jutooru, I.; Chadalapaka, G.; Chintharlapalli, S.; Papineni, S.; Safe, S. Induction of Apoptosis and Nonsteroidal Anti-inflammatory Drug-Activated Gene 1 in Pancreatic Cancer Cells by a Glycyrrhetinic Acid Derivative. *Mol. Carcinog.* **2009**, *48*, 692-702, doi:10.1002/mc.20518.

175. Papineni, S.; Chintharlapalli, S.; Safe, S. Methyl 2-cyano-3,11-dioxo-18 beta-olean-1,12-dien-30-oate is a peroxisome proliferator-activated receptor- gamma agonist that induces receptor-independent apoptosis in LNCaP prostate cancer cells. *Mol. Pharmacol.* **2008**, *73*, 553-565, doi:10.1124/mol.107.041285.

176. Pang, X.F.; Zhang, L.; Wu, Y.G.; Lin, L.; Li, J.J.; Qu, W.J.; Safe, S.; Liu, M.Y. Methyl 2-Cyano-3,11-dioxo-18-olean-1,12-dien-30-oate (CDODA-Me), a Derivative of Glycyrrhetinic Acid, Functions as a Potent Angiogenesis Inhibitor. *J. Pharmacol. Exp. Ther.* **2010**, *335*, 172-179, doi:10.1124/jpet.110.171066.

177. Song, D.D.; Gao, Y.; Wang, R.; Liu, D.; Zhao, L.X.; Jing, Y.K. Downregulation of c-FLIP, XIAP and Mcl-1 protein as well as depletion of reduced glutathione contribute to the apoptosis induction of glycyrrhetinic acid derivatives in leukemia cells. *Cancer Biol. Ther.* **2010**, *9*, 96-108, doi:10.4161/cbt.9.2.10287.

178. Chintharlapalli, S.; Papineni, S.; Lee, S.O.; Lei, P.; Jin, U.H.; Sherman, S.I.; Santarpia, L.; Safe, S. Inhibition of Pituitary Tumor-Transforming Gene-1 in Thyroid Cancer Cells by Drugs That Decrease Specificity Proteins. *Mol. Carcinog.* **2011**, *50*, 655-667, doi:10.1002/mc.20738.

179. Taoka, R.; Jinesh, G.G.; Xue, W.R.; Safe, S.; Kamat, A.M. CF(3)DODA-Me induces apoptosis, degrades Sp1, and blocks the transformation phase of the blebbishield emergency program. *Apoptosis* **2017**, *22*, 719-729, doi:10.1007/s10495-017-1359-1.

180. Kasiappan, R.; Jutooru, I.; Mohankumar, K.; Karki, K.; Lacey, A.; Safe, S. Reactive Oxygen Species (ROS)-Inducing Triterpenoid Inhibits Rhabdomyosarcoma Cell and Tumor Growth through Targeting Sp Transcription Factors. *Mol. Cancer Res.* **2019**, *17*, 794-805, doi:10.1158/1541-7786.mcr-18-1071.

181. Tan, J.N.; Lai, Z.H.; Liu, L.; Long, W.Y.; Chen, T.; Zha, J.; Wang, L.N.; Chen, M.Y.; Ji, H.; Lai, Y.S. ONTD induces apoptosis of human hepatoma Bel-7402 cells via a MAPK-dependent mitochondrial pathway and the depletion of intracellular glutathione. *Int. J. Biochem. Cell Biol.* **2013**, *45*, 2632-2642, doi:10.1016/j.biocel.2013.08.021.

182. Tan, J.N.; Shen, W.X.; Shi, W.J.; Chen, X.; Sun, D.D.; Xu, C.L.; Yan, Q.Y.; Cheng, H.B.; Lai, Y.S.; Ji, H. ONTD induces growth arrest and apoptosis of human hepatoma Bel-7402 cells though a peroxisome proliferator-activated receptor gamma-dependent pathway. *Toxicol. Vitro* **2017**, *45*, 44-53, doi:10.1016/j.tiv.2017.08.012.

183. Gong, P.; Li, K.; Li, Y.; Liu, D.; Zhao, L.X.; Jing, Y.K. HDAC and Ku70 axis- an effective target for apoptosis induction by a new 2-cyano-3-oxo-1,9-dien

glycyrrhetinic acid analogue. *Cell Death Dis.* **2018**, *9*, 11, doi:10.1038/s41419-018-0602-1.

184. Alper, P.; Salomatina, O.V.; Salakhutdinov, N.F.; Ulukaya, E.; Ari, F. Soloxolone methyl, as a 18 beta H-glycyrrhetinic acid derivate, may result in endoplasmic reticulum stress to induce apoptosis in breast cancer cells. *Bioorg. Med. Chem.* **2021**, *30*, 8, doi:10.1016/j.bmc.2020.115963.

185. Markov, A.V.; Odarenko, K.V.; Sen'kova, A.V.; Salomatina, O.V.; Salakhutdinov, N.F.; Zenkova, M.A. Cyano Enone-Bearing Triterpenoid Soloxolone Methyl Inhibits Epithelial-Mesenchymal Transition of Human Lung Adenocarcinoma Cells In Vitro and Metastasis of Murine Melanoma In Vivo. *Molecules* **2020**, *25*, 27, doi:10.3390/molecules25245925.

186. Taylor, R.D.; MacCoss, M.; Lawson, A.D.G. Rings in Drugs. *J. Med. Chem.* **2014**, *57*, 5845-5859, doi:10.1021/jm4017625.

187. Ali, I.; Lone, M.N.; Aboul-Enein, H.Y. Imidazoles as potential anticancer agents. *MedChemComm* **2017**, *8*, 1742-1773, doi:10.1039/c7md00067g.

188. Zhang, L.; Peng, X.M.; Damu, G.L.V.; Geng, R.X.; Zhou, C.H. Comprehensive Review in Current Developments of Imidazole-Based Medicinal Chemistry. *Med. Res. Rev.* **2014**, *34*, 340-437, doi:10.1002/med.21290.

189. Kumar, S.S.; Kavitha, H.P. Synthesis and Biological Applications of Triazole Derivatives - A Review. *Mini-Rev. Org. Chem.* **2013**, *10*, 40-65.

190. Marsilje, T.H.; Pei, W.; Chen, B.; Lu, W.S.; Uno, T.; Jin, Y.H.; Jiang, T.; Kim, S.; Li, N.X.; Warmuth, M., et al. Synthesis, Structure-Activity Relationships, and in Vivo Efficacy of the Novel Potent and Selective Anaplastic Lymphoma Kinase (ALK) Inhibitor 5-Chloro-N2-(2-isopropoxy-5-methyl-4-(piperidin-4-yl)phenyl)-N4-(2-(isop ropylsulfonyl)phenyl)pyrimidine-2,4-diamine (LDK378) Currently in Phase 1 and Phase 2 Clinical Trials. *J. Med. Chem.* **2013**, *56*, 5675-5690, doi:10.1021/jm400402q.

191. Solomon, V.R.; Lee, H. Anti-breast cancer activity of heteroaryl chalcone derivatives. *Biomed. Pharmacother.* **2012**, *66*, 213-220, doi:10.1016/j.biopha.2011.11.013.

192. Santos, R.C.; Salvador, J.A.R.; Marin, S.; Cascante, M.; Moreira, J.N.; Dinis, T.C.P. Synthesis and structure-activity relationship study of novel cytotoxic carbamate and N-acylheterocyclic bearing derivatives of betulin and betulinic acid. *Bioorg. Med. Chem.* **2010**, *18*, 4385-4396, doi:10.1016/j.bmc.2010.04.085.

193. Leal, A.S.; Wang, R.; Salvador, J.A.R.; Jing, Y.K. Synthesis of novel ursolic acid heterocyclic derivatives with improved abilities of antiproliferation and induction of p53, p21(waf1) and NOXA in pancreatic cancer cells. *Bioorg. Med. Chem.* **2012**, *20*, 5774-5786, doi:10.1016/j.bmc.2012.08.010.

194. Thirumurugan, P.; Matosiuk, D.; Jozwiak, K. Click Chemistry for Drug Development and Diverse Chemical-Biology Applications. *Chem. Rev.* **2013**, *113*, 4905-4979, doi:10.1021/cr200409f.

195. Musumeci, F.; Schenone, S.; Desogus, A.; Nieddu, E.; Deodato, D.; Botta, L. Click Chemistry, A Potent Tool in Medicinal Sciences. *Curr. Med. Chem.* **2015**, *22*, 2022-2050.

196. Ma, N.; Wang, Y.; Zhao, B.X.; Ye, W.C.; Jiang, S. The application of click chemistry in the synthesis of agents with anticancer activity. *Drug Des. Dev. Ther.* **2015**, *9*, 1585-1599, doi:10.2147/dddt.s56038.

197. Meghani, N.M.; Amin, H.H.; Leel, B.J. Mechanistic applications of click chemistry for pharmaceutical drug discovery and drug delivery. *Drug Discov. Today* **2017**, *22*, 1604-1619, doi:10.1016/j.drudis.2017.07.007.

198. Pertino, M.W.; Lopez, C.; Theoduloz, C.; Schmeda-Hirschmann, G. 1,2,3-Triazole-Substituted Oleanolic Acid Derivatives: Synthesis and Antiproliferative Activity. *Molecules* **2013**, *18*, 7661-7674, doi:10.3390/molecules18077661.

199. Dangroo, N.A.; Singh, J.; Rath, S.K.; Gupta, N.; Qayum, A.; Singh, S.; Sangwan, P.L. A convergent synthesis of novel alkyne-azide cycloaddition congeners of betulinic acid as potent cytotoxic agent. *Steroids* **2017**, *123*, 1-12, doi:10.1016/j.steroids.2017.04.002.

200. Pokorny, J.; Borkova, L.; Urban, M. Click Reactions in Chemistry of Triterpenes - Advances Towards Development of Potential Therapeutics. *Curr. Med. Chem.* **2018**, *25*, 636-658, doi:10.2174/0929867324666171009122612.

201. Pertino, M.W.; Petrera, E.; Alche, L.E.; Schmeda-Hirschmann, G. Synthesis, Antiviral and Cytotoxic Activity of Novel Terpenyl Hybrid Molecules Prepared by Click Chemistry. *Molecules* **2018**, *23*, 12, doi:10.3390/molecules23061343.

202. Rostovtsev, V.V.; Green, L.G.; Fokin, V.V.; Sharpless, K.B. A stepwise Huisgen cycloaddition process: Copper(I)-catalyzed regioselective "ligation" of azides and terminal alkynes. *Angew. Chem.-Int. Edit.* **2002**, *41*, 2596-+, doi:10.1002/1521-3773(20020715)41:14<2596::aid-anie2596>3.0.co;2-4.

203. Himo, F.; Lovell, T.; Hilgraf, R.; Rostovtsev, V.V.; Noodleman, L.; Sharpless, K.B.; Fokin, V.V. Copper(I)-catalyzed synthesis of azoles. DFT study predicts unprecedented reactivity and intermediates. *J. Am. Chem. Soc.* **2005**, *127*, 210-216, doi:10.1021/ja0471525.

204. Tron, G.C.; Pirali, T.; Billington, R.A.; Canonico, P.L.; Sorba, G.; Genazzani, A.A. Click chemistry reactions in medicinal chemistry: Applications of the 1,3-dipolar cycloaddition between azides and alkynes. *Med. Res. Rev.* **2008**, *28*, 278-308, doi:10.1002/med.20107.

205. Rodrigues, T.; Reker, D.; Schneider, P.; Schneider, G. Counting on natural products for drug design. *Nat. Chem.* **2016**, *8*, 531-541, doi:10.1038/nchem.2479.

206. Rao, G.; Kondaiah, P.; Singh, S.K.; Ravanan, P.; Sporn, M.B. Chemical modifications of natural triterpenes-glycyrrhetinic and boswellic acids: evaluation of their biological activity. *Tetrahedron* **2008**, *64*, 11541-11548, doi:10.1016/j.tet.2008.10.035.

207. Chu, F.H.; Xu, X.; Li, G.L.; Gu, S.; Xu, K.; Gong, Y.; Xu, B.; Wang, M.N.; Zhang, H.Z.; Zhang, Y.Z., et al. Amino Acid Derivatives of Ligustrazine-Oleanolic Acid as New Cytotoxic Agents. *Molecules* **2014**, *19*, 18215-18231, doi:10.3390/molecules191118215.

208. Porchia, M.; Dolmella, A.; Gandin, V.; Marzano, C.; Pellei, M.; Peruzzo, V.; Refosco, F.; Santini, C.; Tisato, F. Neutral and charged phosphine/scorpionate copper(I) complexes: Effects of ligand assembly on their antiproliferative activity. *Eur. J. Med. Chem.* **2013**, *59*, 218-226, doi:10.1016/j.ejmech.2012.11.022.

209. Goncalves, B.M.F.; Salvador, J.A.R.; Marin, S.; Cascante, M. Synthesis and biological evaluation of novel asiatic acid derivatives with anticancer activity. *RSC Adv.* **2016**, *6*, 3967-3985, doi:10.1039/c5ra19120c.

210. Chen, L.; Zhao, Y.; Halliday, G.C.; Berry, P.; Rousseau, R.F.; Middleton, S.A.; Nichols, G.L.; Del Bello, F.; Piergentili, A.; Newell, D.R., et al. Structurally diverse MDM2-p53 antagonists act as modulators of MDR-1 function in neuroblastoma. *Br. J. Cancer* **2014**, *111*, 716-725, doi:10.1038/bjc.2014.325.

211. Antunovic, M.; Kriznik, B.; Ulukaya, E.; Yilmaz, V.T.; Mihalic, K.C.; Madunic, J.; Marijanovic, I. Cytotoxic activity of novel palladium-based compounds on leukemia cell lines. *Anti-Cancer Drugs* **2015**, *26*, 180-186, doi:10.1097/cad.0000000000000174.

212. Rajic, Z.; Zorc, B.; Raic-Malic, S.; Ester, K.; Kralj, M.; Pavelic, K.; Balzarini, J.; De Clercq, E.; Mintas, M. Hydantoin derivatives of L- and D-amino acids: Synthesis and evaluation of their antiviral and antitumoral activity. *Molecules* **2006**, *11*, 837-848, doi:10.3390/11110837.

213. Cheng, J.; Haas, M. FREQUENT MUTATIONS IN THE P53 TUMOR SUPPRESSOR GENE IN HUMAN LEUKEMIA T-CELL LINES. *Mol. Cell. Biol.* **1990**, *10*, 5502-5509.

214. Drag-Zalesinska, M.; Kulbacka, J.; Saczko, J.; Wysocka, T.; Zabel, M.; Surowiak, P.; Drag, M. Esters of betulin and betulinic acid with amino acids have improved water solubility and are selectively cytotoxic toward cancer cells. *Bioorg. Med. Chem. Lett.* **2009**, *19*, 4814-4817, doi:10.1016/j.bmcl.2009.06.046.

215. Csuk, R.; Schwarz, S.; Siewert, B.; Kluge, R.; Strohl, D. Synthesis and Cytotoxic Activity of Methyl Glycyrrhetinate Esterified with Amino Acids. *Z.Naturforsch.(B)* **2012**, *67*, 731-746, doi:10.5560/znb.2012-0107.

216. Roughley, S.D.; Jordan, A.M. The Medicinal Chemist's Toolbox: An Analysis of Reactions Used in the Pursuit of Drug Candidates. *J. Med. Chem.* **2011**, *54*, 3451-3479, doi:10.1021/jm200187y.

217. Lal, G.S.; Pez, G.P.; Pesaresi, R.J.; Prozonic, F.M.; Cheng, H.S. Bis(2-methoxyethyl)aminosulfur trifluoride: A new broad-spectrum deoxofluorinating agent with enhanced thermal stability. *J. Org. Chem.* **1999**, *64*, 7048-7054, doi:10.1021/jo990566+.

218. White, J.M.; Tunoori, A.R.; Turunen, B.J.; Georg, G.I. Bis(2-methoxyethyl)amino sulfur trifluoride, the deoxo-fluor reagent: Application toward one-flask transformations of carboxylic acids to amides. *J. Org. Chem.* **2004**, *69*, 2573-2576, doi:10.1021/jo035658k.

219. Carpino, L.A.; Beyermann, M.; Wenschuh, H.; Bienert, M. Peptide synthesis via amino acid halides. *Accounts Chem. Res.* **1996**, *29*, 268-274, doi:10.1021/ar950023w.

220. Kangani, C.O.; Kelley, D.E. One pot direct synthesis of amides or oxazolines from carboxylic acids using Deoxo-Fluor reagent. *Tetrahedron Lett.* **2005**, *46*, 8917-8920, doi:10.1016/j.tetlet.2005.10.068.

221. Kangani, C.O.; Kelley, D.E.; Day, B.W. One pot direct synthesis of oxazolines, benzoxazoles, and oxadiazoles from carboxylic acids using the Deoxo-Fluor reagent. *Tetrahedron Lett.* **2006**, *47*, 6497-6499, doi:10.1016/j.tetlet.2006.07.032.

222. Kangani, C.O.; Day, B.W.; Kelley, D.E. Direct, facile synthesis of acyl azides and nitriles from carboxylic acids using bis(2-methoxyethyl)aminosulfur trifluoride. *Tetrahedron Lett.* **2007**, *48*, 5933-5937, doi:10.1016/j.tetlet.2007.06.119.

223. Sakano, K.; Ohshima, M. MICROBIAL CONVERSION OF GLYCYRRHETINIC ACIDS .2. MICROBIAL CONVERSION OF 18BETA-GLYCYRRHETINIC ACID AND 22-ALPHA-HYDROXY-18BETA-GLYCYRRHETINIC ACID BY CHAINIA-ANTIBIOTICA. *Agricultural and Biological Chemistry* **1986**, *50*, 1239-1245, doi:10.1080/00021369.1986.10867532.

224. High yield 11-de:oxo:glycyrrhetic acid prepn. - by reducing glycyrrhetic acid in solvent using zinc and hydrochloric acid. JP59070638-A; JP90024264-B, JP59070638-A 21 Apr 1984 198422.